Stony Brook University

The Role of Connexin26 Mutations in Keratitis-Ichthyosis-Deafness Syndrome

A Dissertation Presented

by

Jack Lee

to

The Graduate School

in Partial Fulfillment of the

Requirements

for the Degree of

Doctor of Philosophy

in

Physiology and Biophysics

Stony Brook University

December 2011

Stony Brook University

The Graduate School

Jack Lee

We, the dissertation committee for the above candidate for the

Doctor of Philosophy degree, hereby recommend

acceptance of this dissertation.

Dr. Thomas W. White – Dissertation Advisor
Associate Professor,
Department of Physiology and Biophysics

Dr. Peter R. Brink - Chairperson of Defense
Professor,
Department of Physiology and Biophysics

Dr. Richard Mathias
Professor,
Department of Physiology and Biophysics

Dr. Linda Musil – Outside Member
Associate Professor, Department of Biochemistry and Molecular Biology
Oregon Health and Science University

This dissertation is accepted by the Graduate School

Lawrence Martin
Dean of the Graduate School

Abstract of the Dissertation

The Role of Connexin26 Mutations in Keratitis-Ichthyosis-Deafness Syndrome

by

Jack Lee

Doctor of Philosophy

in

Physiology and Biophysics

Stony Brook University

2011

Gap junctions are intercellular channels formed by connexin (Cx) proteins which create a pathway for the transport of ions and small metabolites between two adjacent cells that are in contact. In individual cells connexin proteins can form hemichannels, single ion channels, which interact with the extracellular solution. Connexin proteins are found ubiquitously throughout the body and naturally occurring mutations within their genes are associated with a range of diseases. Connexin related diseases can manifest from a variety of differing functions of the resulting protein. Mutations in the Cx26 gene (*GJB2*) are a major cause of non-syndromic deafness and also can result in syndromic deafness associated with skin disease. While the function of the mutations which cause

non-syndromic deafness can be related to a complete loss of channel functionality, the role of mutations associated with syndromic deafness is not understood. It has been theorized that this complication may result from aberrantly active hemichannels which disrupt normal homeostasis within the epidermis. It was also theorized that dominant negative inhibition or trafficking defects could be responsible for syndromic disorders where mutations do not lead to an increase in hemichannel activity. Six naturally occurring mutations (Gly12Arg, Asn14Lys, Asn14Tyr, Ser17Phe, Asp50Asn, and Asp50Tyr) were selected to investigate what differences the proteins may have compared to wild-type Cx26 activity. Gap junction activity was quantified using the *Xenopus* oocyte expression system via dual whole-cell voltage clamp on paired cells, and hemichannel activity was determined by single whole-cell voltage clamp in unpaired cells. Immunofluorescent staining in cultured and transfected HeLa cells was used to detect the trafficking patterns of the mutants and wild-type protein. All tested mutations resulted in single cells with altered hemichannel activity compared to wild-type Cx26 cells. Three tested mutations (Gly12Arg, Asn14Lys, and Asp50Asn) saw robust outward currents several fold larger than wild-type, and three mutations (Asn14Tyr, Ser17Phe, and Asp50Tyr) resulted in cells with negligible currents compared to wild-type injected cells. Cells injected with mutations associated with larger aberrant hemichannels also resulted in an increased rate of cell death. All but one mutation (Asn14Lys, equivalent) tested

had severely lowered gap junction conductance in paired oocytes compared to wild-type Cx26 pairs. Four of these mutations (Asn14Lys, Asn14Tyr, Asp50Asn, and Asp50Tyr) were selected to determine trafficking patters of Cx26 mutant proteins in HeLa cells. All cells transfected with mutant proteins showed altered trafficking patterns compared to wild-type Cx26 transfected cells. These findings lead to the conclusion that while some mutations may operate through robust and aberrant hemichannels as originally hypothesized, there also seems to a second pathway related to protein trafficking which creates the same phenotype associated with Syndromic Deafness.

Table of Contents

List of Figures

List of Tables

List of Abbreviations

35ΔG – Mutation at the 35th Residue that Results in a Frame-Shift Stop Codon

167ΔT – Mutation of the 167th Residue that Results in a Frame-Shift

235ΔC – Mutation of the 235th Residue that Results in a Frame Shift

A – Gating Charge

A40V – Mutation of Alanine at 40 into Valine

A88V – Mutation of Alanine at 88 into Valine

ATP – Adenosine Triphosphate

BPS – Bart-Pumphrey Syndrome

Ca^{2+} - Calcium Ion

$CaCl_2$ - Calcium Chloride

CL – Cytoplasmic Loop

Cx – Connexin

Cx26 – Connexin 26

Cx30 – Connexin 30

Cx30.3 – Connexin 30.3

Cx31 – Connexin 31

Cx38 – Connexin 38

Cx43 – Connexin 43

D50A – Mutation of Aspartic Acid at 50 into Alanine

D50N – mutation of Aspartic Acid at 50 into Asparagine

D50Y – Mutation of Aspartic Acid at 50 into Tyrosine

D66H – Mutation of Aspartic Acid at 66 into Histidine

DAPI - 4',6-diamidino-2-phenylindole Fluorescent Nuclear Marker

Del42E – Deletion of Glutamic Acid at 42

DFNA3 – Autosomal Dominant Non-Syndromic Deafness

DFNB1 – Autosomal Recessive Non-Syndromic Deafness

EC1 – Extracellular Domain 1

EC2 – Extracellular Domain 2

EGTA - Ethylene glycol tetraacetic acid

EDTA - Ethylenedinitrilotetraacetic acid

ER – Endoplasmic Reticulum

Exp - exponential

F142L – Mutation of Phenylalanine at 142 into Leucine

Fe^{2+} - Iron Ion

FFA – Flufenamic Acid

G11E – Mutation of Glycine at 11 into Glutamic Acid

G11R – Mutation of Glycine at 11 into Arginine

G12R – Mutation of Glycine at 12 into Arginine

G130V – Mutation of Glycine at 130 into Valine

G45E – Mutation of Glycine at 45 into Glutamic Acid

G59 – Glycine at 59

G59S – Mutation of Glycine at 59 into Serine

G59A – Mutation of Glycine at 59 into Alanine

G59R – Mutation of Glycine at 59 into Arginine

Gj - Junctional Conductance

Gjss – Macroscopic Steady State Junctional Conductance

Gjmax – Maximum Conductance Normalized to Utility

Gjmin – Residual Conductance at Large Values of Vj

GJB2 – Gap Junction Beta-2 Coding Domain

GJB6 – Gap Junction Beta-6 Coding Domain

H73R – Mutation of Histidine at 73 into Arginine

H_2O – Water

HEPES - 4-(2-hydroxyethyl)-1-piperazineethanesulfonic Acid

HID – Histrix-like Icthyosis Deafness Syndrome

I30N – Mutation of Isoleucine at 30 into Asparagine

Ij – Junctional Current

Ijss – Steady State Junctional Current

IP_3 – Inositol Triphosphate

k – Boltzmann Constant

K^+ - Potassium Ion

KCl – Potassium Chloride

KID – Keratitis-Ichthyosis-Deafness Syndrome

M – Molar

MΩ – MegaOhms

MB – Modified Barth's Medium

MB+ - Modified Barth's Medium with 0.8mM Calcium

MB- - Modified Barth's Medium without Additional Calcium

$MgCl_2$ - Magnesium Chloride

mg – Milligrams

ml – Milliliter

mm – Millimeter

mM – Millimolar

mM – Micromolar

mV – Millivolts

n – Number of Electron Charges

ng – Nanograms

N14K – Mutation of Asparagine at 14 into Lysine

N14Y – Mutation of Asparagine at 14 into Tyrosine

N54 – Asparagine at 54

N54K – Mutation of Asparagine at 54 into Lysine

N54H – Mutation of Asparagine at 54 into Histidine

Na^+ - Sodium Ion

NaN_3 – Sodium Azide

PBS – Phosphate Buffer Solution

PCR – Polymerase Chain Reaction

PPK – Palmoplantar Keratoderma

q – Electron Charge

R75Q – Mutation of Asparagine at 75 into Glutamine

R75W – Mutation of Asparagine at 75 into Tryptophan

S17F – Mutation of Serine at 17 into Phenylalanine

S183F – Mutation of Serine at 183 into Phenylalanine

SD – Standard Deviation

SE – Standard Error

SNHL – Sensorineural Hearing Loss

T – Absolute Temperature

TM1-4 – Transmembrane Domains 1 through 4

V0 – Transjunctional Voltage at Which Gjss=(Gjmax-Gjmin)/2

V1 – Voltage of Cell 1

V2 – Voltage of Cell 2

Vj – Transjunctional Potential

VS – Vohwinkel Syndrome

W24X – Mutation of Tryptophan at 24 into a missense mutation

Zn^{2+} - Zinc Ion

Acknowledgments

First and foremost I would like to thank my advisor Dr. Thomas White. His calm and friendly demeanor transcends lab work and radiates to all of his co-workers and students. This quality makes working in his lab a very pleasant experience that generally goes unnoticed at first, as if it's a sort of normalcy. He helps alleviate unnecessary stresses that are commonly found around many other places of work and let's you focus on science. I am forever grateful for his guidance both in my work and my life. His expertise in this field is exceptional, but my favorite characteristic is that he knows the limitations of what the data proves. While eager young graduate students may not at first grasp the proper depth of their work, Dr. White always seems to have a keen sense of how the pieces fit together. I am extremely thankful for his advisement.

I cannot thank Dr. White alone though, I must also thank the members of his lab who hold together the daily operations and long term work. Caterina and Helen are some of the most helpful and talented people I've met. My fellow students that I've shared the lab with have always been able to put a smile on my face. I have to thank Dwan, Adam, Gulistan, Teresa, Zunaira, Pallavi, Noah, Jen, Lukasz, and Daniel for helping me work, laugh, and generally enjoy the time I have spent there.

I also have to give a special thank you to Dr. Peter Brink, Dr. Richard Mathias, and Dr. Linda Musil for the time they have taken out of their busy schedules during this entire process. Their expertise in the field of connexins has been very beneficial to helping me understand many things. Dr. Musil has had the arduous task of flying in from Oregon for both my proposal and defense and I am extremely thankful for her making that sacrifice. While I graded papers for both Dr. Mathias and Dr. Brink, I think I enjoyed grading the cell physiology exams for Dr. Mathias a bit more. However, I am forever grateful to Dr. Brink for helping me find a lab to work in when I first arrived here and his advice is second to none. I often find myself trying to listen as much as possible when he offers up thoughts on science or the scientific community. Thank you to my committee for continually pushing and guiding me.

I would like to acknowledge the Department of Physiology and Biophysics. The collection of professors that represents this Department is quite exceptional. They are extremely helpful, friendly, and intelligent. I have to thank staff of the office for keeping things running smoothly. I want to give a special thank you to Melanie Bonnette for being an amazing administrator who always has everything in order. I also would like to thank the graduate students of the department for sitting through my presentations and joking around with me. It's always nice to have a group to talk with about general graduate student life.

Lastly and most importantly I want to thank my family. I specifically want to thank my mother, Frances Guichard, who has raised me to be the person I am today. She has always been the most important person in my life and I will never be able to thank her enough. I want to thank my sisters (Amber and Shannon) and father (Jack R. Lee Sr.) for always being there and helping me whenever I need it. I also want to thank Hannah, she is the person I turn to everyday. She has always been there to listen to me gripe and laugh. I am grateful for her keeping me sane and grounded. I also want to thank my close friends Travis, Jon, and Dave who have been there to talk to whenever.

Chapter 1

Introduction

Gap Junctions: Function, Structure, and Communication

A principle development that has lead to complex multicellular organisms is the role of communication between cells and organs to help respond to environmental conditions and changes. This key function helps groups of cells and entire tissues co-ordinate events such as growth regulation or responses to stimuli. Gap junctions are protein channels found throughout the body that take part in many processes which are necessary for normal physiological function [1]. They are formed by connexin (Cx) proteins which are encoded by over 20 connexin genes that are expressed throughout the body in overlapping and unique patterns [2]. Gap Junctions facilitate intracellular communication by creating a channel that connects the cytoplasm of two adjacent cells. Six connexin proteins come together to form a connexon hemichannel on the cells surface[3]. A connexon can dock with the adjacent cells hemichannel (Figure I-1) to form a complete gap junction [4]. In nonjunctional membranes hemichannels function as an ion channel

that facilitates diffusion of ions and small molecules between the cytoplasm and extracellular space [5,6]. Due to the heterogeneous expression of connexin genes, hemichannels may be formed from mixtures of connexin sub-units as either homomeric or heteromeric channels and gap junction channels may be assembled from the same connexin (homotypic), or a combination of different connexins (heterotypic) depending on the cell type (Figure I-1). This allows for a wide variety of functional hemichannels and gap junctions throughout the body with unique properties, though their ultimate function as a facilitator of communication remains mostly the same. Each connexin protein has four transmembrane domains (TM1-4), connected by two extracellular loops (EC1 and EC2) and a cytoplasmic loop (CL). The two extracellular loops are thought to play a role in docking two connexon hemichannels together to form a complete gap junction [7]. The amino and carboxy termini of the protein also extend into the cytoplasm of the cell. The amino terminus is thought to play a role in gating of some connexin proteins [8,9].

The biosynthesis of gap junctions begins in the endoplasmic reticulum (ER) where the synthesized protein is inserted into the membrane. The oligomerization of the connexon hemichannel from individual proteins occurs after synthesis in the ER as the protein becomes incorporated in the trans-golgi network [10]. While this has been shown for many connexin proteins, Cx26 proteins specifically appear to traffic from the ER to the plasma membrane in an

alternative and quicker route that bypasses the golgi network [11,12]. Presumably this would have a profound effect on the oligomerization process. Once at the plasma membrane the connexin proteins form junctional plaques [13,14], but the alternative trafficking theory was challenged and it was suggested that the only difference was in microtubule dependence and not in overall pathway differences [15]. This would resolve the previous observations but allow for a similar connexin trafficking pathways. Insertion into the plasma membrane of most cells is relatively short lived as connexin hemichannels have a quick turnover rate with a half-life of only a few hours [16,17]. Removal of the gap junction from the plasma membrane occurs via internalization of the gap junction in a double membrane structure into one of the two adjacent cells [18]. Internalized gap junctions may either be re-inserted into the membrane or targeted for normal lysosomal degradation.

Gap Junction Physiology

Mutations in connexin genes are associated with diverse hereditary human diseases [19-22]. Sensorineural hearing loss (SNHL) is the most common connexin related disease which can be either non-syndromic, or syndromic, when associated with skin disorders and other ectodermal abnormalities [23-26]. SNHL is commonly linked to mutations in the Cx26 encoding gene *GJB2* [27]. Although

mutations in Cx26 have been linked to a few rare autosomal dominant cases of non-syndromic deafness (DFNA3), autosomal recessive mutations account for the vast majority of non-syndromic hearing loss associated with *GJB2* (DFNB1) [28]. Cx26 mutations are present with a high frequency in the human population, and genetic screening for Cx26 is routine in cases of pediatric hearing impairment [29-31]. Mutations that cause non-syndromic deafness are distributed throughout the Cx26 coding region, while syndromic mutations that cause skin disease are predominantly found in the amino terminus and first extracellular domain (Figure I-2). There is ample evidence suggesting that simple loss of function mutations in Cx26 cause non-syndromic deafness, but not the syndromic forms exhibiting epidermal pathology [32-34]. Both autosomal recessive and autosomal dominant non-syndromic deafness have been associated with mutations in Cx26 [35,36]. The most frequent recessive Cx26 mutation is a single base deletion (35ΔG) that results in a frame-shift at the 12th amino acid and premature termination of the protein. Other common recessive Cx26 mutations include nonsense mutations and small deletions/insertions, most of which also lead to premature termination of protein translation [27,36]. Therefore, many of the commonly observed recessive mutations result in severely truncated connexin proteins that fail to retain any channel activity and recessive hearing loss may largely be a result of null mutations in Cx26. In contrast, the Cx26 mutations causing skin diseases and deafness are all single amino acid changes, and the mechanism(s) whereby they lead to skin

pathology are unclear. The identification of mutations in Cx26 that cause either non-syndromic hearing loss, or syndromic deafness associated with skin disease, presents an interesting paradox that arises from the observation that complete loss of Cx26 function correlates with deafness, but not skin disease. Thus, human skin does not need functional Cx26 to maintain homeostasis. Certain mutations in this gene dramatically perturb epidermal homeostasis, possibly through dominant gain of function mechanisms.

Anatomy of the Inner Ear

The transduction of the auditory impulses takes place within the cochlea of the inner ear. This organ is a long coiled like structure which houses the hair cells responsible for converting the physical pressure waves associated with sound into an electrical stimulus for the brain to process. A complex array of proteins work to carry out this conversion of the sound wave into a nerve impulse. However, Cx26 is not directly involved in the process of sound wave conversion and is not found between the hair cells and supporting cells which surround these sensory cells [32,37]. Gap junctions, including Cx26, are found in the nonsensory epithelial cells among which the hair cells are located and the connective tissue which surrounds the scala media of the cochlea [38-40].

The sensory cells (hair cells) of the inner ear are located in a series of fluid filled spaces that comprise the organ of corti within the cochlea. The basolateral surface of hair cells is bathed in a solution known as the perilymph which has a similar ionic composition to other extracellular solutions (Figure I-3). The apical surface of the hair cells contains the hair like stereocilia that project into the scala media and a solution known as the endolymph. This solution has a unique ionic concentration of high K^+ and low Na^+, which is unlike other extracellular solutions. When pressure waves pass through the scala media the force pushes over hair cells and starts the transduction process by which pressure is converted into an electrical impulse. The hair cells experience a flow of K^+ ions from the endolymph into the cell. The K^+ ions eventually are deposited from the hair cell into the interstitial space of the organ of corti [41]. There K^+ channels on the supporting epithelial cells plasma membrane uptake the ions into the cell [42]. The endolymph is continually re-supplied with K^+ ions and there are various theories about the role of connexins in shunting these ions back to the endolymph from the interstitial space in a cyclical manner.

The Role of Connexins in the Auditory Process

Although gap junctions are not found within the sensory hair cells, there are a few theories about their role in the auditory process. This is highlighted by

the manifestation of SNHL which was discussed previously. In one theory passive diffusion is used to allow K^+ ions to flow through gap junctions in supporting cells from the perilymph to the endolymph [43-45]. This theory suggest that K^+ ions are taken into the supporting cells where they flow in a gradient dependent manner from the area near the hair cells laterally toward the lower area of the spiral ligament. This allows K^+ to pass the basal cell layer of the spiral ligament via the connective tissue gap junction system and into the extracellular space near the stria vascularis (Figure I-3). Marginal cells can then recycle the K^+ ions via transporters back into the endolymph [46,47]. This would help explain how the endolymph maintains a high concentration of K^+ ions relative to the surrounding compartments without the necessity of pulling them from vascular areas. A second theory elaborates upon this idea by also including IP_3 signaling and Ca^{2+} waves that pass through cochlear gap junction networks to facilitate active diffusion of K^+ along a similar pathway back to the endolymph from the perilymph [48,49]. While both theories suggest that K^+ is shunted along the gap junction network in the cochlea from the perilymph to the endolymph, there are differences in proposed active or passive mechanisms to determine this end.

Anatomy of the Epidermis

The skin is a unique organ which is designed to facilitate many physiological functions that maintain homeostasis. The primary function is to serve as a regenerative barrier that prohibits the entrance of pathogens into the other organs of the body [50]. It also assists in thermoregulation of the body via the secretion of sweat which is evaporated to cool the body's temperature. The epidermis tightly controls this watertight barrier to simultaneously monitor interstitial osmolarity. Within the epidermis are nerve endings and mechanoreceptors associated with the sense of touch and pain receptors for temperature and other physiologically relevant sensations. All of these functions are carried out by the largest organ in the human body, and one which continually sheds the outermost layer and replenishes cells of the other layers in a tightly regulated fashion so that normal epidermal thickness can be held at optimal levels to carry out these required duties [51]. The skin is made up of the dermis and epidermis. There are four layers in the epidermis; they are the basal, spinuous, granular, and cornified layers (Figure I-4). The external layer, the cornified layer, is continually shed as humans make contact with abrasive surfaces and through normal daily function. So out of necessity the skin continually proliferates and differentiates starting at the basal layer and ending in the cornified layer. This continual state of growth aims to maintain a constant thickness that is optimal for all of the skin's functions.

The barrier of the epidermis is a finely tuned to maintain Ca^{2+} gradients which influence cell growth and differentiation [52,53]. In low levels of Ca^{2+} keratinocytes in culture proliferate rapidly, but do not differentiate. It is only after the addition of higher levels of Ca^{2+} that keratinocytes stop proliferating and begin differentiating and cornifying [52]. When wounding occurs which disrupts the established barrier, Ca^{2+} gradients dissipate and normal skin physiological function does not return until the re-establishment of the barrier function and Ca^{2+} gradients[54]. As such it is suggested that extracellular Ca^{2+} levels are an important component of normal skin proliferation and differentiation. However, Ca^{2+} does not have a constant concentration across all epidermal barriers (Figure I-5). Since it is a key component in signaling the switch from proliferating keratinocytes to differentiating ones, Ca^{2+} concentration is higher in outer layers of the skin [53,55].

The Role of Connexins in the Epidermis

Gap junctions have been discovered between the cells of all but the cornified layers [56,57], and dye-transfer experiments have been used to show gap junctional coupling between keratinocytes of the three inner most layers of the epidermis [58,59]. These dye transfer studies discovered that within the epidermis there were clusters of 20-25 cells that were gap junctionally connected, but discrete from other clusters in the surrounding areas and lead to the postulation

that gap junctions played an integral role in keratinocyte growth and differentiation [58].

The epidermis contains a large variety of connexin types which display overlapping spatial and temporal patterns throughout the differentiation of keratinocytes prior to being incorporated into the cornified layer. There are at least 9 different connexin proteins found within the skin which show these varied patterns of expression [22,60,61]. Cx26 protein expression is typically confined to the lower layers of the epidermis (the basal and spinuous layers) and not commonly found in the upper spinuous or granular layer [62]. The suggestion that gap junctions are involved in synchronous growth in the skin [58] is reinforced by the numerous skin pathologies associated with connexins such as Cx26, Cx30, Cx30.3, Cx31, and Cx43 [24]. In several experiments a large up regulation of Cx26 (greater than that of other connexins) in all layers except the cornified layer and hyperproliferation was observed after wounding of human skin [63,64]. It was also observed that down regulation of Cx26 is necessary for the proper formation of the skin barrier, excessive Cx26 expression kept wounded skin in a state of hyperproliferation, and Cx26 induced ATP release which promoted an inflammatory response [65]. The role of Cx26 in the skin still is not well understood. While wounding and barrier dysfunction up regulates the protein's expression, it is down regulation that is necessary for barrier acquisition after wounding. The hyperproliferative growth associated with Cx26 up regulation

may play an integral role in the preliminary stages of wound healing. Indeed the lowered extracellular Ca^{2+} associated with barrier disruption may trigger the immune response properties of Cx26, and lead to hyperproliferation. Mutations which result in extremely early truncation of the protein during the translation process such as 35ΔG, result in short peptide sequences which cannot form functional channels [27,36]. These mutations do not result in skin complications, only deafness. Thus normal physiology of the skin does not seem to require Cx26 specific function. Either the function is redundant and carried out by one of the numerous other connexins within the epidermis or it is completely unnecessary. In either case, mutations in Cx26 can result in severe skin pathologies which must be related to a gain of some function in Cx26 that disturbs homeostasis. It is worth noting that Cx26 may have the function of passing ATP, among other ions and small metabolites, in the inner ear theory involved in IP_3 signaling and in the epidermis in immune responses [65,66].

Non-Syndromic Deafness

Naturally occurring mutations in connexins can cause a variety of disease, and Cx26 related mutations typically result in one of two forms of deafness. Non-syndromic deafness is defined as hearing loss in the absence of any other clinical complication. Mutations that cause this disorder are mostly recessive, but in a

few cases they've been found to be dominant. Mutations in other connexins can cause non-syndromic or syndromic deafness, but up to 50% of genetic non-syndromic hearing loss is caused by mutations in the *GJB2* gene which codes for the Cx26 protein [35,67-70]. These mutations are found at amino acid residues scattered through the entire Cx26 protein (Figure I-6). In determining how the mutations in the *GJB2* gene produce this pathology there are several very informative changes which can be examined. A handful of very commonly occurring changes in the *GJB2* gene produce severely truncated proteins from nonsense mutations or deletions producing frame shifts [71].

The most common mutation in Cx26 is the 35ΔG frame shift which causes a stop codon and results in a 13 amino acid long peptide that does not insert into the membrane. This does not produce a functional channel protein [28]. In some studies the mutation was found in a high percentage of Italian (88%), Spanish (55%), and Greek (54%) subjects who reported hearing impairment [72,73]. A similar mutation, W24X, also creates a severely truncated protein. It is found in a high percentage of recessive deafness alleles in the Spanish Romani gypsy population (79%), sensorineural deafness patients in India (5-33%), and deafness alleles in the European Romani population (23-93%) [74-77]. Similar results can be found in other truncation mutations such as 167ΔT and 235ΔC in various other populations [71,78-81].

In many populations the leading causes of non-syndromic deafness are mutations that lead to a severe truncation of Cx26. This suggests that mere removal of the functional channel is enough to cause deafness and can be described as loss of function mutations. These recessive modifications phenocopy homozygous knockout of Cx26, resulting in deafness from a complete loss of Cx26 function [28]. In the inner ear there are several different connexins which are expressed in overlapping patterns [40,43,82-88]. This suggests that the other connexins cannot compensate and take over the role Cx26 typically carries in the inner ear. It follows that Cx26 related non-syndromic deafness results from loss of function mutations.

Syndromic Deafness

The second form of deafness that is associated with connexin proteins is syndromic deafness, which is characterized by hearing loss in addition to other observable phenotypes. Mutations in Cx26 specifically can cause syndromic deafness that display hearing loss in addition to skin disorders and ecotodermal dysfunction [23-26]. As opposed to non-syndromic hearing loss, the mutations in Cx26 that cause syndromic hearing loss are all autosomal dominant mutations and found primarily in the amino terminal or 1st extracellular domain and can be seen near the pore of the protein structure (Figure I-6). These mutations can cause a

variety of skin complications ranging from mild to severe and are identified as Vohwinkel syndrome (VS), Bart-Pumphrey syndrome (BPS), palmoplantar keratoderma (PPK), Keratitis-ichthyosis-deafness syndrome (KID), and histrix-like ichthyosis deafness syndrome (HID) depending on their clinical complications (Table I-1). While non-syndromic mutations can be related to loss of function changes which create severely truncated proteins, the patients with these conditions by definition have no skin complications. Thus, simple loss of function cannot be associated with syndromic deafness related mutations in Cx26. Instead these dominant mutations must result in some unknown gain of function which manifests as the resulting skin complication.

To better analyze these various syndromic deafness sub-types it, each class was analyzed for similarities and differences. It was noted that VS, BPS, and PPK all had complications that were confined to the epidermis of the hands and feet (Table I-1). Also striking was that the mutation G59S was clinically diagnosed as causing both VS and BPS, and other mutations at the G59 amino acid residue also resulted in PPK. You can observe similar cross listings for the N54 residue. These similarities seem to place VS, BPS, and PPK into a single sub-group that are responsible for a distinct set of observed complications.

Mutations causing KID and HID however, displayed hyperkeratosis and ichthyosis which was found throughout the body. There has been only one

described condition of HID, but the mutation associated with it (D50N) is a commonly occurring mutation that is overwhelming diagnosed as causing KID. Again, this seems to suggest that KID and HID are really one broad sub-group of syndromic deafness complications. KID syndrome typically presents with mild to severe sensorineural hearing loss associated with keratitis, loss of eyebrows/eyelashes, ichthyosis and an increased susceptibility to mucocutaneous infections [89-91]. Similar to the deafness degrees, keratitis typically is mild to severe and bilateral, but can lead to complete blindness [92]. The mucocutaneous infections which are sometimes found in patients with KID can be traced back to a complete breakdown of the skin barrier and can at times be associated with severe carcinomas [89,93,94]. The phenotype associated with KID syndrome is more severe than that observed in the syndromic deafness diseases of the VS, BPS, and PPK class. There are nearly a dozen known mutations which can cause KID syndrome: G11E, G12R, N14K, N14Y, S17F, I30N, A40V, G45E, D50A, D50N, D50Y, and A88V [36,92,93,95-105]. The mutations are found primarily in the amino terminal through the 1st extracellular loop (Figure I-2) and can be seen near the pore of the channel as opposed to the protein's surface (Figure I-6). A few of these mutations had previously been tested for certain properties (Table I-2), but there had not been a common cause which was indicated in the channels function and the ultimate gain of function causing the disease remained mostly unknown.

Hypothesis and Aims

It has become apparent that Cx26 plays a distinct role in development of skin diseases in patients who suffer from syndromic deafness. This observation makes it clear that non-syndromic mutations are distinctly different from syndromic mutations, and that different mutations result in different protein functions. The purpose of this dissertation will be to elucidate the differences that must occur in the mutated Cx26 proteins in patients with syndromic deafness due to KID syndrome as opposed to the mere loss of function associated with non-syndromic deafness. **We hypothesize that mutations associated with KID syndrome cause a gain of function which disturbs the natural homeostasis of the skin.** There are three aims associated with this hypothesis and proposal. First, we will examine several Cx26 mutations associated with KID syndrome and test whether there are any detectable differences in channel function. Second, we will then determine the differences between Cx26 mutations for KID syndrome that occur at the same residues. Lastly, we will examine the effects of connexon channel blockers to determine if there is any influence upon the activity we observe from the mutations described.

Specific Aim 1: **Determine the channel activity of Cx26 mutations G12R, N14K, S17F, and D50N.**

Preliminary data for KID mutations suggested that the altered proteins may form aberrant hemichannel activity as well as altered gap junction activity [98,106]. We hypothesize that mutations associated with KID syndrome result in altered hemichannel and gap junction activity that disrupts normal physiological function in the epidermis. We will test this hypothesis by injecting wild-type and mutant Cx26 RNA into *Xenopus* oocytes and then record hemichannel as well as gap junctional conductances in response to voltage steps. We will then look at protein expression levels to determine if there are any changes to the amount of protein found within cells.

Specific Aim 2: Compare different mutations associated with KID in Cx26 occurring at the same amino acid residues and determine trafficking patterns for KID mutations.

At both the 14th and 50th amino acid residues of Cx26 there are multiple mutations resulting in KID syndrome. We hypothesize that in addition to altered hemichannel activity found in mutations at these residues there may be altered protein trafficking within the cell which causes further complications. To test this hypothesis we will first record hemichannel and gap junction currents from *Xenopus* ooctyes expressing RNA encoding the mutations N14K, N14Y, D50N, and D50Y in Cx26. We will then transfected cell lines with the same mutated

DNA sequences and use cell markers to determine where the mutated proteins localize. We will also co-stain HeLa cells to observe cellular markers of the early endosome, golgi apparatus, and endoplasmic reticulum to determine where connexin protein is located within the cell.

Specific Aim 3: Test the effects of channel blockers on Cx26 mutations associated with KID syndrome.

Preliminary data suggested that KID syndrome mutations found in Cx26 proteins produce variable channel activity. However, it is also known that Cx26 wild-type channel activity is not necessary for normal epidermal homeostasis. We hypothesize that channel blockers may help alleviate some of the altered channel activity associated with KID syndrome and may lead to a potential therapeutic strategy to treat syndromic mutations. To test this hypothesis we will inject *Xenopus* ooctyes with RNA of Cx26 for wild-type and KID syndrome associated mutations. We will then record hemichannel currents in the presence and absence of blockers to determine the effect on the aberrant hemichannel activity from mutations in Cx26 that cause KID syndrome. We will test several molecules suspected to block Cx26 channel activity to help determine if developed blockers can be used in therapeutic ranges.

Figure Legends and Figures:

Figure I-1: Connexin channel formation.

Diagram shows how connexons (hemichannels) form at cell membranes and the terminology used to describe the different types of combinations. Connexin proteins assemble into hemichannels (connexons) and intercellular channels (gap junctions). Connexons may be homomeric or heteromeric, and gap junction channels may be homotypic or heterotypic [107].

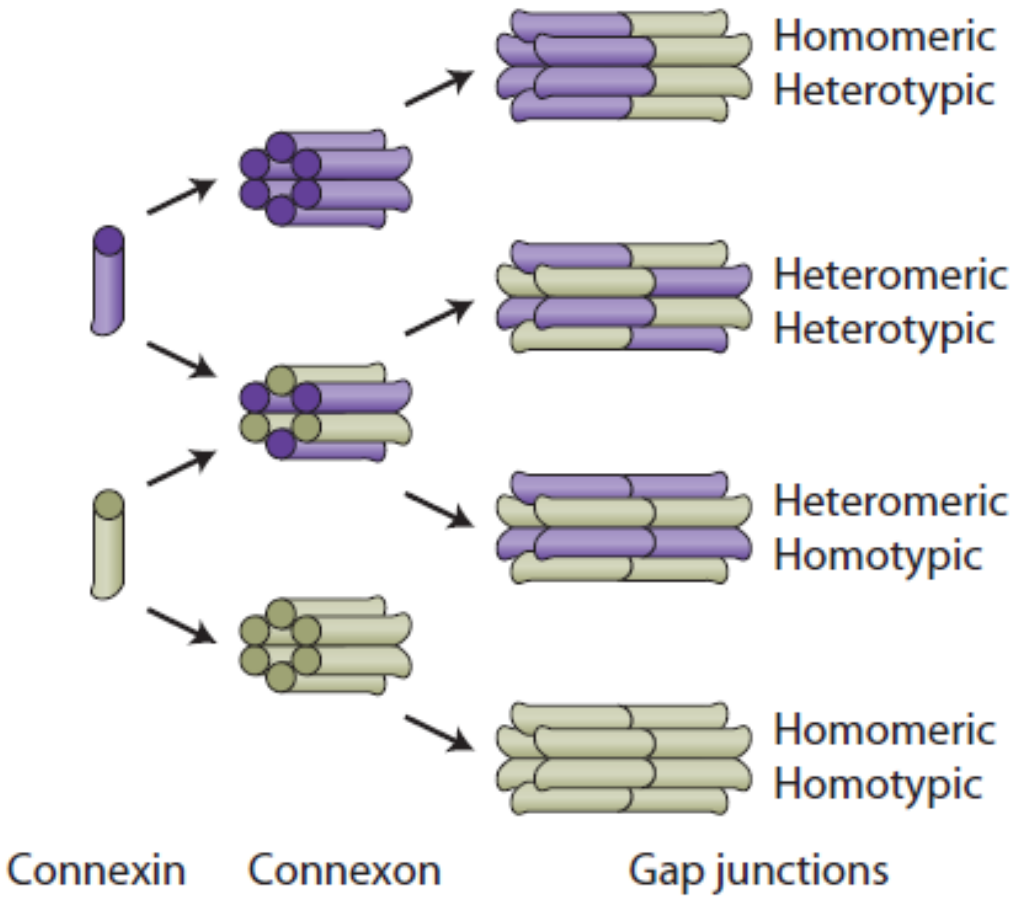

Connexin channel formation

Figure I-2: Connexin26 Topology and Mutated Residues

This illustration displays the location of amino acid residues in Cx26 relative to the membrane. Purple residues are not mutated. Blue amino acids are mutated residues found in nonsyndromic deafness and can be seen throughout the protein. Brown residues represent amino acids mutated in syndromic deafness, which are generally found within the N-terminus and first extracellular loop [107].

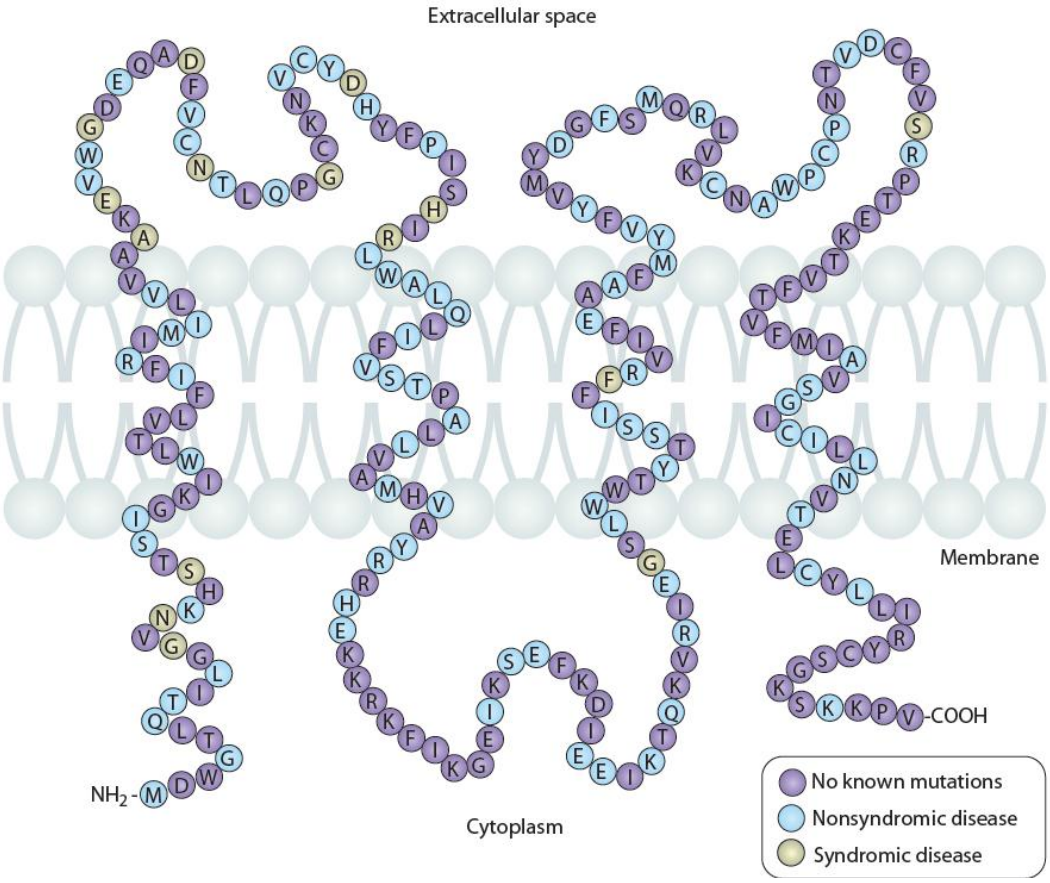
Extracellular space
Membrane
Cytoplasm
NH2 -M
-COOH
No known mutations
Nonsyndromic disease
Syndromic disease

Figure I-3: Structure and Function of the Organ of Corti.

Hair cells are show with their stereocilia bathing in the endolymph of the scala media and their basal surfaces near the perilymph where they rest on the Basilar membrane. This diagram displays the theoretical flow of K^+ ions from the outer hair cells, through the gap junction network and back to the endolymph where they originated [45].

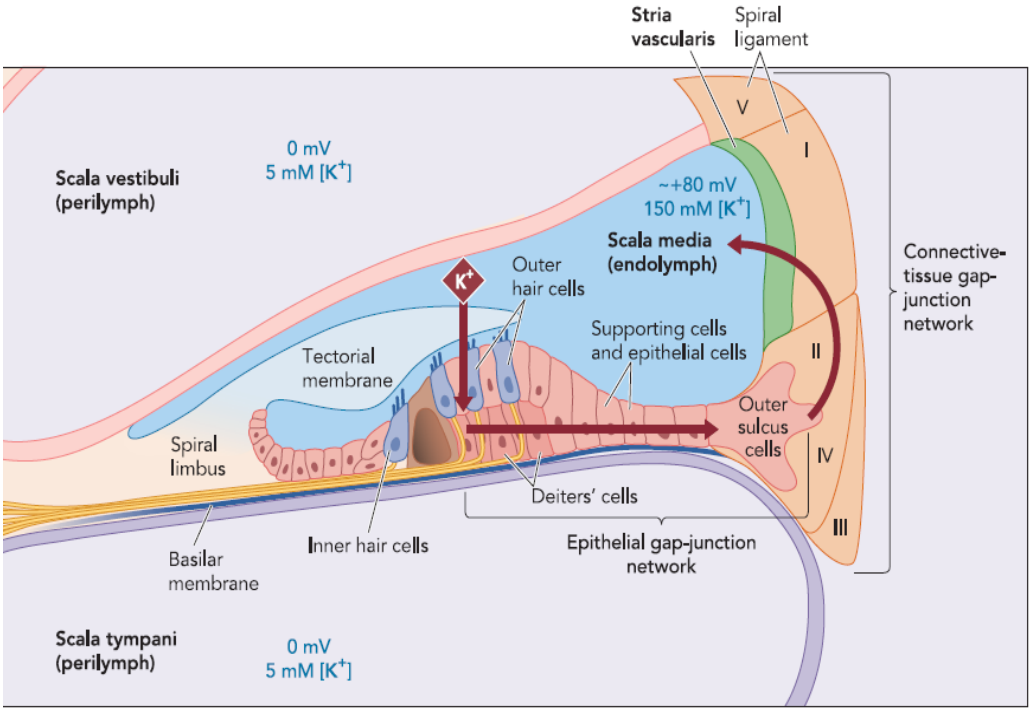
Stria vascularis
Spiral ligament
V
I
0 mV
5 mM [K+]
Scala vestibuli (perilymph)
~+80 mV
150 mM [K+]
Scala media (endolymph)
K+
Outer hair cells
Supporting cells and epithelial cells
Connective-tissue gap-junction network
Tectorial membrane
II
Outer sulcus cells
Spiral limbus
IV
Deiters' cells
III
Basilar membrane
Inner hair cells
Epithelial gap-junction network
Scala tympani (perilymph)
0 mV
5 mM [K+]

Figure I-4: Layers of the Epidermis.

This diagram is a schematic representation of the skin. The epidermis rests on the dermis and contains four layers called the stratum basale, stratum spinosum, stratum granulosum, and stratum corneum. The cornified outer layer known as the stratum corneum contains keratinocytes which have become corneocytes while the rest of the 3 layers contain proliferating and differentiating keratinocytes. The desmosomes are markers of differentiation which begins to occur when proliferating cells from the startum basale migrate towards the higher calcium environment of the upper layers of the epidermis [108].

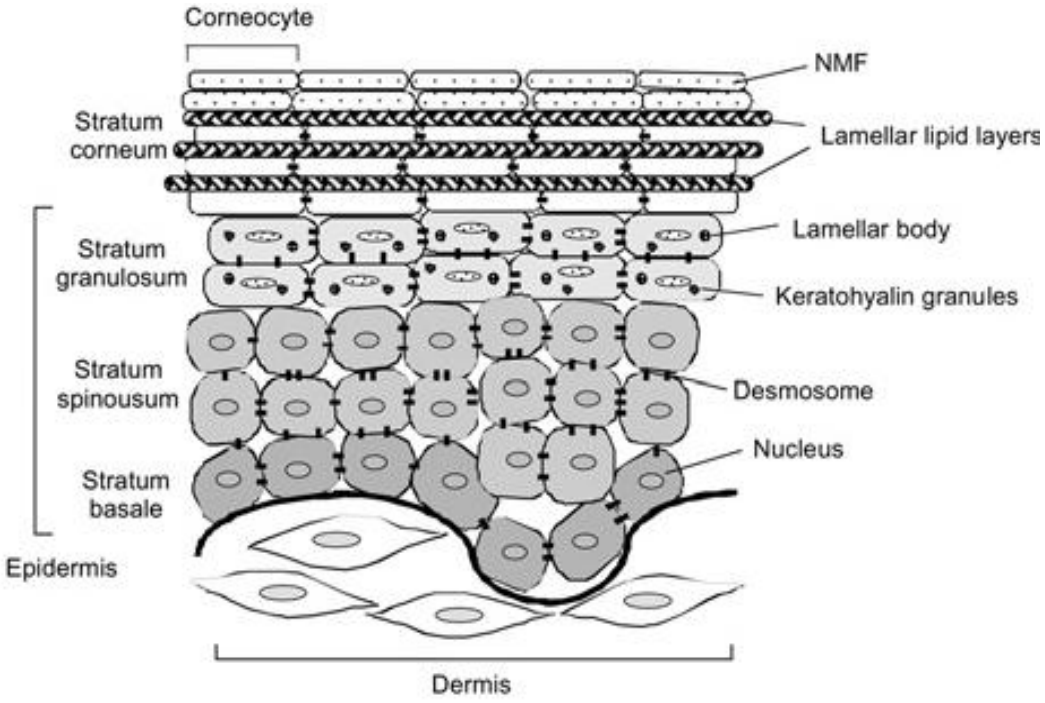
Corneocyte
NMF
Stratum corneum
Lamellar lipid layers
Lamellar body
Stratum granulosum
Keratohyalin granules
Stratum spinousum
Desmosome
Nucleus
Stratum basale
Epidermis
Dermis

Figure I-5: Distributions of Different Ions in the Skin.

This graph shows the amounts of ions found at different depths of the epidermis. Ca20 is the level of Ca^{2+}, Zn30 is the level of Zn^{2+}, and Fe26 is the level of Fe^{2+}. The Dermis is noted. Germ. is the stratum basale, Spin. is the stratum spinosum, Gran. is the stratum granulosum, and Corn. is the stratum corneum. Ca^{2+} levels increase from the basal layer as you approach the surface of the epidermis [55].

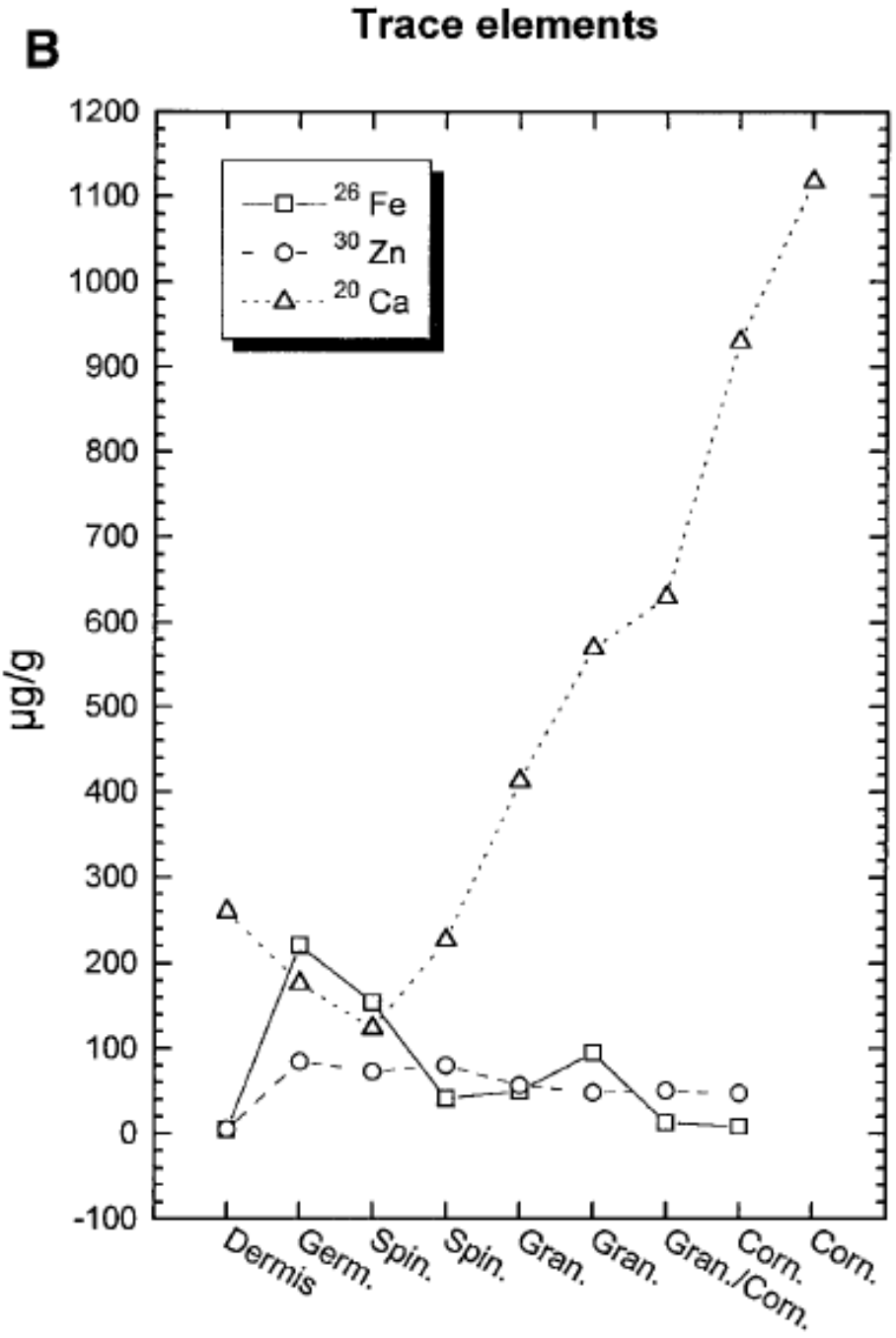
B
Trace elements
µg/g
1200
1100
1000
900
800
700
600
500
400
300
200
100
0
-100
26 Fe
30 Zn
20 Ca
Dermis
Germ.
Spin.
Spin.
Gran.
Gran.
Gran./Corn.
Corn.
Corn.

Figure I-6: Three Dimensional Structure of Connexin26.

Syndromic and nonsyndromic mutations mapped onto the reported crystal structure of Cx26 [109]. Red residues are reported syndromic mutations, green residues are known nonsyndromic mutations, and blue residues are not reported to have a mutation. (a) Side view of a Cx26 hemichannel with six protein subunits. The structure has the extracellular portion of the protein at the top of the diagram and the cytoplasmic segment at the bottom. (b) Cut away side view of a Cx26 hemichannel with three protein subunits removed allowing a view of residues lining the pore domain. (c) View from the extracellular surface of the complete hemichannel looking down onto the protein and into the cell through the pore domain. (d) View from the cytoplasmic surface of the complete hemichannel looking out of the cell through the pore domain [107].

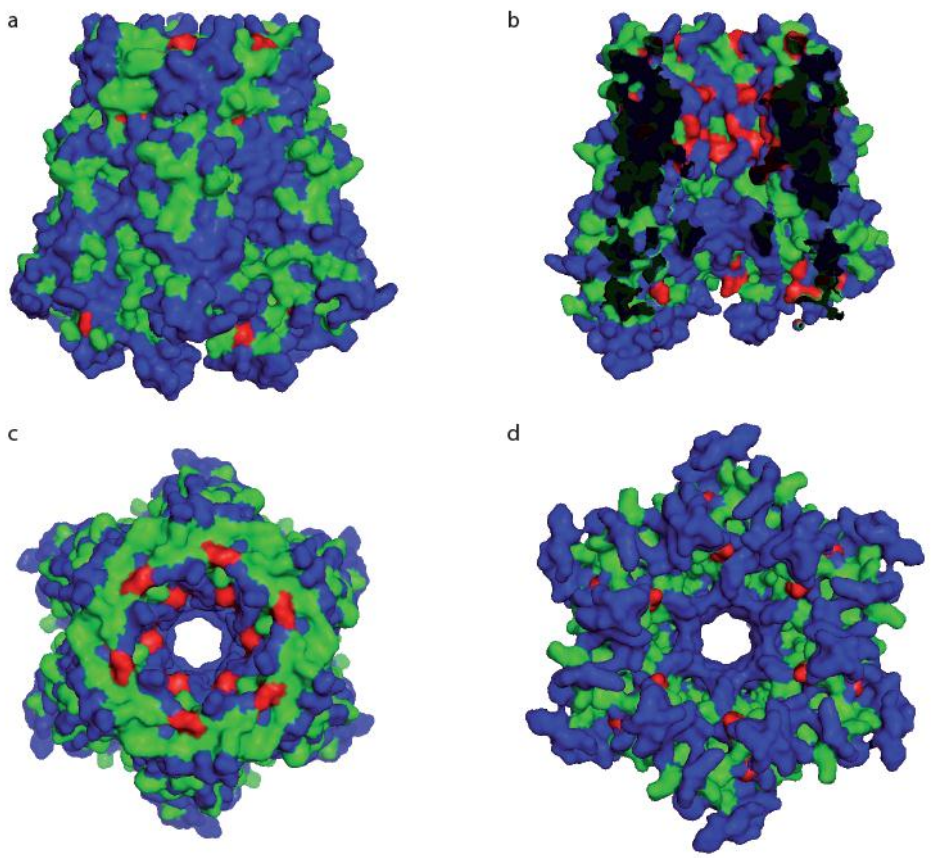
a
b
c
d

Table I-1. Connexin26 Syndromic Deafness Disorders.

The different syndromic deafness disorders associated with Cx26 and the mutations associated with each disorder. The typical characteristics of each disorder are listed [107].

Cx26 Syndromic Deafness Disorders			
Syndrome	**Mutations**	**Features**	**References**
Vohwinkel's Syndrome	G59S, D66H, G130V	Hyperkeratosis, Constriction Bands, Deafness	[110-112] [113] [114] [115] [116] [117]
Bart-Pumphrey Syndrome	N54K, G59S	Hyperkeratosis, Knuckle Pads, Leukonychia, Deafness	[118] [119] [120] [121]
PPK	Del42E, N54H, G59A, G59R, H73R, R75Q, R75W, G130V, S183F	Palmoplantar Hyperkeratosis, Deafness	[122] [123] [35] [124] [125] [126] [62] [127] [128] [129] [130]
Keratitis-Ichthyosis-Deafness Syndrome	G12R, N14K, N14Y, S17F, A40V, G45E, D50N, D50Y	Hyperkeratosis, Keratitis, Ichthyosis, Mucocutaneous Infection, Deafness	[89] [90] [91] [131] [89] [93] [94] [93] [95] [96] [97] [98] [92] [99] [36] [100] [101]
Histrix-like Ichthyosis Deafness syndrome	D50N	Hyperkeratosis (spiky), Ichthyosis (cobblestone appearance), Deafness	[132] [133] [134] [95]
Undetermined	F142L	Deafness, Erythematous patches and Scaly Plaques	[135]

		on the scalp, Calcinosis Cutis in the heels.	

Table I-2. Know Syndromic Mutations in *GJB2*.

A list of known syndromic mutations in Cx26, their associated syndrome, and many of the tested parameters. Abbreviations: BPS, Bart–Pumphrey syndrome; HID, hystrix-like icthyosis deafness syndrome; KID, keratitis–ichthyosis-deafness syndrome; PPK, palmoplantar keratoderma; VS, Vohwinkel syndrome [107].

Mutation	Syndrome	Trafficking to Plasma Membrane	Gap Junction Channels	Hemi-channels	Dominant Inhibition	Reference
G12R	KID	Yes	No	Yes	-	[107] [93]
N14K	KID	Yes	Yes	Yes	-	[107]
N14Y	KID	-	No?	-	-	[100]
S17F	KID	Yes	No	No	-	[107] [93]
A40V	KID	Yes	-	Yes	-	[98] [106]
DeltaE42	PPK	Yes	No	-	26, 37, 43	[62] [136]
G45E	KID	Yes	Yes	Yes	-	[106]
D50N	KID/HID	Yes	No	Yes	-	[107]
D50Y	KID	-	-	-	-	N/A
N54K	BPS	-	-	-	-	N/A
N54H	PPK	-	-	-	-	N/A
G59A	PPK	No	No	-	26, 30, 32, 43	[137] [136] [137]
G59R	PPK	-	-	-	-	
G59S	VS/BPS	-	-	-	-	
D66H	VS	No	No	-	26, 43	[62] [137] [136] [138]

H73R	PPK	No	-	-	26	129
R75Q	PPK	Yes	No	-	26	139
R75W	PPK	Yes	No	Yes	26, 30, 43	128 62 137 138 140 136 141
G130V	PPK/VS	-	-	-	-	
F142L	unclassified	-	-	-	-	
S183F	PPK	-	-	-	-	

Chapter II

Channel activity of Cx26 mutations G12R, N14K, S17F, and D50N which are known to cause KID syndrome

Abstract:

Mutations in the *GJB2* gene-encoding connexin 26 (Cx26) have been linked to skin disorders and genetic deafness. However, the severity and type of the skin disorders caused by Cx26 mutations are heterogeneous. Here we explored the effect of Cx26 KID syndrome-associated mutations, G12R, N14K, S17F, and D50N on channel function. The proteins were all expressed in *Xenopus* oocytes with levels equal to wild-type Cx26. Single *Xenopus* oocytes were tested for hemichannel currents and paired oocytes were tested for junctional conductances. The G12R, N14K, and D50N mutations resulted in larger hemichannel currents than the wild-type-expressing cells, but the S17F mutation resulted in a complete loss of hemichannel activity. Functional gap junctions were only produced by paired N14K cells, which had a similar conductance level to wild type, even though they exhibited a complete loss of voltage sensitivity. This set of data confirms that aberrant hemichannel activity is a common feature of most Cx26 mutations associated with KID syndrome, and this may contribute to a loss of cell viability and tissue integrity.

Introduction

Syndromic mutations in Cx26 are associated with a variety of skin disorders such as Vohwinkel syndrome, Bart– Pumphrey syndrome, palmoplantar keratoderma, or keratitis (and hystrix-like) ichthyosis deafness syndrome (KID/HID) and always present with autosomal dominant inheritance [23,24,26,96] The lack of associated skin disorders in cases of non-syndromic SNHL shows that the function and development of the epidermis is not affected by the simple loss of Cx26 function as in the case of homozygous 35ΔG patients. Thus, the Cx26 mutations that can cause syndromic deafness associated with skin disease must show some type of alteration of function, but the mechanisms whereby Cx26 mutation leads to pathological changes in the epidermis remain to be elucidated. Historically, the formation of complete gap junction channels was thought to be the primary function of connexin subunits, although recently non-junctional hemichannels have been speculated to play a role in cellular homeostasis under different physiological conditions [6,142]. As hemichannels may contribute to normal cell function, disease causing connexin mutations could also mediate their effects through alteration of hemichannel activity. Analysis of connexin mutations causing syndromic SNHL associated with skin disease has supported this idea. Examples include the A40V and G45E mutations of Cx26, both of which cause severe forms of KID syndrome, producing neonatal fatality in the case of G45E

[36,92,98]. Both of these mutations displayed aberrant hemichannel activity leading to cell death *in vitro*, and constitutively active hemichannels was suggested to be the cause of the resultant epidermal pathology [98,99,106]. These observations suggested that abnormal hemichannel activity may be a general feature of Cx26 mutations associated with KID/HID disorders. Four additional Cx26 mutations G12R, N14K, S17F, and D50N have also been linked to cases of KID/HID syndrome [93,95-97]. All patients exhibited SNHL symptoms, but the accompanying skin disorders varied in both clinical features and severity. KID/HID disorders cover a broad clinical spectrum, although several subtypes can be distinguished based on prevailing clinical features [97]. However, there is not yet sufficient data to establish clear genotype–phenotype correlations, or to associate specific reported Cx26 mutations with distinct subtypes. The functional properties of G12R, N14K, S17F, and D50N were characterized using an *in vitro* expression assay comprised of cRNA-injected *Xenopus* oocytes. All four mutations displayed significantly different membrane currents than wild-type Cx26. Two of the mutations, G12R and D50N, produced large hemichannel currents that increased with cell depolarization and failed to induce any gap junctional conductance between paired cells. N14K also showed abnormal hemichannel activity that was activated at positive voltages, in addition to producing robust junctional conductance in cell pairs. The voltage-gating sensitivity of junctions formed by N14K channels was greatly reduced compared to wild-type Cx26. The results for the final mutation

tested, S17F, differed from both the other mutations and wild-type Cx26. S17F expression induced neither hemichannel currents nor gap-junctional conductance. When cultured in solutions with higher extracellular Ca^{2+} concentrations, all three of the hemichannel forming mutations had reduced levels of activity and increased cell survival. Three of the four KID mutations tested demonstrated significantly increased hemichannel activity compared to the wild-type protein. Taken together with the aforementioned G45E and A40V mutations, increased hemichannel activity appears to be a common feature among most *GJB2* mutations responsible for KID/HID syndrome.

Materials and Methods

Molecular cloning

Human wild-type Cx26 was cloned into the BamHI restriction site of the pCS2+ expression vector for functional studies in *Xenopus* laevis oocytes [62]. DNA primers (Table S1) with BamHI restriction sites (Integrated DNA Technologies, Inc., Coralville, IA) were designed to generate the G12R, N14K, S17F, and D50N mutations by standard PCR mutagenesis [106,143]. The G12R-, N14K-, and S17F-specific sense primers were paired with a Cx26 wild-type antisense primer and amplified by PCR with conditions of 95°C for 4 minutes, followed by 25 cycles of 94°C for 30 seconds, 60°C for 30 seconds, 72°C for 45 seconds, and 72°C for 2 minutes. The D50N mutation was created by the overlap extension method [144], using D50N-specific primers in conjunction with Cx26 sense and antisense primers. PCR products were gel purified using the QIAquik gel extraction kit (Qiagen, Valencia, CA), digested with BamHI and cloned into pBlueScript (Stratagene, La Jolla, CA), and sequenced on both strands (GeneWiz North Brunswick, NJ). Mutants with the correct sequence were subcloned into the pCS2+ vector [145].

In vitro transcription, oocyte microinjection, and pairing

Use of frogs was approved by the Institutional Animal Care and Use Committee. Human Cx26, G12R, N14K, S17F, and D50N were linearized using the NotI restriction site of pCS2+, and transcribed using the SP6 mMessage mMachine (Ambion, Austin, TX). Adult *Xenopus* females were anesthetized with ethyl-3-aminobenzoate methanesulfonate, and ovarian lobes were surgically removed and digested for 1.5 hours in a solution containing 50 $mgml^{-1}$ collagenase B, and $50mgml^{-1}$ hyaluronidase in MB without Ca^{2+}. Stages V–VI oocytes were collected and injected first with 10 ng of antisense *Xenopus* Cx38 oligonucleotide to eliminate endogenous connexins [9,146]. Antisense oligonucleotide-treated oocytes were then injected with wild-type Cx26, G12R, N14K, S17F, and D50N cRNA transcripts (5 ng per cell), or H_2O as a negative control. cRNA-injected oocytes were then cultured in Ca^{2+}-free MB, or MB with elevated Ca^{2+} (4mM $CaCl_2$) and cultured until ready for electrophysiological recording or image capture. For measurements of gap junctional conductance, the vitelline envelopes were removed in a hypertonic solution (200mM aspartic acid, 10mM HEPES, 1mM $MgCl_2$, 10mM EGTA, and 20mM KCl at pH 7.4), and the oocytes were manually paired with the vegetal poles apposed in MB with elevated Ca^{2+}.

Electrophysiological hemichannel current recordings

At 8–12 hours after cRNA injection, macroscopic recordings of hemichannel currents were recorded from single *Xenopus* oocytes using a GeneClamp 500

amplifier controlled by a PC-compatible computer through a Digidata 1320 interface (Axon Instruments, Foster City, CA). pClamp 8.0 software (Axon Instruments) was used to program stimulus and data collection paradigms. To obtain hemichannel I–V curves, cells were initially clamped at -40mV and subjected to 5 seconds depolarizing voltage steps ranging from -30 to +60mV in 10mV increments. To test the effect of extracellular Ca^{2+} on hemichannel currents, oocytes were switched between MB media without Ca^{2+} , or MB supplemented with elevated Ca^{2+} (1, 2, and 4mM $CaCl_2$) via a perfusion system that washed 25 ml of solution through the 35mm dish before recording. Cells were allowed to rest in the new solution for 2–5 minutes before recording.

Dual whole-cell voltage clamp

Gap junctional coupling between oocyte pairs was measured using the dual whole-cell voltage clamp technique [147]. Current and voltage electrodes (1.2mm diameter, omega dot; Glass Company of America, Millville, NJ) were pulled to a resistance of 1–2MΩ with a horizontal puller (Narishige, Tokyo, Japan) and filled with solution containing 3M KCl, 10mM EGTA, and 10mM HEPES, pH 7.4. Dual voltage clamp experiments were performed using the same amplifier, data acquisition interface, computer, and software used for hemichannel current recordings. For measurements of junctional conductance, both cells in a pair were

initially clamped at -40mV to eliminate any transjunctional potential. One cell was then subjected to alternating pulses of ±20 mV, whereas the current produced by the change in voltage was recorded in the second cell. The current delivered to the second cell was equal in magnitude to the junctional current, and the junctional conductance was calculated by dividing the measured current by the voltage difference, Gj=Ij/(V1-V2). To determine voltage-gating properties, transjunctional potentials (Vj) of opposite polarity were generated by hyperpolarizing or depolarizing one cell in 20mV steps (range, ±120 mV) while clamping the second cell at -40 mV. Currents were measured at the end of the voltage pulse, at which time they approached steady state (Ijss). Macroscopic conductance (Gjss) was calculated by dividing Ijss by Vj, normalized to the values determined at ±20 mV, and plotted against Vj. Data describing the relationship of Gjss as a function of Vj were analyzed using Origin 6.1 (Microcal Software, Northampton, MA) and fit to a Boltzmann relation of the form: Gjss=(Gjmax-Gjmin)/ 1+exp(A(Vj-V0))=Gjmin, where Gjss is the steady-state junctional conductance, Gjmax (normalized to unity) is the maximum conductance, Gjmin is the residual conductance at large values of Vj, and V0 is the transjunctional voltage at which Gjss=(Gjmax-Gjmin)/2. The constant A=nq/kT represents the voltage sensitivity in terms of gating charge as the equivalent number (n) of electron charges (q) moving through the membrane, k is the Boltzmann constant, and T is the absolute temperature.

Preparation of oocyte samples for western blot analysis and quantification

Oocytes used for electrophysiological recording were collected in 2ml tubes and frozen at -80°C. Oocytes were homogenized in 1ml of buffer containing 5mM Tris, pH 8.0, 5mM EDTA and protease inhibitors using a series of mechanical passages through needles of diminishing caliber (20, 22, 26 gauge). Extracts were centrifuged at 1,000 g at 4°C for 5 min. The supernatant was then centrifuged at 100,000 g at 4°C for 30 min. Membrane pellets were resuspended in SDS sample buffer (1 ml per oocyte), samples were separated on 15% SDS gels and transferred to nitrocellulose membranes. Blots were blocked with 5% BSA in 1x phosphatebuffered saline with 0.02% NaN_3 for 1 hour and probed with a polyclonal Cx26 antibody, at a 1:500 dilution (Zymed Laboratories, San Francisco, CA), followed by incubation with alkaline-phosphatase conjugated anti-rabbit secondary antibody (Jackson ImmunoResearch Laboratories, West Grove, PA). Band intensities were quantified using Kodak 1D Image Analysis software (Eastman Kodak, Rochester, NY). Values from three independent experiments were normalized to the mean value of band intensity of the wild-type Cx26 sample.

Results

Gap junction hemichannel currents in single *Xenopus* oocytes The *GJB2* mutations G12R, N14K, S17F, and D50N are the result of single amino-acid substitutions in the N-terminus and first extracellular loop of Cx26 and are associated with KID/HID syndrome. To assess the functionality of these mutations, wild type, G12R, N14K, S17F, and D50N-Cx26 proteins were expressed in *Xenopus* oocytes. Single cells were subjected to depolarizing voltage pulses and membrane currents were recorded (Figure II-1). Oocytes injected with H_2O showed negligible current flow for voltages from -30 to +60 mV. The hemichannel activity of wild-type Cx26-injected cells was previously reported and was characterized by outward currents that increased with greater depolarization [106,148,149]. Three of the KID mutants, G12R, N14K, and D50N, all showed a significant increase in this outward current when compared to the either H_2O or Cx26 injected cells. This increased membrane current is associated with a reduction in cell membrane resistance and suggests the presence of hemichannels. Conversely, the S17F mutant showed a reduction in membrane current when compared to Cx26-injected cells, and S17F-injected cells were similar to H_2O injected negative control cells. This suggested that G12R, N14K, and D50N mutants induced aberrant hemichannel activity, whereas S17F mutants completely eliminated normal hemichannel activity. Mean steady-state currents were plotted as a function of membrane potential to quantify the hemichannel currents (Figure

II-2). Control cells injected with H_2O showed negligible currents at all tested voltages. Wild-type Cx26-injected cells displayed larger outward currents than H_2O-injected cells that increased at greater depolarizing voltages. At the highest voltage tested, wild-type cells showed a maximum current more than 17 times greater than the control cells (+60 mV, $p<0.05$, Student's t-test). The G12R-, N14K-, and D50N-expressing cells produced large outward currents at all voltages tested. At +60 mV, these three mutations exhibited currents that were approximately three times larger than wild type and more than 40 times larger than control cells, differences that were statistically significant ($p<0.05$, one-way analysis of variance). This change represents a difference in membrane conductance associated with each mutation that could be attributed to increased hemichannel activity. Conversely, expression of the S17F mutation in cells caused a significant reduction of current compared to wild-type cells and closely mimicked control cells across all voltages. The introduction of this mutation can be attributed to a reduction in hemichannel activity at increased membrane potentials. The hemichannel currents recorded from cells expressing the four KID-associated mutations were dramatically different from the wild-type currents. This could have been due to changes in relative quantities of the protein that was produced by the cell or due to a change in activity of the hemichannel. To draw a distinction between these two possibilities, we quantified the amount of protein expressed in the *Xenopus* oocytes by western blot analysis (Figure II-3).

The band density for each mutation mimicked that of the wild-type expression, with an intensity normalized to wild-type of close to 1 for all mutations. This showed that the alterations in current in the hemichannels were not the result of a change in total connexin protein levels.

Gap junctions in paired *Xenopus* oocytes

The rescue of cells expressing G12R, N14K, and D50N proteins by elevated Ca^{2+} allowed us to test whether any of our mutations created fully functional intercellular channels using dual whole-cell voltage clamp in paired oocytes (Figure II-4). Cells injected with the cRNAs for G12R, N14K, S17F, D50N, or wild-type Cx26 were incubated and paired in 4mM Ca^{2+}. Water-injected cells were used as a negative control. Cell pairs expressing wild-type Cx26 proteins showed junctional conductances that were 12-fold higher than those for control pairs. Oocyte pairs for G12R, S17F, and D50N showed conductances that were significantly lower than wild-type pairs ($p<0.05$) and were tantamount to control pairs. This suggested the lack of properly functioning gap junctions for these mutations. It has previously been shown by dye transfer assay that S17F showed no gap junctional coupling [93]. Curiously, pairs of N14K-expressing cells showed a junctional conductance that was significantly higher than negative controls ($p<0.05$) and indistinguishable from wild-type values. The formation of gap

junction channels by N14K allowed for analysis of the voltage gating properties. Oocyte pairs expressing N14K showed an apparent loss of the voltage gating seen in their wild-type counterparts. A common feature of wild type Cx26 traces was the asymmetric nature of decay at higher voltages that was not seen in N14K cell pairs (Figure II-5 a and b). The steady-state conductance values were normalized, plotted against transjunctional voltage, and fit to a Boltzmann equation (Figure II-5 c). The complete loss of voltage gating can clearly be seen by the linearity of the N14K data that has a value of unity at all voltages tested and a slope near zero. This apparent difference can be attributed to the N14K mutation and may be part of observed variation in KID phenotype for individuals with this mutation.

Discussion

The appearance of KID syndrome is marked by syndromic deafness and associated skin diseases. Mutations causing non-syndromic deafness are found throughout the *GJB2* protein, but KID syndrome variants are restricted to the N-terminus and first extracellular loop. It was previously shown that the KID mutations G45E and A40V resulted in increased hemichannel activity [98,106]. The increased hemichannel currents caused cell death that could be blocked through the addition of extracellular Ca^{2+}. In this study, we examined the behavior of four additional *GJB2* mutations associated with SNHL and skin disorders. The G12R,

N14K, and D50N mutations led to increased hemichannel activity and cell death. The S17F mutation produced a distinct loss of hemichannel activity altogether, with no cellular lethality observed in oocytes. The cell death phenotype of G12R, N14K, and D50N could be rescued through the addition of extracellular Ca^{2+}. These findings are consistent with previous studies describing hemichannel activity associated with Cx26 and suggest a common characteristic among the KID-associated mutations [98,99,106]. The most commonly occurring KID mutation analyzed in this paper is D50N. Reported cases display profound SNHL, photophobia, keratitis, and associated skin disorders [93,94,97]. The recorded properties of D50N and G12R agreed with the theory that KID mutations displayed aberrant hemichannel activity and both mutations failed to induce electrical coupling between paired cells. The cellular death observed in these cases could be rescued by introduction of Ca^{2+} to the extracellular media during incubation. However, the main difference between the two mutations was an apparent change in their sensitivity to the concentration of Ca^{2+}. Hemichannel activity in D50N was less responsive to changes in the extracellular concentration. The response of G12R was quicker and more complete. Both cell populations could be rescued from cell death, but they showed a different reaction to extracellular Ca^{2+} levels. The reduction of D50N currents was smaller than G12R; however, D50N also had a lower magnitude of hemichannel activity in 0mM Ca^{2+}. Elevation of external Ca^{2+} reduces the amplitude of hemichannel currents by

shifting the voltage activation curve to more positive potentials [150], such that the mutations with larger hemichannel activity (G12R and N14K) may reflect different activation voltages and experience a larger reduction in current. The underlying cause remains unknown, but may be attributed to the location of the mutations relative to the membrane. The G12R and N14K mutations are bathed in the intracellular solution and D50N is found on the first extracellular loop. The reported case of N14K was found to have SNHL similar to all of the other mutations reported [96]. However, the patient bearing this mutation was described as having a phenotype more similar to Clouston syndrome (caused by mutations in *GJB6*) than KID syndrome due to the lack of keratitis and overall mild-associated skin conditions. These observations were consistent with our functional data. The mutant channels led to cell death and elevated hemichannel activity similar to other KID-associate mutations in addition to the formation of complete gap junctions with a conductance similar to wild-type channels. The difference between N14K channels and Cx26 wild-type gap junctions was the complete loss of voltage-dependent gating. The N terminus has been shown to be crucial for voltage-gating properties of channels [8,9]. It was also reported that the N-terminus of Cx26 has a region of flexibility around the first 12–14 amino-acid residues that is important to cellular function [100]. The loss of voltage gating seen for N14K also suggests that this residue plays a key role in voltage gating. Although several KID mutations have shown no electrical coupling between cells, G45E cells were

coupled and the resulting channels demonstrated an increase in voltage sensitivity [106]. This suggests that KID mutations that form gap junction channels have reduced conductance at modest transjunctional potentials. The relative loss of conductance compared to wild type could be another property shared by KID mutations. The lack of voltage sensitivity seen by N14K cells may be responsible for causing a phenotype closer to Clouston syndrome by producing conductances across all transjunctional voltages. One of the most severe phenotypes observed in patients was due to S17F mutation. It has been reported that this condition lead to SNHL, visual impairment, and in one case lethal carcinoma of the tongue [93,97]. Oddly enough, this mutation also had a different phenotype in our results, displaying a complete lack of both gap junctional coupling and hemichannel activity. It was similar to negative controls in both experimental recordings. It was also reported that S17F showed a complete lack of coupling in HeLa cells via a dye transfer assay with caboxyfluorescein [93]. This was consistent with our observations that demonstrated the inability of S17F mutant channels to couple cells. These data suggest that S17F may operate by an alternative method of function previously not classified. After classification of the functional activity of the four mutations analyzed in this paper, we concluded that aberrant hemichannel activity is a common feature among KID associated mutations. It has been shown that Cx26 is important in keratinocyte growth and differentiation [151]. There seems to be a distinct pathology for syndromic hearing loss and skin-associated

disorders. As was displayed with the N14K mutation, a combination of effects can be caused by the dual activity of Cx26 as both an intercellular channel and a hemichannel interacting with the extracellular solution. With the data from G12R, N14K, S17F, A40V, G45E, and D50N mutations of Cx26, one can conclude that the altered hemichannel activity of these mutants is important in cell signaling [106]. The mutation of G11R in Cx30 was also reported to produce hemichannel activity and leads to cell death [152]. This group also showed the association of A88V with induced cell death in *Xenopus* oocytes. Aberrant hemichannel activity and cell death are common features of Cx26 and Cx30 mutations associated with KID syndrome and other epidermal disorders; however, the precise mechanism whereby this may contribute to a loss of cell viability and tissue integrity remains to be elucidated.

Figures and Figure Legends:

Figure II-1. Hemichannel currents recorded from *Xenopus* oocytes.

Cells were held at a potential of -40mV and then membrane currents were recorded at pulses between -30 and +60mV in 10mV steps. (a) H_2O-injected cells displayed small currents at all potentials. Cells injected with Cx26 (b), G12R (c), N14K (d), and D50N (f) displayed hemichannel currents with different magnitudes. S17F cells (e) had a negligible current at all voltages recorded.

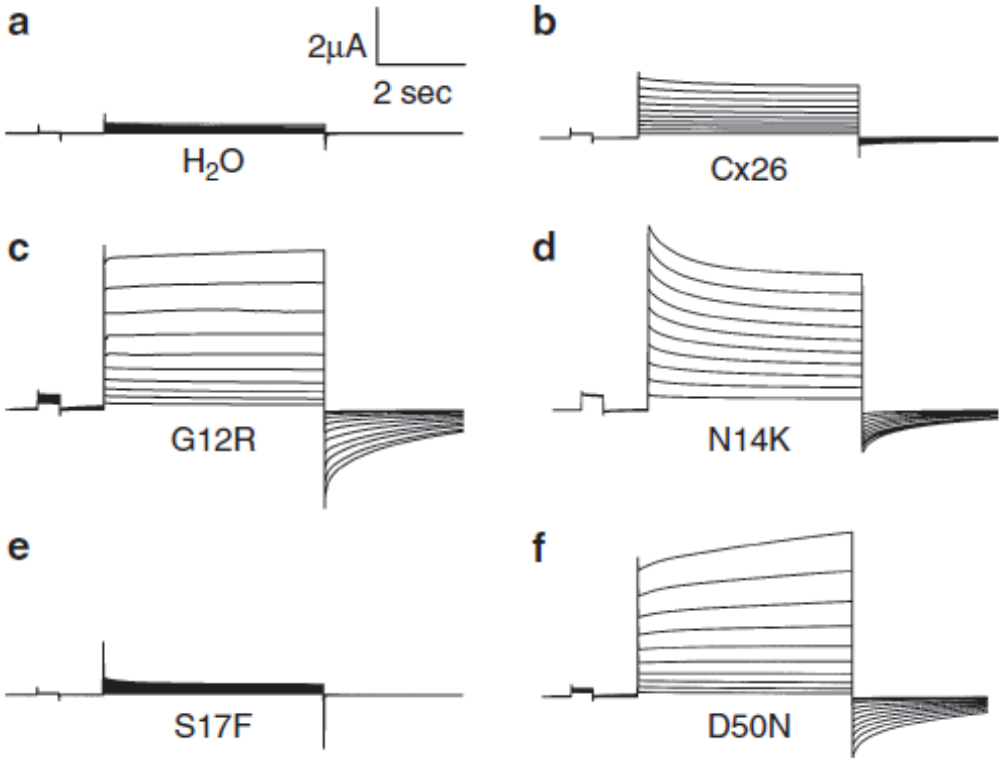
a
2μA
2 sec
H2O
b
Cx26
c
G12R
d
N14K
e
S17F
f
D50N

Figure II-2. Current-voltage relationship of the wild-type and mutant hemichannels.

Cells expressing each mutation were plotted along with H_2O (n=10, open upside down triangle) and Cx26 (n=8, filled diamond)-injected cells to give a comparison of hemichannel activity. H_2O-injected cells displayed negligible currents at all voltages tested. Cells injected with (a) G12R (n=7, open circle), (b) N14K (n=9, open square), and (d) D50N (n=12, open triangle) all had currents that were similar to Cx26 at lower voltages but became dramatically larger than Cx26 at increasingly positive potentials. Oocytes injected with (c) S17F (n=11, open sideways triangle) were similar to H_2Oinjected cells and displayed a relative lack of current at all voltages tested.

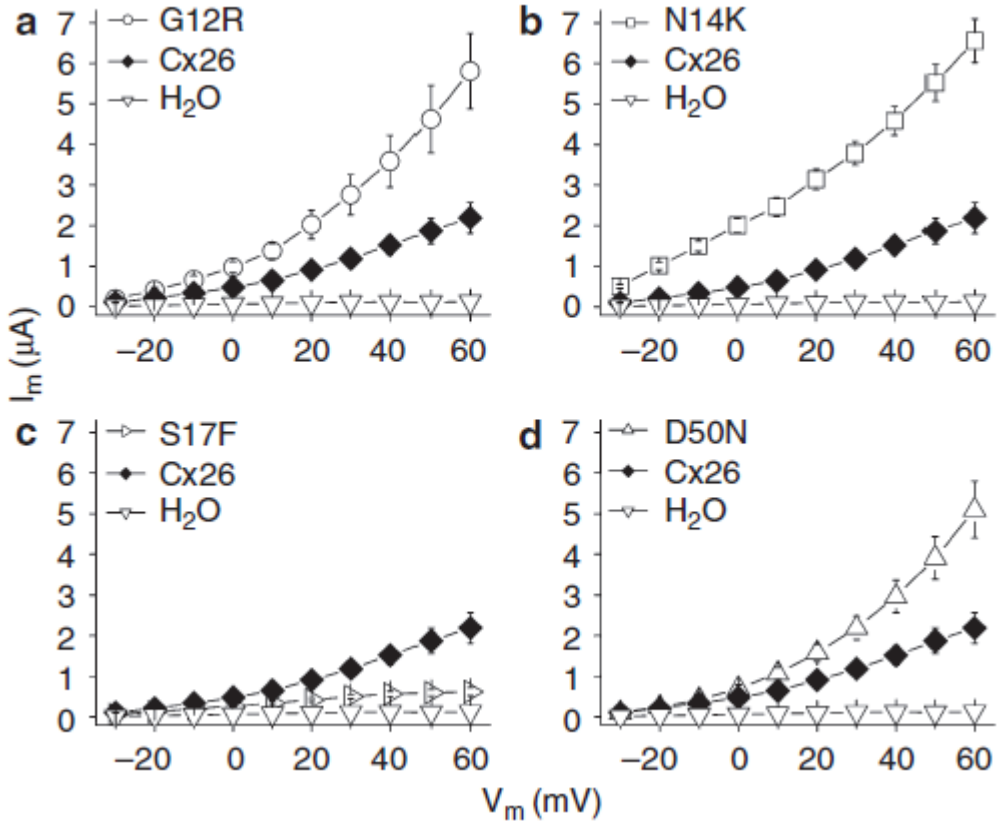
a
G12R
Cx26
H2O
b
N14K
Cx26
H2O
c
S17F
Cx26
H2O
d
D50N
Cx26
H2O
Im (μA)
Vm (mV)
0
1
2
3
4
5
6
7
–20
0
20
40
60

Figure II-3. Western blot analysis of protein content from *Xenopus* oocytes.

The expression level of each mutation (G12R, N14K, S17F, and D50N) was similar to Cx26. (a) Membrane extracts were obtained from an equal number of cells and stained with Cx26 antibodies. H_2O-injected cells were used as a negative control. Cx26, G12R, N14K, S17F, and D50N were seen in their corresponding lanes and in relatively equal amounts. (b) The expression levels were tested via densitometry (n=3) and were found to be equal for all mutations and wild type ($p<0.05$). Data are means±SE.

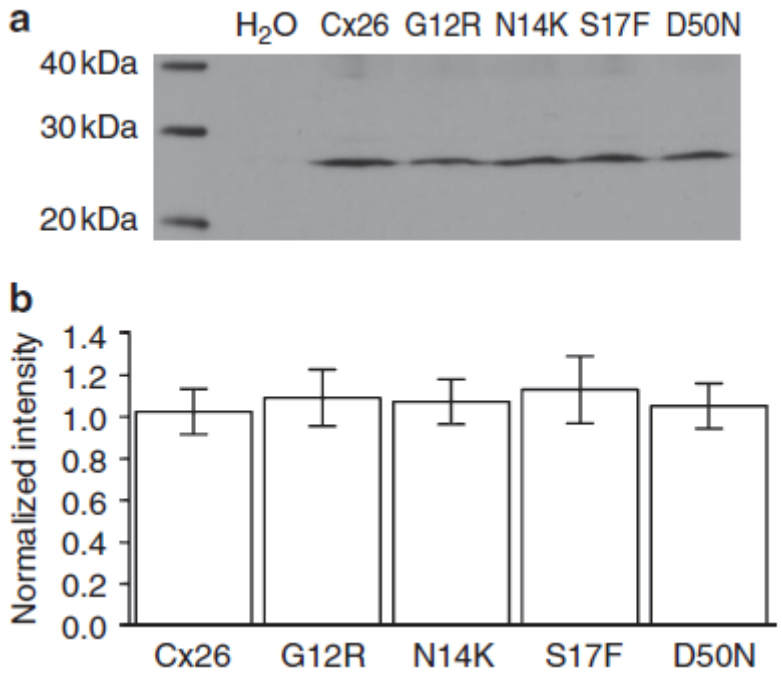
a
H2O Cx26 G12R N14K S17F D50N
40 kDa
30 kDa
20 kDa
b
Normalized intensity
1.4
1.2
1.0
0.8
0.6
0.4
0.2
0.0
Cx26
G12R
N14K
S17F
D50N

Figure II-4. Comparison of junctional conductances recorded from paired *Xenopus* oocytes via dual whole-cell voltage clamp.

Pairs of cells expressing Cx26 (n=43), D50N (n=17), G12R (n=12), N14K (n=19), S17F (n=22), and H_2O (n=41) were clamped and held at -40 mV. One cell of the pair was subjected to a voltage pulse whereas the other cell was held constant. The junctional current between cells was recorded and divided by the voltage step to calculate junctional conductance. N14K was the only expressed mutation with a conductance greater than that of H_2O cells. Oocytes with Cx26 and N14K produced a similar junctional conductance. Data are means±SE.

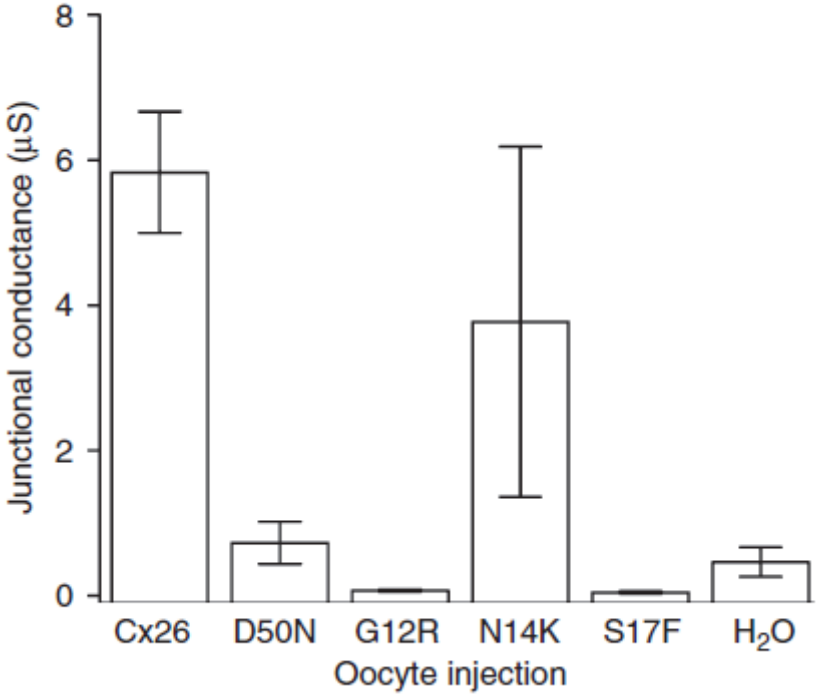
Junctional conductance (μS)
8
6
4
2
0
Cx26
D50N
G12R
N14K
S17F
H2O
Oocyte injection

Figure II-5. Properties of Cx26 and N14K intercellular junctions.

(a) Cx26 gap junctions displayed an asymmetric decay in junctional current at transjunctional potentials ±100 mV. (b) Gap junctions from pairs of N14Kexpressing cells showed a complete loss of voltage sensitivity. (c) When normalized junctional conductance was plotted against transjunctional potential, the slope of the line produced by N14K pairs was zero. The Cx26 gap-junctional data could be fit to a Boltzmann equation.

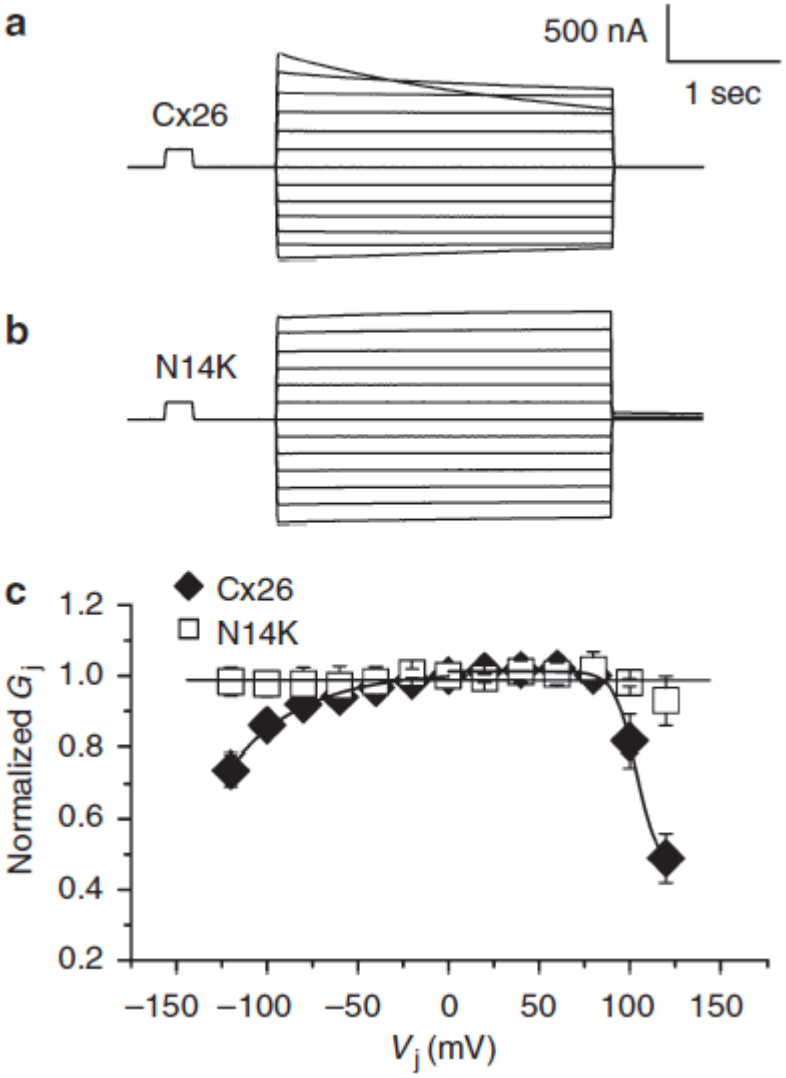
a
500 nA
1 sec
Cx26
b
N14K
c
Cx26
N14K
Normalized G_j
1.2
1.0
0.8
0.6
0.4
0.2
–150
–100
–50
0
50
100
150
V_j (mV)

Chapter III

Comparison of channel activity for different mutations associated with KID syndrome in Cx26 which occur at the same amino acid residues and trafficking patterns for these mutations

Abstract:

KID syndrome causing mutations in *GJB2* had been linked to aberrant hemichannel activity. While the majority increased hemichannel activity, one of the tested mutations (S17F) caused a decrease in that activity. To further examine what role hemichannels had in KID syndrome, we decided to test a pair of naturally occurring KID-causing mutations at the same residue. Luckily there are two residues in Cx26 which have multiple single amino acid substitutions which cause KID syndrome (N14 and D50). Here we tested N14K against N14Y and D50N against D50Y to determine what differences might exist between similar positioned substitutions with the same phenotype. The proteins were expressed in *Xenopus* ooctyes. We tested single cells for hemichannel currents and paired cells for gap junctional conductance. The previous data for N14K and D50N were confirmed and both caused a larger aberrant hemichannel, but the N14Y and D50Y mutations displayed significant reductions in the hemichannel currents that

brought them down to 0 (similar to previously tested S17F). To determine if these difference were the result of a possible trafficking defect which completely removed the hemichannel capabilities of the wild-type channel we transfected the 4 mutations into cultured cells and stained with antibodies for Cx26 as well as for antibodies for proteins localized to the early endosome (EEA1), the golgi (Golgin 97), and endoplasmic reticulum (ERp72). We then analyzed the mutations and found that the mutations which complete loss of hemichannel currents appeared to not transport to the surface in typical fashion and were stuck in the perinuclear region. However, mutations which caused an increase in hemichannel activity appeared to transport rather diffusely throughout the cell but did not make gap junctional plaques similar to like what the wild-type protein did. These data raise the prospect that there may be two distinct pathways by which KID mutations create the same phenotype. One pathway would be mediated by connexin hemichannel currents, while the other would be the result of trafficking defects.

Introduction:

Connexin proteins are found expressed throughout the body and have been implicated in many different types of disease. Their function is primarily as a channel between two adjacent cells. It had previously been suggested that connexin hemichannels could function in non-junctional plaques [6,142]. This would

allow connexins to operate as single ion channels (hemichannels) in contact with the extracellular solution. Other findings showed that hemichannel activity that differed from wild-type due to mutations in Cx26 could be related to the progressions of disease like KID syndrome [98,99,106,107]. While simple loss of Cx26 function can cause non-syndromic deafness [28], it has been suggested that the aforementioned aberrant hemichannel activity therefore could account for clinical complications that arise in syndromic deafness. The deafness portion of this disease would presumably be due to a loss of function within the inner ear, but the resulting skin complications could arise due to a gain of function associated with this hemichannel activity.

Mutations in the *GJB2* gene that encodes the Cx26 protein have been found to cause both syndromic and non-syndromic deafness. Further analysis of mutations related to the syndromic deafness disease KID syndrome [98,99,106 2009] analyzed how each mutation could affect channel activity compared to wild-type. These studies suggested that cell death as a result of hemichannel activity or trafficking defects could be responsible for the manifestation of the disease phenotype in the skin. It was recently discovered that the D50 and N14 amino acid residues could be mutated to several other amino acids and each mutation still resulted in KID syndrome (N14K/N14Y and D50N/D50Y/D50A). Across each of these mutations the channel still had the same gain of function that caused the skin complications for KID syndrome. We analyzed these mutations in the

Cx26 protein to see if they had similar changes in function and trafficking. Gap junction conductances recorded from paired oocytes for N14K previously showed similar levels as wild-type cells, while D50N injected pairs failed to produce such coupling. Cells injected with N14Y or D50Y did not produce coupled cells with any level of conductance and were well below wild-type injected cells. While N14K and D50N were previously characterized as having aberrantly large hemichannel related single cell currents, when N14Y or D50N were expressed in *Xenopus* oocytes they displayed no currents across many tested voltage ranges. These were identical to currents recorded for negative control cells injected with H_20 and differed greatly from wild-type Cx26 injected positive controls. It seemed that while mutations occurring at the same residue could cause the same disease, they may use different pathways to create the associated phenotype.

We next tested to determine if there were any trafficking differences between Cx26 wild-type proteins and the proteins of the 4 KID related mutations (N14K, N14Y, D50N, and D50Y). We transfected cultured HeLa cells with cDNA for each condition and used Immunocytochemistry techniques to stain for Cx26 protein antibodies in addition to early endosome (EEA1), golgi apparatus (Golgin 97), and endoplasmic reticulum (ERp72) antibodies to help analyze the location of any clustering which may occur related to the protein. Cells transfected with wild-type Cx26 cDNA showed typical gap junctions at interfaces between adjacent cells suggesting most of the protein incorporated into the

membrane and created gap junction plaques. Cells transfected with N14K or D50N cDNA displayed altered trafficking and did not display robust gap junction plaques like wild-type. They were found rather spread out around the cell in what appeared to be cell membrane clusters. Cells transfected with N14Y or D50Y also did not result in gap junction plaques at interfaces between cells, but also appeared different from N14K and D50N cells. The N14Y and D50Y cells had perinuclear protein expression in several robust dots that seemed to be close to many cellular organelles. This suggests that maybe the N14Y and D50Y proteins do not traffic to the membrane, but instead become stuck within the cell. These findings support the idea that mutations linked to KID syndrome have altered channel function compared to wild-type Cx26 protein. Also, there seems to be 2 different gain of functions which can lead to the skin complications in KID syndrome, large aberrant hemichannel activity and a protein trafficking defect.

Materials and Methods

Molecular cloning

The BamHI restriction site of the pCS2+ vector was used to incorporate human wild-type Cx26 for functional studies in *Xenopus* laevis oocytes [62]. DNA primers with BamHI restriction sites (Integrated DNA Technologies, Inc. Coralville, IA)

were created to produce the N14K, N14Y, D50N, and D50Y mutations by standard PCR mutagenesis [106,143]. The N14K primer was 5'- ACG TGG ATC CAT GGA TTG GGG CAC GCT GCA GAC GAT CCT GGG GGG TGT GAA GAA ACA CTC CAC C -3', the N14Y primer was 5'- ACG TGG ATC CAT GGA TTG GGG CAC GCT GCA GAC GAT CCT GGG GGG TGT GTA CAA ACA CTC CAC C -3', the D50N sense and anti-sense primers were 5'-GAT GAG CAG GCC AAC TTT GTC TGC AAC-3' and 5'-GTT GCA GAC AAA GTT GGC CTG CTC ATC-3', and the D50Y sense and anti-sense primers were 5'-GAT GAG CAG GCC TAC TTT GTC TGC AAC- 3' and 5' – GTT GCA GAC AAA GTA GGC CTG CTC ATC – 3'. Cx26 wild-type antisense primer 5'-TGT TGT GGA TCC TTA AAC TGG CTT TTT TGA CTT CCC AG-3' were paired with the N14K and N14Y specific sense primers and amplified via polymerase chain reaction (PCR) with settings of 95°C for 4 minutes, followed by 25 cycles of 94°C for 30s, 60°C for 30s, 72°C for 45s, and 72°C for 2 minutes. Using D50N and D50Y specific primers in conjunction with a Cx26 (sense) 5'-TGT TGT GGA TCC ATG GAT TGG GGC ACG CTG CAG ACG-3' and Cx26 antisense primer, the D50N and D50Y sequences were produced by the overlap extension method [144]. PCR products were gel purified using the QIAquik gel extraction kit (QIAGEN, Valencia, CA), digested with BamHI and cloned into pBlueScript (Stratagene, La Jolla, CA) and sequenced on both strands (GeneWiz

North Brunswick, NJ). Mutants with the correct sequence were subcloned into the pCS2+ vector [145].

In vitro transcription, oocyte microinjection, and pairing

Human Cx26, N14K, N14Y, D50N and D50Y were linearized using the NotI restriction site of pCS2+, and transcribed using the SP6 mMessage mMachine (Ambion, Austin, TX). Adult *Xenopus* females were anesthetized with ethyl 3-aminobenzoate methanesulfonate and ovarian lobes were surgically removed and digested for 15 mins while being incubated at 37°C in a solution containing 50mgml^{-1} collagenase B, and 50mgml^{-1} hyaluronidase in modified Barth's medium (MB) without Ca^{2+}. Stage V-VI oocytes were collected and injected first with 10ng of antisense *Xenopus* Cx38 oligonucleotide to eliminate endogenous connexins [9,146]. The treated oocytes were then injected with wild-type Cx26, N14K, N14Y, D50N and D50Y cRNA transcripts (5ng/cell), or H_2O as a negative control. Injected oocytes were then cultured in MB with elevated Ca^{2+} (4 mM $CaCl_2$) until ready for electrophysiological recording. The vitelline envelopes were removed in a hypertonic solution (200mM aspartic acid, 10mM HEPES, 1mM $MgCl_2$, 10mM EGTA, and 20mM KCl at pH 7.4) for measurements of gap junctional conductance, and the oocytes were manually paired with the vegetal poles apposed in MB with elevated Ca^{2+}.

Electrophysiological hemichannel current recordings

Macroscopic recordings of hemichannel currents were recorded from single *Xenopus* oocytes 10-12 hours after cRNA injection using a GeneClamp 500 amplifier controlled by a PC-compatible computer through a Digidata 1320 interface (Axon Instruments, Foster City, CA). pClamp 8.0 software (Axon Instruments) was employed to program stimulus and data collection paradigms. To acquire hemichannel I-V curves, cells clamped at -40mV were subjected to 5 second depolarizing voltage steps ranging from -30 to +60mV in 10mV increments.

Dual whole-cell voltage clamp

Oocyte pairs were measured for gap junctional coupling using the dual whole-cell voltage clamp technique [147]. Current and voltage electrodes (1.2mm diameter, omega dot; Glass Company of America, Millville, NJ) were pulled to a resistance of 1-2MΩ with a horizontal puller (Narishige, Tokyo, Japan) and filled with solution containing 3M KCl, 10mM EGTA, and 10mM HEPES, pH 7.4. Dual voltage clamp experiments were performed using the same amplifier, data acquisition interface, computer, and software used for hemichannel current

recordings. Both cells in a pair were initially clamped at -40mV to eliminate any transjunctional potential. To measure junctional conductance, one cell was then subjected to alternating pulses of ±20mV, while the current produced by the change in voltage was recorded in the second cell. The current delivered to the second cell was equal in magnitude to the junctional current, and the junctional conductance was calculated by dividing the measured current by the voltage difference, Gj = Ij/(V1-V2).

Cell Culture

HeLa cells were transiently transfected with the cDNAs for wild-type, N14K, N14Y, D50N or D50Y Cx26 in the pCS2+ vector. The cDNAs were transfected into the cells using Lipofectamine 2000 reagent (Invitrogen, Carlsbad, CA) according to the protocol provided by the manufacturer. HeLa cells were plated on coverslips 2 days prior to transfection so that they would be 50-60% confluent on the day of transfection. DNA (4ng) and Lipofectamine 2000 (2ul) were placed into separate tubes and mixed with 100ul of OPTI-MEM medium (GIBCO) at room temperature. After 15 mins the solutions were combined and incubated for 20 mins. The mixture was added onto the plated HeLa cells in fresh media slowly via pipette. The cells were cultured for 24 h at 37°C and 5% CO_2.

Immunocytochemistry

Transfected HeLa cells were fixed in a solution containing Methanol and Acetone at a 1:1 ratio and pre-cooled to -20°C. The cells were bathed in the solution at -20°C for 10 mins and then removed and blocked by placing them in a solution of 3% BSA in PBS with 0.1% Tween20 for 45 min. Cx26 mouse monoclonal or rabbit polyclonal antibodies at a dilution of 1:1000 were mixed with either anti-Early Endosome (EEA1) rabbit polyclonal or anti-Golgi (58k) mouse monoclonal antibodies (Abcam) at 1:250 dilution and applied to the coverslips to be incubated overnight at 4°C. The following day the coverslips were washed and then incubated at 37°C for 1h with the secondary antibody. To keep the Cx26 signal the same color, CY3-conjugated AffiniPure goat anti-mouse was mixed with CY2-conjugated AffiniPure goat anti-rabbit for cells with the golgi primary antibody and CY3-conjugated goat anti-rabbit was mixed with CY2-conjugated goat anti-mouse for cells with the early endosome primary antibody. The coverslips were washed again and then mounted with using Vectashield with DAPI (Vector Laboratories, Burlingame, CA). Protein expression was monitored using an Olympus BX51 microscope (Olympus America, Center Valley, PA) and photographed with a MagnaFire digital camera (Optronics, Goleta, CA).

Results

Connexin Hemichannels in *Xenopus* Oocytes

Aberrant hemichannel activity has been suggested to be linked with causing KID syndrome in patients who have dominant single amino acid substitutions in Cx26. Here we examined multiple mutations that occurred at either the Asparagine 14 (N14) or Aspartic Acid 50 (D50) amino acid in the protein to determine if there was a difference between the hemichannel function of single substitutions at the same residue. To test this, wild-type, N14K, N14Y, D50N and D50Y-Cx26 proteins were expressed in *Xenopus* oocytes. Single oocytes were clamped at depolarizing voltage steps from -30 to +60 mV in order to observe changes in whole-cell current associated with the mutated protein. Membrane currents were recorded from the cells (Figure III-1) and showed that wild-type Cx26 injected cells had outward currents that increased with increasing positive depolarization as has been previously reported [106,148,149]. Cells expressing N14K or D50N mutant protein had a significant increase in current compared to wild-type and negative controls similar to what we previously reported [107], but cells expressing N14Y or D50Y proteins had a reduction in membrane currents that was below wild-type Cx26 injected cells and comparable to H_2O injected negative control cells. While the N14K and D50N mutants exhibited aberrant

hemichannel activity, the N14Y and D50Y mutants completely knocked out hemichannel activity.

To quantify these differences, mean steady-state currents were plotted for each mutant protein as well as positive and negative controls at each voltage tested. Cells injected with H_2O resulted in negligible currents at all voltages. As the depolarization increased, Wild-type Cx26 injected cells displayed increasingly large outward currents which were greater than H_2O injected negative controls. Cells expressing N14K or D50N protein produced large outward currents at all voltages tested (Figure III-2 and Figure III-3). Conversely, cells expressing N14Y or D50Y lead to a dramatic reduction in current at the voltages tested, and were comparable to H_2O injected controls. At +60 mV N14K was three times larger than wild-type and eight times larger than H_2O injected cells, but at the same voltage N14Y caused a significant reduction of current which was three times lower than wild-type and mirrored H_2O injected cells. When D50N was tested at +60 mV it produced currents that were four times larger than wild-type and thirteen times larger than H_2O control cells, but D50Y injected cells tested at the same voltage produced negligible currents that were sixteen times below wild-type injected cells. While cells expressing N14K or D50N mutant protein are shown to dramatically increase outward hemichannel currents compared to wild-type cells with positive voltage steps, cells expressing their substitution position counterparts N14Y or D50Y do the exact opposite and cause a dramatic reduction

in outward hemichannel currents. In all cases, cells expressing Cx26 proteins with KID-associated mutations were significantly different from cells expressing wild-type Cx26 protein.

Gap Junctions in Paired *Xenopus* Ooctyes

The differences in hemichannel function lead us to test whether mutant proteins expressed in paired *Xenopus* oocytes could form fully functioning gap junction channels. Cells injected with H_2O, wild-type Cx26, N14K, N14Y, D50N or D50Y RNA were incubated in 4 mM Ca^{2+} MB solution and tested via dual whole-cell voltage clamp (Figure III-4). Oocyte pairs expressing Cx26 wild-type protein displayed junctional conductance that were eight times larger than H_2O injected negative control pairs. Cells expressing mutant N14Y resulted in negligible amounts of current that were significantly smaller than Cx26 wild-type pairs and were comparable to H_2O injected pairs. This was in contrast to previously tested N14K paired oocytes [107] which had a junctional conductance similar to wild-type. Cells injected with wild-type, D50N, and D50Y RNA were also paired and tested for gap junctional coupling. Wild-type pairs had a conductance that was 37 times higher than H_2O injected negative control cells (Figure III-5). Oocyte pairs expressing D50Y and D50N had negligible amounts of conductance compared to wild-type and were comparable to H_2O injected

negative control pairs. Both the N14Y and D50Y mutations resulted in cells that had no hemichannel activity and no gap junction activity. This was in contrast to N14K and D50N which had large hemichannel activity and varying gap junctional conductances.

Immunofluorescence

As the majority of KID-associated Cx26 mutations have been found to increase the whole-cell currents of tested cells at positive depolarization, it has been suggested that this was related to an increase in hemichannel function. Previously we reported that the S17F mutation [107] displayed a dramatic decrease in whole-cell current to levels comparable to H_2O injected negative control cells, and this paper examines 2 more mutations (N14Y and D50Y) which have similar results. These results lead us to question if there were trafficking differences between mutations which display larger hemichannel associated currents and those which lacked hemichannel associated currents. The potential lack of a hemichannel current in this case could be the result of the lack of channel proteins on the plasma membrane. We used antibodies for Cx26 in conjunction with antibodies (Abcam) for the golgi apparatus (Golgin 97), early endosome (EEA1), or endoplasmic reticulum (ERp72). HeLa cells were transfected with Cx26 wild-type, N14K, N14Y, D50N or D50Y cDNA and stained for connexin protein

localization as well as golgi apparatus, early endosome, or endoplasmic reticulum. Cx26 wild-type transfected cells (Figure III-6 a-c) showed typical gap junctional plaques at the plasma membrane of apposing cells, as well as some intracellular anti-Cx26 staining consistent with organelles including the golgi. HeLa cells with N14K cDNA (Figure III-6 d-f) had a punctate staining pattern throughout the cell and potentially the plasma membrane, which was not restricted to sites of cell-cell interaction. The N14K mutant protein did not appear to be expressed overwhelmingly near the Golgi. Cells which contained N14Y cDNA (Figure III-6 g-i) did not produce junctional plaques at cellular interfaces and could be found clustered in the perinuclear region. These were unlike the N14K expression pattern and did not overlap with the marker for the golgi apparatus. When D50N cDNA was placed in the cells (Figure III-6 j-l) it also did not produce gap junction plaques like the wild-type protein did. The D50N protein was not restricted to locations near the Golgi specifically. HeLa cells transfected with D50Y (Figure III-6 m-o) also did not make gap junctional plaques as the wild-type cells did. The D50Y protein was not concentrated near the Golgi markers. This suggests that wild-type Cx26 protein created gap junctions, but none of the KID-associated mutations produced typical gap junctional plaques. Proteins for the N14K mutations were found in a diffuse manner around the cell, while protein for the N14Y, D50N, and D50Y proteins seemed to form localized clusters

around the cell in various locations, but did not overlap with the golgi marker to any large extent.

Cells transfected with cDNAs for Cx26 wild-type, N14K, N14Y, D50N, or D50Y were also stained for connexin expression and an early endosome marker. HeLa cells transfected with Cx26 wild-type (Figure III-7 a-c) overwhelmingly showed typical gap junction plaques at the plasma membrane as well as some protein in normal trafficking pathways. Cells with N14K cDNA (Figure III-7 d-f) lacked this typical gap junction formation and the connexin protein was found scattered throughout the cell but not overwhelming adjacent to early endosome concentrations. This is consistent with N14K connexins primarily forming hemichannels on the cell surface and being expressed fairly evenly throughout the cell. When cells were transfected with N14Y (Figure III-7 g-i), they showed a complete lack of gap junction formation as well as perinuclear connexin concentrations nearly identical to early endosome markers. D50N expressing cells (Figure III-7 j-l) showed diffuse connexin protein expression that did not overlap with any early endosome staining and had a distinct lack of gap junctional plaques. This suggests that D50N is found primarily on the cellular surface where it creates hemichannels (Figure II-2). Cells with D50Y (Figure III-7 m-o) also had a distinct lack of gap junctional plaques. The connexin protein in these cells were concentrated in a perinuclear fashion again and adjacent to early endosome staining. These results suggest that Cx26 wild-type protein forms gap

junctions as expected, but these KID causing mutations result in proteins that cannot form typical junctional plaques.

Lastly, a marker for the endoplasmic reticulum (ERp72) was also co-stained for with Cx26 proteins to help determine the trafficking patterns of the N14K, N14Y, D50N, and D50Y mutations. When HeLa cells were transfected with wild-type protein they displayed typical gap junction plaques as well as normal trafficking throughout the sub-cellular organelles consistent with protein synthesis (Figure III-8 a-c). Cells transfected with N14K cDNA did not result in typical gap junction formation, but instead showed a protein expression pattern that was diffuse throughout the entire cell and possibly the plasma membrane (Figure III-8 d-f). This suggests that N14K proteins traffic but do not form connexon plaques on the membrane and did not appear to localize in the ER with any sort of specificity. N14Y expressing cells had perinuclear localization, consistent with a failure of the protein to properly traffic to the membrane (Figure III-8 g-i). It appears that N14Y protein and the ER marker were in close proximity to each other in the cell. When HeLa cells were transfected with D50N cDNA they produced gap junctions that can be found in what appears to be typical pathways for connexin expression, but do no form typical gap junctional plaques (Figure III-8 j-l). It does not appear that D50N localizes specifically with the ER marker, but it is possible the some clusters of the protein may be in close proximity. Finally, D50Y cells appeared to express proteins in the

perinuclear region and did not form typical gap junctions (Figure III-8 m-o), and appeared to be transported in a manner similar to N14Y.

Discussion

While mutations in Cx26 often cause deafness, the syndromic mutations associated with skin disease like KID syndrome lead to severe phenotypes that differ in their role that they play within cells of the cochlea and skin. Our hypothesis is that KID causing mutations lead to a gain of function that exceeds the typical behavior of the wild-type channel and disrupts homeostasis within the epidermis. Of the naturally occurring mutations studied prior to this it was observed that there may be a gain of function mechanism related to aberrant hemichannel activity. To further examine this and other gain of function mechanisms that had been proposed we examined four naturally occurring mutations (N14K, N14Y, D50N, and D50Y) related to KID syndrome to determine if there was any functional similarities between different mutations which occurred at the same amino acid residue. While we observed that the N14K and D50N mutations lead to increased hemichannel activity several fold higher than wild-type with moderate changes in voltage, but N14Y and D50Y mutations resulted in non-functional channels that were several fold lower than wild-type at nearly all voltages tested.

Mutations associated with KID that cause an increase in hemichannel activity (N14K and D50N) again showed a diffuse staining pattern, leading us to conclude that they are found randomly on the cell surface in agreement with their ability to form hemichannels. However, KID mutations that cause a decrease in hemichannel activity (N14Y and D50Y) appear to not traffic to the plasma membrane, consistent with their lack of gap junction and hemichannel activity. These two mutations also appear to be concentrated in perinuclear sub-cellular regions in close proximity to early endosome and endoplasmic reticulum staining. This suggests that wild-type Cx26, N14K, and D50N can traffic to the plasma membrane, which is consistent with their ability to form either gap junctions or hemichannels. The two mutations tested, N14Y and D50Y, which don't form either gap junctions or hemichannels also do not appear to traffic to the plasma membrane and appear to be stuck somewhere near the early endosome and endoplasmic reticulum, potentially headed to lysosomal areas for degradation.

There have been several studies which have examined the role of Cx26 related KID mutations in cells. Most of these have focused on cell death, hemichannel activity, and dye transfer [98,99,106,107]. Most KID causing mutations lead to larger than normal hemichannels in tested cells. It's been previously suggested that some KID mutations may have altered channel function though certain dye transfer assays that test how far dyes can spread through gap junctions and even hemichannels [100,153]. In this experiment we discovered that the N14Y

and D50Y mutations that are associated with KID syndrome do not have functional channels through direct measurement of channel function. These mutations are similar to the results that S17F [107] did not form a functional channel either. This suggests that some large hydrophobic substitutions (N14Y, S17F, and D50Y) can result in channels that result in a pathology of syndromic deafness with skin disease. We also looked at the trafficking patterns of these proteins and found that they are located in perinuclear clusters (Figures III 5-7). Thus it seems likely that there is some internal response to these mutations which bypasses the typical hemichannel pathway that's associated with the gain of function mechanism for other mutations in Cx26, and instead there seems to be an internal cellular mechanism that disrupts epidermis homeostasis.

Figures and Legends:

Figure III – 1. Hemichannel currents recorded from *Xenopus* oocytes.

Cells were held at a potential of -40mV and then membrane currents were recorded at pulses between -30 and +60mV in 10mV steps. (a) Cx26wt-injected cells displayed typical current traces. Cells with N14K (b) or D50N (c) had currents that were larger than those of wild-type. Negative control cells injected with H_2O (d) had no currents, similar to N14Y (e) and D50Y (f) cells.

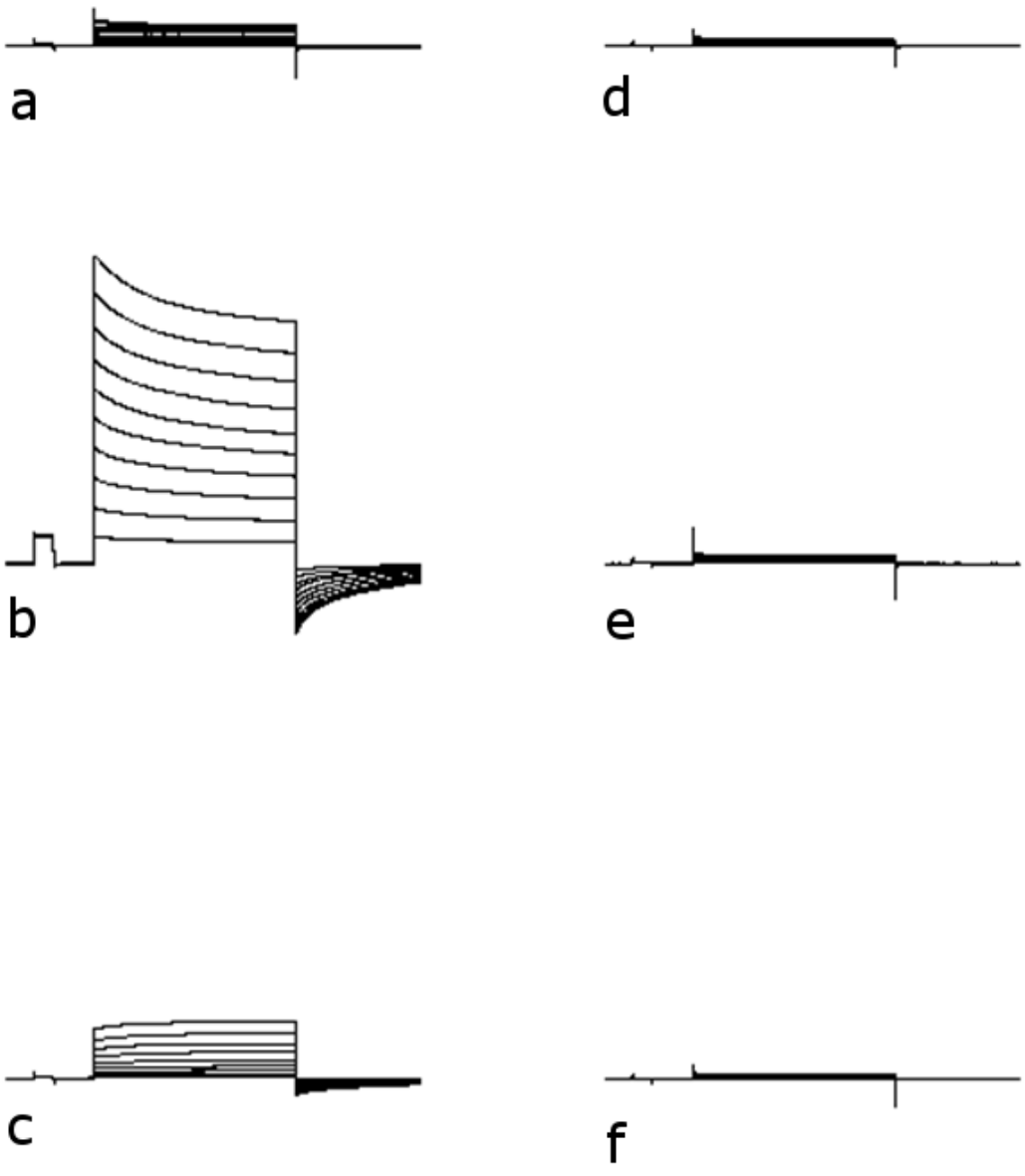
a
d
b
e
c
f

Figure III-2. Current-voltage relationship of the wild-type and mutant hemichannels.

Cells expressing each mutation were plotted along with H_2O and Cx26-injected cells to give a comparison of hemichannel activity. H_2O-injected cells (open triangles) displayed negligible currents at all voltages tested. Cells injected with N14K (filled diamonds) were larger than wild-type (open squares) and cells injected with with N14Y (filled circles) were the same as H_2O injected negative controls.

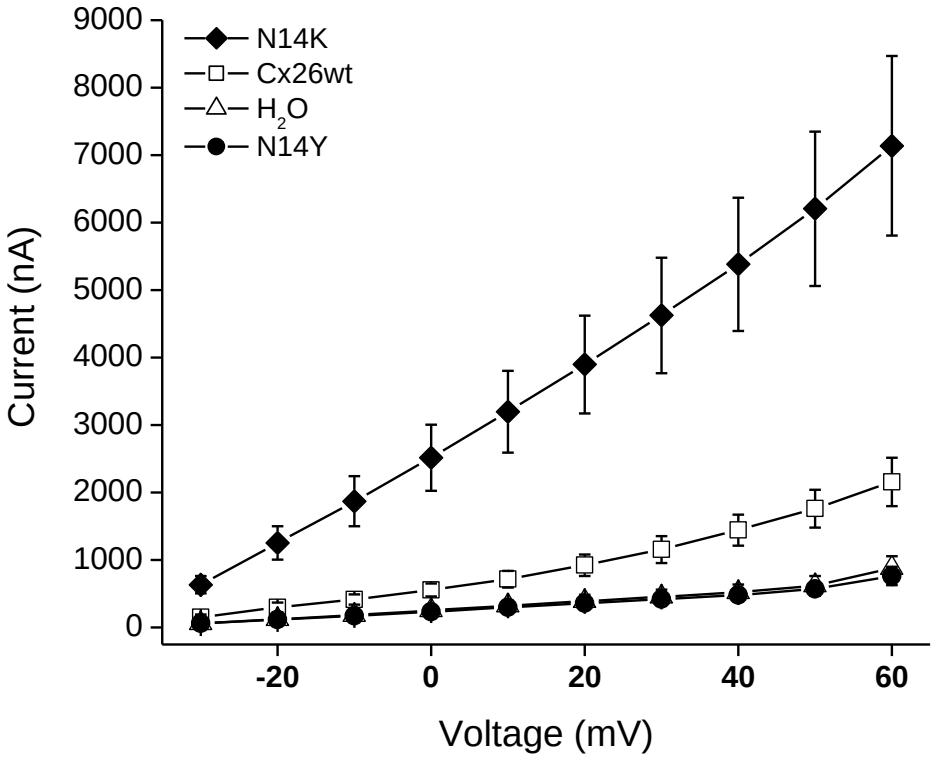
9000
8000
7000
6000
5000
4000
3000
2000
1000
0
Current (nA)
N14K
Cx26wt
H2O
N14Y
-20
0
20
40
60
Voltage (mV)

Figure III-3. Current-voltage relationship of the wild-type and mutant hemichannels.

Cells expressing each mutation were plotted along with H_2O and Cx26-injected cells to give a comparison of hemichannel activity. H_2O-injected cells (open triangles) displayed negligible currents at all voltages tested. Cells injected with D50N (filled diamonds) were larger than wild-type (open squares) and cells injected with with D50Y (filled circles) were the same as H_2O injected negative controls.

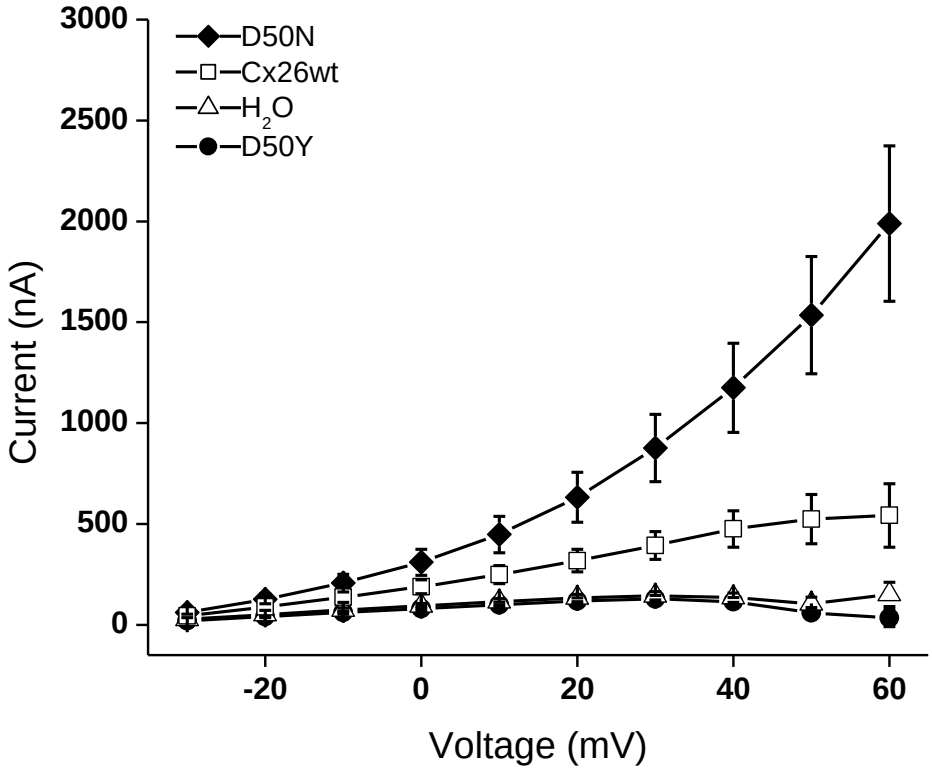
3000
2500
2000
1500
1000
500
0
Current (nA)
D50N
Cx26wt
H2O
D50Y
-20
0
20
40
60
Voltage (mV)

Figure III-4. Gap Junctional Conductance for Mutations Compared to Wild-Type.

Xenopous ooctyes were injected with RNA and paired to their junctional conductance by holding both cells at -40mV and then doing a +20 mV voltage step to test junctional conductance between paired cells. Cells injected with H_2O (n=25) had a negligible level of conductance. Pairs of wild-type Cx26 (n=27) or N14K (n=19 data from Lee et al, 2009) had a modest level of gap junction coupling. However, pairs of N14Y (n=10) injected cells did not have any conductance between them. (Data ± SE).

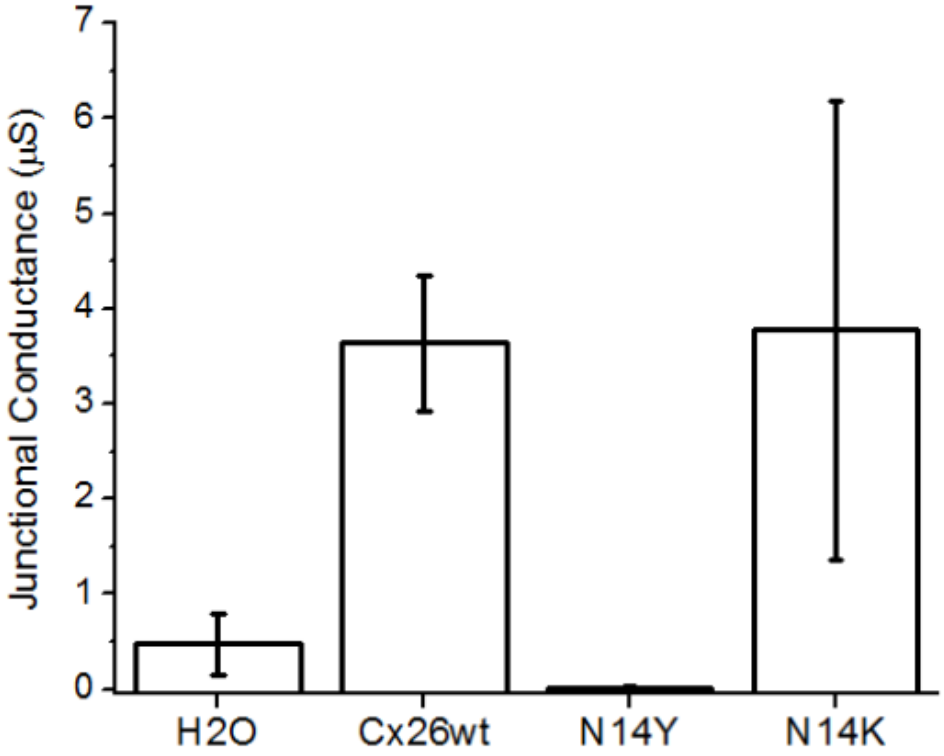
Junctional Conductance (μS)
7
6
5
4
3
2
1
0
H2O
Cx26wt
N14Y
N14K

Figure III-5. Gap Junctional Conductance for Mutations Compared to Wild-Type.

Xenopous ooctyes were injected with RNA and paired to their junctional conductance by holding both cells at -40mV and then doing a +20 mV voltage step to test junctional conductance between paired cells. Cells injected with H_2O (n=15) had a negligible level of conductance. Pairs of wild-type Cx26 (n=16) had a modest level of gap junction coupling. However, pairs of D50Y (n=15) or D50N (n=6) injected cells did not have any conductance between them. (Data ± SE).

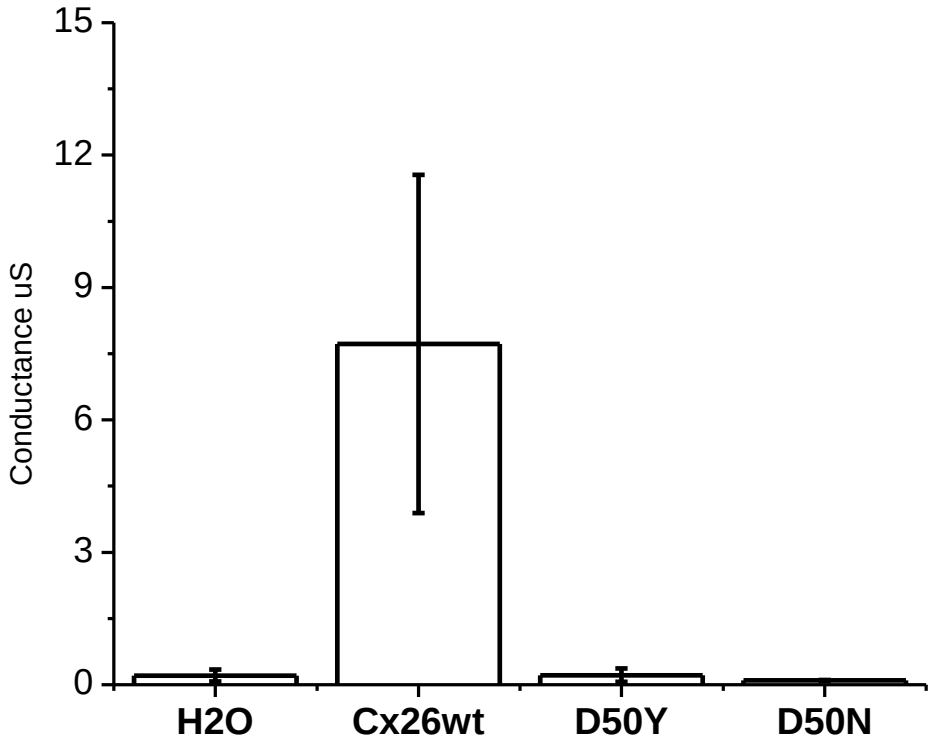
15
12
9
6
3
0
Conductance uS
H2O
Cx26wt
D50Y
D50N

Figure III-6 Immunocytochemical Staining of Cx26 Antibodies and Golgin-97 Antibody, a Golgi Marker.

HeLa cells were cultured and transfected with cDNA for wild-type Cx26, N14K, N14Y, D50N, and D50Y. When wild-type Cx26 was expressed in cells (a-c) gap junctional plaque formation can be noted (a) and when merged with a golgi apparatus marker (b) typical Cx26 trafficking is observed (c). N14K (d-f), N14Y (g-i), D50N (j-l), and D50Y (m-o) cells did not display typical gap junction formation.

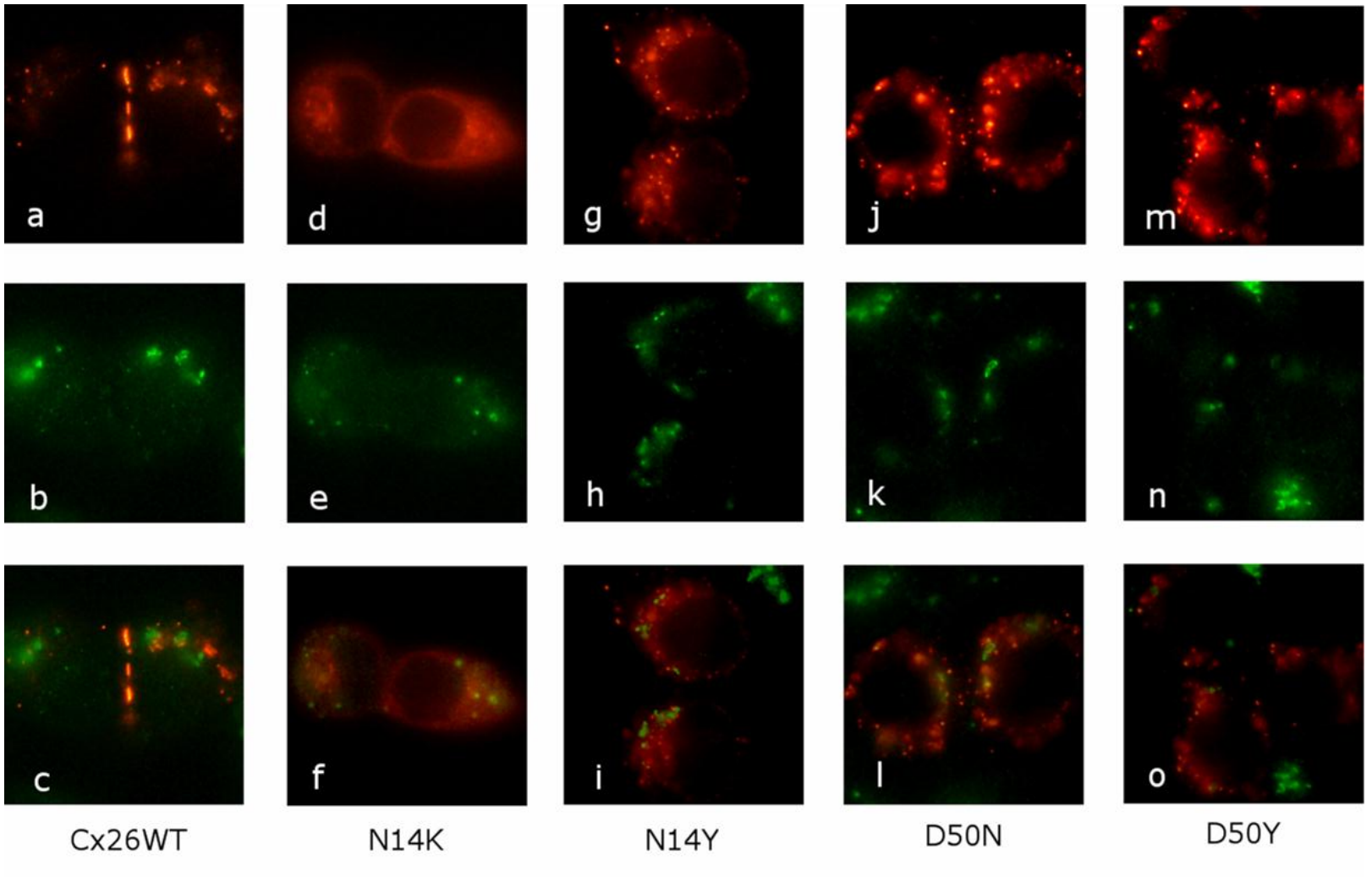
a
d
g
j
m
b
e
h
k
n
c
f
i
l
o
Cx26WT
N14K
N14Y
D50N
D50Y

Figure III-7 Immunocytochemical Staining of Cx26 Antibody and EEA1 Antibody, an Early Endosome Marker.

HeLa cells were cultured and transfected with cDNA for wild-type Cx26, N14K, N14Y, D50N, and D50Y. When wild-type Cx26 was expressed in cells (a-c) gap junctional plaque formation can be noted (a) and when merged with an early endosome marker (b) typical Cx26 trafficking is observed (c). N14K (d-f), N14Y (g-i), D50N (j-l), and D50Y (m-o) cells did not display typical gap junction formation.

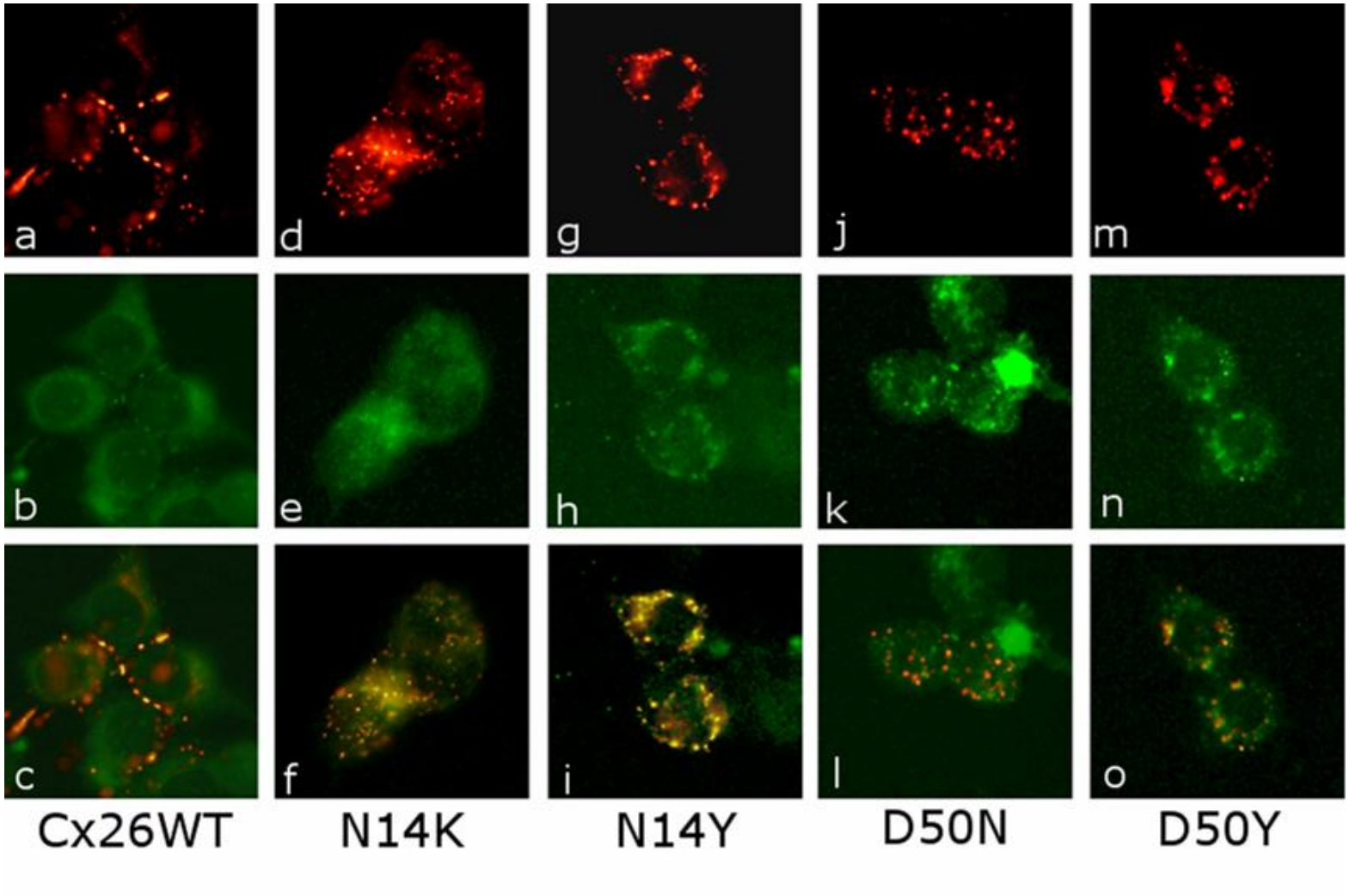
a
d
g
j
m
b
e
h
k
n
c
f
i
l
o
Cx26WT
N14K
N14Y
D50N
D50Y

Figure III-8 Immunocytochemical Staining of Cx26 Antibody and ERp72 Antibody, an Endoplasmic Reticulum Marker.

HeLa cells were cultured and transfected with cDNA for wild-type Cx26, N14K, N14Y, D50N, and D50Y. When wild-type Cx26 was expressed in cells (a-c) gap junctional plaque formation can be noted (a) and when merged with an endoplasmic reticulum marker (b) typical Cx26 trafficking is observed (c). N14K (d-f), N14Y (g-i), D50N (j-l), and D50Y (m-o) cells did not display typical gap junction formation.

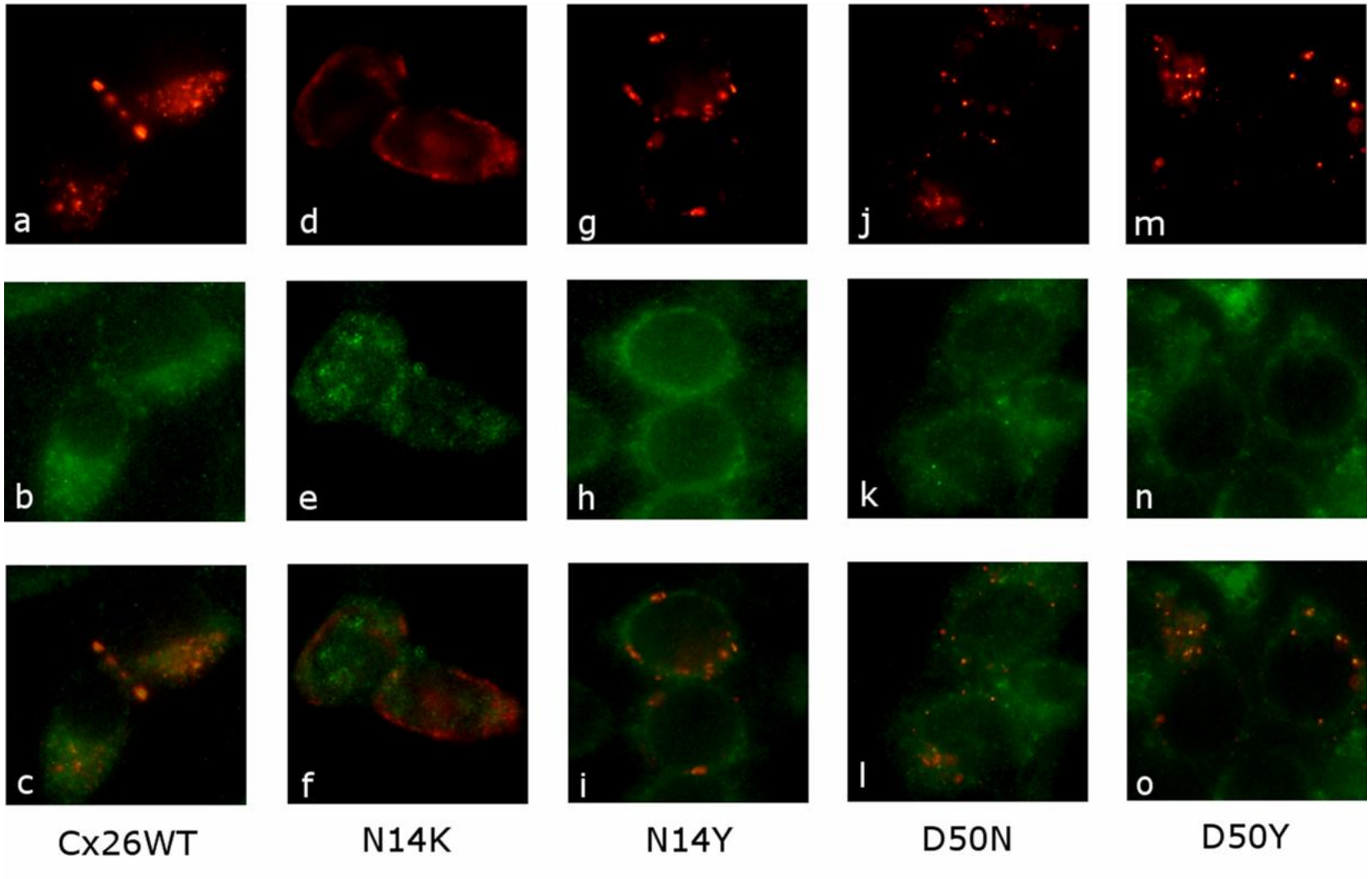
a
d
g
j
m
b
e
h
k
n
c
f
i
l
o
Cx26WT
N14K
N14Y
D50N
D50Y

Chapter IV

The effects of channel blockers on Cx26 mutations associated with KID syndrome

Abstract

Connexin proteins are essential for homeostasis in the inner ear as mutations in Cx26 that create severely truncated non-functional channels result in hearing pathologies. While Cx26 is found within the epidermis, it has a somewhat less vital role there. Mutations that cause severely truncated channels do not result in skin pathologies. Therefore the mutations in Cx26 that cause severe skin phenotypes associated with syndromic deafness diseases such as KID syndrome must have some gain of function that allows for the protein to alter homeostasis in the skin. Here we aim to knock down some of that gain of function by treating cells with channel blockers to determine if thing like aberrantly large hemichannel currents can be significantly reduced. This would hopefully rescue the skin phenotype by knocking out the action of the channel (which is not essential). We tested G12R, N14K, D50N, and S17F injected ooctyes with a variety of possible channel blocking techniques. When cells were treated with increasing extracellular Ca^{2+} concentrations, the hemichannel activity of G12R,

N14K and D50N could be reduced significantly. Also the survival rate of the cells increased dramatically. Similar results could be obtained by using extracellular Zn^{2+} in increasing concentration, although Zn^{2+} was a more potent blocker. Lastly, when cells were treated with known connexin channel blocker Flufenamic Acid (FFA) the currents of N14K injected cells could be blocked in the μM range and the drug could be washed out in a reversible manner. This suggests that the skin disease pathology associated with aberrant hemichannels in KID syndrome can be alleviated by reducing channel currents with drugs similar to FFA or extracellular Zn^{2+}. A therapeutic solution could be sought out.

Introduction

In the inner ear connexin function is responsible for helping maintain homeostasis. It has been shown that mutations in Cx26 that cause severely truncated proteins that fail to create connexon channels are some of the leading causes of deafness [28]. This suggests that Cx26 channel function is essential to normal hearing. While Cx26 is expressed with a variety of other connexins in the epidermis [22,60,61], mutations that result in severely truncated proteins and fail to create connexon channels do not cause syndromic deafness, only non-syndromic deafness. Therefore the cause of the skin pathologies in Cx26 cannot be associated with the complete lack of channel function, but instead must be some

gain of function that the channel receives due to the mutations that occur. Cells expressing mutated Cx26 proteins associated with KID syndrome have been shown to alter channel function.

Studies have been used to try to discover the mechanism that KID syndrome mutations gain that result in various skin pathologies. It's been proposed that the mutations cause over-active hemichannels or trafficking defects [98,99,106,153]. Also, previous studies have shown that some of these mutations (G45E and A40V) cause an increased rate of cell death. This change is part of the pathology expressed in vitro for KID mutations and a large number of connexin protein related skin disorders [154,155]. Increased rates of cell death could have a profound impact on skin physiology considering how tightly regulated the turnover rate of the epidermis is. If cells with increased hemichannel activity are also experiencing cell death in vitro, we wondered if a reduction to hemichannel activity could alleviate some of the symptoms associated with the pathology. This was especially interesting because as was pointed out early, reduction or even complete loss of Cx26 channel function would not be harmful to normal skin homeostasis. Thus the only effect of blocking abnormal Cx26 specific channel activity in cases of mutated Cx26 protein associated with KID syndrome may be to alleviate the pathology.

It was previously shown that elevated extracellular Ca^{2+} levels are known to inhibit connexin hemichannels [150] and prolong the lifespan of G45E expressing cells [99,106]. We further examined this by testing whether addition of extracellular Ca^{2+} could inhibit large single-cell currents caused by mutations associated with KID syndrome. Oocytes were injected with G12R, N14K, S17F, and D50N RNA and cultured in media with raised extracellular Ca^{2+} concentrations to determine if the rapid onset of cell death observed in cells with KID mutations that caused large single channel currents could be alleviated. G12R, N14K, and D50N all expressed large single channel currents that were several fold greater than wild-type Cx26 expressing cells. The same mutations also had increased rates of cell death compared to wild-type. When the cells with these mutations were cultured in media with increased extracellular Ca^{2+} all of their cell survival rates increased to the range near wild-type and S17F injected cells with >90% viability of oocytes after 24 hrs. This suggests that the extracellular Ca^{2+} helped alleviate hemichannel activity and thus thwarted the cell death phenotype associated with the mutations.

To examine whether extracellular Ca^{2+} actually was interacting with hemichannel currents and not causing a secondary influence on cells we recorded single-cell currents in the presence of various extracellular Ca^{2+} concentrations. The large hemichannels associated with KID causing Cx26 mutations G12R, N14K, and D50N were increasingly reduced as extracellular levels of Ca^{2+}

increased from 0mM to 4mM. Another divalent cation, Zn^{2+}, was tested on N14K injected cells and also reduced hemichannel activity but was a much more potent blocker of the channel. When the connexin channel blocker Flufenamic Acid (FFA) was tested, it could reversibly block the hemichannel currents caused by the N14K mutation at μM ranges. This suggests that therapeutic solutions to excessive hemichannel activity that would alleviate the skin diseases seen in KID syndrome can be sought if indeed the pathology is the result of excessive hemichannel activity.

Materials and Methods

Molecular cloning

Human wild-type Cx26 was cloned into the BamHI restriction site of the pCS2+ expression vector for functional studies in *Xenopus* laevis oocytes [62]. DNA primers (Table S1) with BamHI restriction sites (Integrated DNA Technologies, Inc., Coralville, IA) were designed to generate the G12R, N14K, S17F, and D50N mutations by standard PCR mutagenesis [22,106]. The G12R-, N14K-, and S17F-specific sense primers were paired with a Cx26 wild-type antisense primer and amplified by PCR with conditions of 95°C for 4 minutes, followed by 25 cycles of 94°C for 30 seconds, 60°C for 30 seconds, 72°C for 45 seconds, and 72°C for 2

minutes. The D50N mutation was created by the overlap extension method [144], using D50N-specific primers in conjunction with Cx26 sense and antisense primers. PCR products were gel purified using the QIAquik gel extraction kit (Qiagen, Valencia, CA), digested with BamHI and cloned into pBlueScript (Stratagene, La Jolla, CA), and sequenced on both strands (GeneWiz North Brunswick, NJ). Mutants with the correct sequence were subcloned into the pCS2+ vector [145].

In vitro transcription, oocyte microinjection, and pairing

Use of frogs was approved by the Institutional Animal Care and Use Committee. Human Cx26, G12R, N14K, S17F, and D50N were linearized using the NotI restriction site of pCS2+, and transcribed using the SP6 mMessage mMachine (Ambion, Austin, TX). Adult *Xenopus* females were anesthetized with ethyl-3-aminobenzoate methanesulfonate, and ovarian lobes were surgically removed and digested for 1.5 hours in a solution containing 50 mg/ml collagenase B, and 50mg/ml hyaluronidase in MB without Ca^{2+}. Stages V–VI oocytes were collected and injected first with 10ng of antisense *Xenopus* Cx38 oligonucleotide to eliminate endogenous connexins [9,146]. Antisense oligonucleotide-treated oocytes were then injected with wild-type Cx26, G12R, N14K, S17F, and D50N cRNA transcripts (5ng per cell), or H_2O as a negative control. cRNA-injected oocytes

were then cultured in Ca^{2+}-free MB, or MB with elevated Ca^{2+} (4mM $CaCl_2$) and cultured until ready for electrophysiological recording or image capture.

Electrophysiological hemichannel current recordings

At 8–12 hours after cRNA injection, macroscopic recordings of hemichannel currents were recorded from single *Xenopus* oocytes using a GeneClamp 500 amplifier controlled by a PC-compatible computer through a Digidata 1320 interface (Axon Instruments, Foster City, CA). pClamp 8.0 software (Axon Instruments) was used to program stimulus and data collection paradigms. In order to obtain hemichannel I–V curves, cells were initially clamped at -40mV and subjected to 5 seconds depolarizing voltage steps ranging from -30 to +60mV in 10mV increments. To test the effect of extracellular Ca^{2+} on hemichannel currents, oocytes were switched between MB media without Ca^{2+} , or MB supplemented with elevated Ca^{2+} (1, 2, and 4mM $CaCl_2$) via a perfusion system that washed 25 ml of solution through the 35mm dish before recording. Cells were allowed to rest in the new solution for 2–5 minutes before recording.

Results

Mutations known to cause increased hemichannel activity compared to wild-type seemed to have an accelerated rate of cell death when oocytes were

cultured for recording. Cells were injected with injected with RNA for wild-type, G12R, N14K, S17F, and D50N Cx26 protein and cultured in either 0 or 4mM Ca^{2+} media overnight before the oocytes were observed to determine the effect extracellular calcium might have on the survivability of the cells (Figure IV-1). Wild-type Cx26 and H_2O injected cells were incubated as controls. The effects of Ca^{2+} on the cell viability depended on the expressed mutation. There was no apparent difference between cells incubated in high Ca^{2+} or no Ca^{2+} for conditions with wild-type levels of hemichannel activity or lower (H_2O control, Cx26wt, and S17F). These cells were healthy upon visual inspection (Figure IV-1) and showed no signs of cell death after being incubated in media with or without Ca^{2+}. Incubation in media with no Ca^{2+} had a profound effect for cells expressing G12R, N14K, and D50N (Figure IV-1). The membranes of these cells exhibited blebbing and ooplasm began leaking from the cells within 8 to 10 hours.

To determine if the change in the observed rates of cell death in different Ca^{2+} concentrations were statistically significant, cell viability was scored by counting the number of cells with visible blebbing every hour between 12 and 24 hours post cRNA injection. Cells expressing wild-type or S17F cRNA showed little variation between 0 and 4 mM Ca^{2+} media (Figure IV-2). Oocytes injected with G12R, N14K, and D50N showed very different rates between 0 and 4 mM Ca^{2+}. When incubated in 0 mM Ca^{2+} these three mutations were statistically different from wild-type after 24 hours, while S17F injected oocytes were not.

This confirms the observation that cells expressing G12R, N14K, and D50N mutations died at a significantly faster rate than their wild-type counterparts. In contrast, rates of death for S17F injected oocytes were indistinguishable from wild-type. When all cells are incubated in 4 mM Ca^{2+} instead of 0 mM Ca^{2+} all of the 4 mutations displayed normal rates of cell death.

Cells injected with RNA coding for the G12R, N14K and D50N mutations in Cx26 also displayed sensitivity to extracellular Ca^{2+} concentrations (Figure IV-3). Cells containing mutant Cx26 G12R (Figure IV-3 a), N14K (Figure IV-3 b), and D50N (Figure IV-3 c) proteins showed large outward currents in 0mM Ca^{2+} solutions as documented earlier. The substitution of 1mM Ca^{2+} led to a significant reduction in membrane currents ($p<0.05$) but did not display a total reduction in outward current. The aberrant hemichannel currents produced by the mutated proteins in 2 and 4mM Ca^{2+} continued to decrease. The currents were significantly reduced in a concentration dependent manner, but each mutation showed a different sensitivity to extracellular Ca^{2+} (Figure IV-3 d).

Lastly we blocked oocytes expressing N14K Cx26 protein with Zn^{2+} and FFA to determine if these compounds could block the hemichannel activity common to this mutation. Both Zn^{2+} and FFA worked as efficient blockers across many ranges of concentrations (Figure IV-4 and Figure IV-5), but were most effective on the 100μM range. Cells treated with 100 μM extracellular FFA could

then be washed with MB solution without calcium and the hemichannel activity would return (Figure IV-5).

Discussion

Some mutations in Cx26 associated with KID syndrome (G45E and A40V) cause an increased rate of cell death [106] that could be alleviated by adding extracellular Ca^{2+} to the culture media. This change is part of the pathology expressed in vitro for KID mutations and a large number of connexin protein related skin disorders [154,155]. It was observed while culturing oocytes injected with RNA for KID mutations G12R, N14K, and D50N that the cells were not as viable as wild-type injected ones after being cultured overnight. We tested whether these cells could be rescued by adding Ca^{2+} to the culture media. When the media contained 4mM Ca^{2+} as opposed to 0mM, the cells injected with G12R, N14K, and D50N were all rescued and their viability increased. They experienced very little discoloration or blebbing which was common in the 0mM Ca^{2+} media. Thus it became apparent that extracellular Ca^{2+} had rescued the cells. It has been suggested that this mechanism occurs by shifting the I-V curve of the hemichannel to more positive potentials and thus limit the ability of the channel to open in physiological conditions and act as a sort of block against channel activation.

Previously it was reported that elevated extracellular Ca^{2+} could inhibit connexin hemichannels [150] and prolong the lifespan of G45E expressing cells [99,106]. Since Ca^{2+} was a known blocker of hemichannel currents, we were curious if it would have an impact on KID causing mutations in Cx26 that resulted in large hemichannels. We examined this by testing whether addition of extracellular Ca^{2+} could inhibit these associated currents. We injected cells with RNA for G12R, N14K, or D50N RNA and recorded currents from single oocytes over a variety of different membrane voltages in the presence of different concentrations of extracellular Ca^{2+}. The single cell currents, associated with hemichannel activity of the cell, were reduced for all mutations as we moved to progressively higher concentrations of Ca^{2+}. If the I-V curve for Cx26 hemichannels was shifted to higher membrane potentials by increasing the extracellular Ca^{2+} concentration, which also rescues cells injected with aberrant hemichannel activity (G12R, N14K, and D50N) from cell death, it is likely that the cell death phenotype and gain of function for KID mutations may be overly active hemichannels. It then becomes possible to alleviate some of the skin complications associated with KID syndrome by using channel blockers specific to Cx26.

To further examine if over active Cx26 hemichannels produced by KID mutations could be reduced by adding blockers to the extracellular medium, we added known connexin inhibitors such as the divalent cation Zn^{2+} and FFA to

N14K expressing cells while recording channel currents. This lead to a complete reduction of hemichannel currents by both Zn^{2+} and FFA within μM ranges. It is possible that potential therapeutic blockers to Cx26 hemichannels could be developed which would help alleviate some of the skin symptoms for patients with KID syndrome related mutations that result in aberrant hemichannels.

Figure Legends and Figures:

Figure IV-1. Hemichannel activity-dependent cell death.

(a) Cells were injected with either H_2O, Cx26, G12R, N14K, S17F, or D50N and incubated in MB solution overnight. Cells injected with H_2O and Cx26 wild type remained viable and intact. Mutations that caused hemichannel activity (G12R, N14K, and D50N) displayed obvious blebbing and an increased rate of cell death compared to Cx26 cells. The S17F mutation that lacked hemichannel activity did not experience the increased rate of cell death. (b) Injected cells were incubated in 4mM Ca^{2+} MB solution overnight. The increased rate of cell death and physical deformation of the membrane experienced by mutations with active hemichannels was rescued by elevated Ca^{2+}. Scale bar = 1 mm. [107]

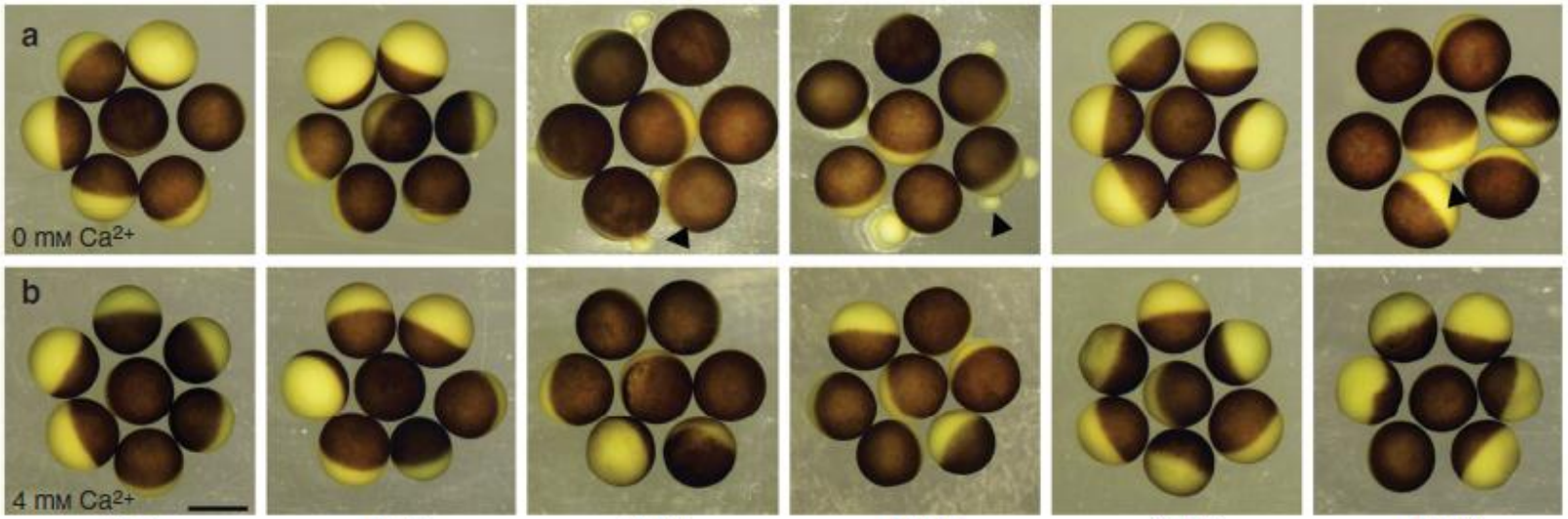
a
0 mM Ca2+
b
4 mM Ca2+
H2O
Cx26
G12R
N14K
S17F
D50N

Figure IV-2. Viability of Cx26 wild-type and mutant expressing cells.

(a) Cells in 0mM Ca^{2+} media were scored for cell viability based on the appearance of blebbing. Cells were injected with wild-type Cx26, G12R, N14K, S17F, or D50N cRNA and monitored for 24 hours. These data are based on 20 injected cells per experimental condition. (b) Equal numbers of cells expressing the same cRNAs were incubated in 4mM Ca^{2+} media overnight and scored in the same fashion. (c) Cell viability at 24 hours post-injection for all five conditions. The G12R-, N14K-, and D50N-injected cells are statistically different ($P<0.05$, Student's t-test) from wild-type-injected cells. Cells injected with S17F were not statistically different from wild type. Data are the mean±SE from four experiments. [107]

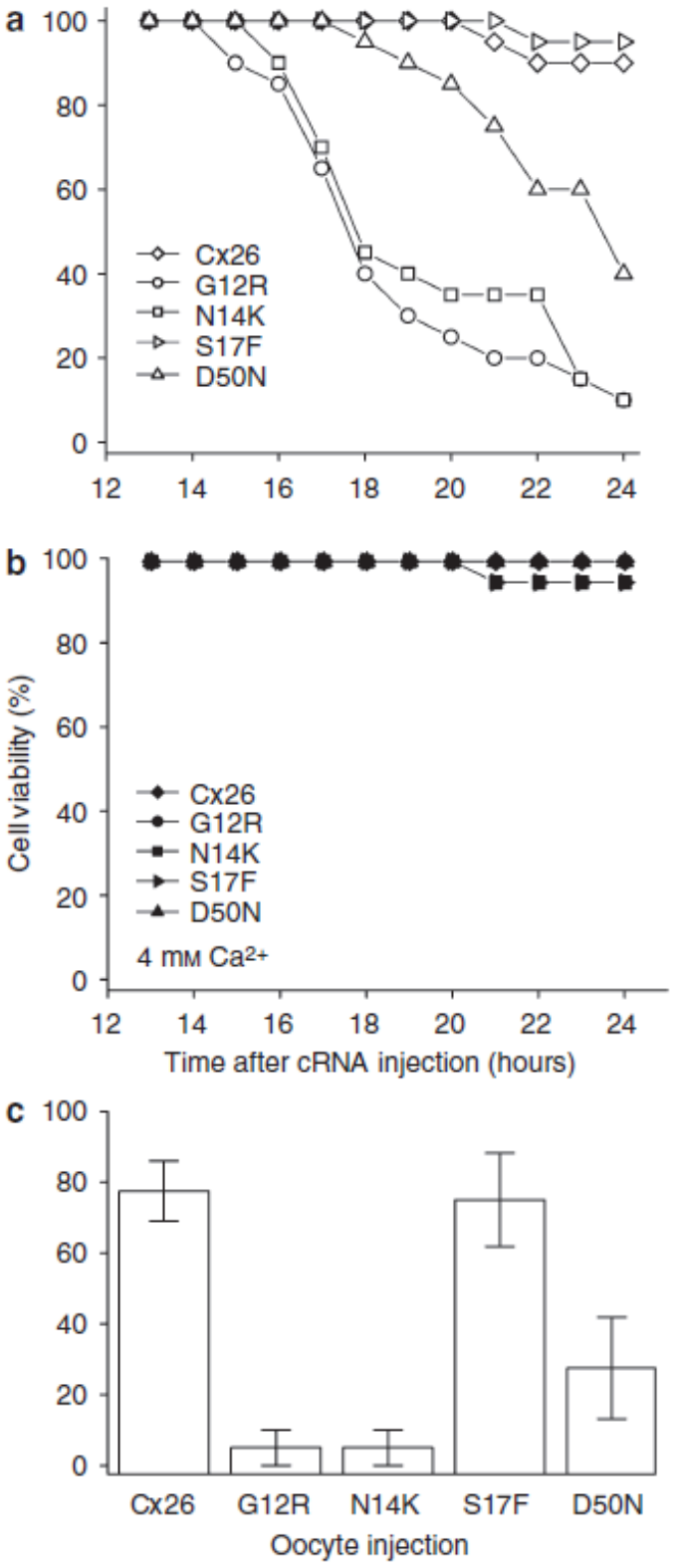
a
100
80
60
40
20
0
12
14
16
18
20
22
24
Cx26
G12R
N14K
S17F
D50N
b
Cell viability (%)
4 mM Ca2+
Time after cRNA injection (hours)
c
Cx26
G12R
N14K
S17F
D50N
Oocyte injection

Figure IV-3. Current–voltage relationships of cells recorded in MB with 0, 1, 2, or 4mM Ca^{2+} (open, top closed, bottom closed, and completely closed, respectively).

Only cells that expressed hemichannels were recorded. (a–c) Cells were clamped at -40mV and then tested with pulses from -30 to +60mV via +10mV steps. G12R (circle), N14K (square), and D50N (triangle) mutations caused hemichannel activity that increased at positive potentials. The magnitude of hemichannel current was reduced at all potentials as the extracellular concentration of Ca^{2+} increased. (d) Currents for each mutation were normalized for steady-state maximal values at each concentration and plotted against the concentration of extracellular Ca^{2+}. There was a distinct difference in the degree and rate of current reduction induced by Ca^{2+}. [107]

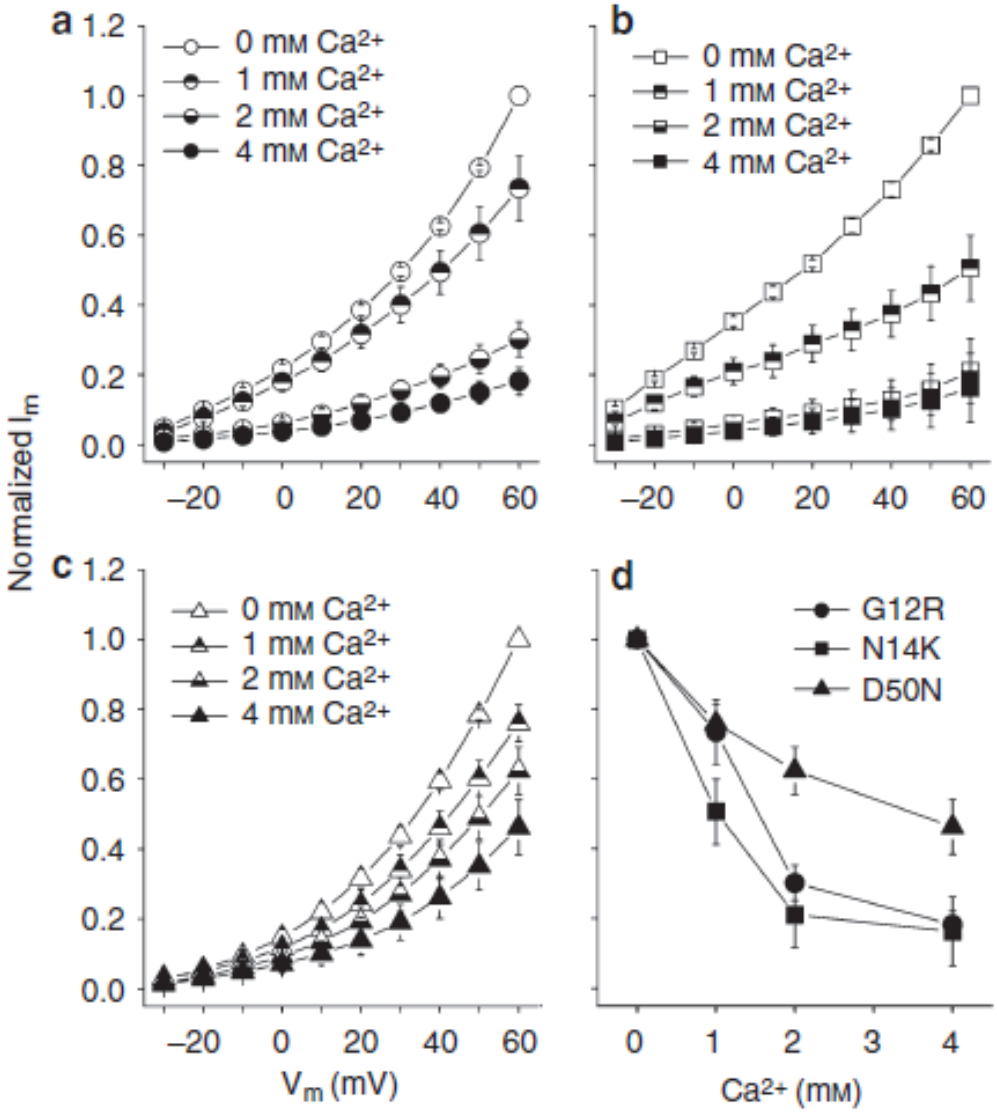
a
b
c
d
0 mM Ca2+
1 mM Ca2+
2 mM Ca2+
4 mM Ca2+
Nomalized Im
Vm (mV)
G12R
N14K
D50N
Ca2+ (mM)

Figure IV-4. *Xenopus* oocytes expressing Cx26 mutation N14K in different Zn^{2+} extracellular concentrations.

(a) Current traces for 0mM, 10 μM, 100μM, and 1mM Zn^{2+} concentrations. (b) Mean hemichannel currents for N14K proteins in ooctyes at different Zn^{2+} concentrations.

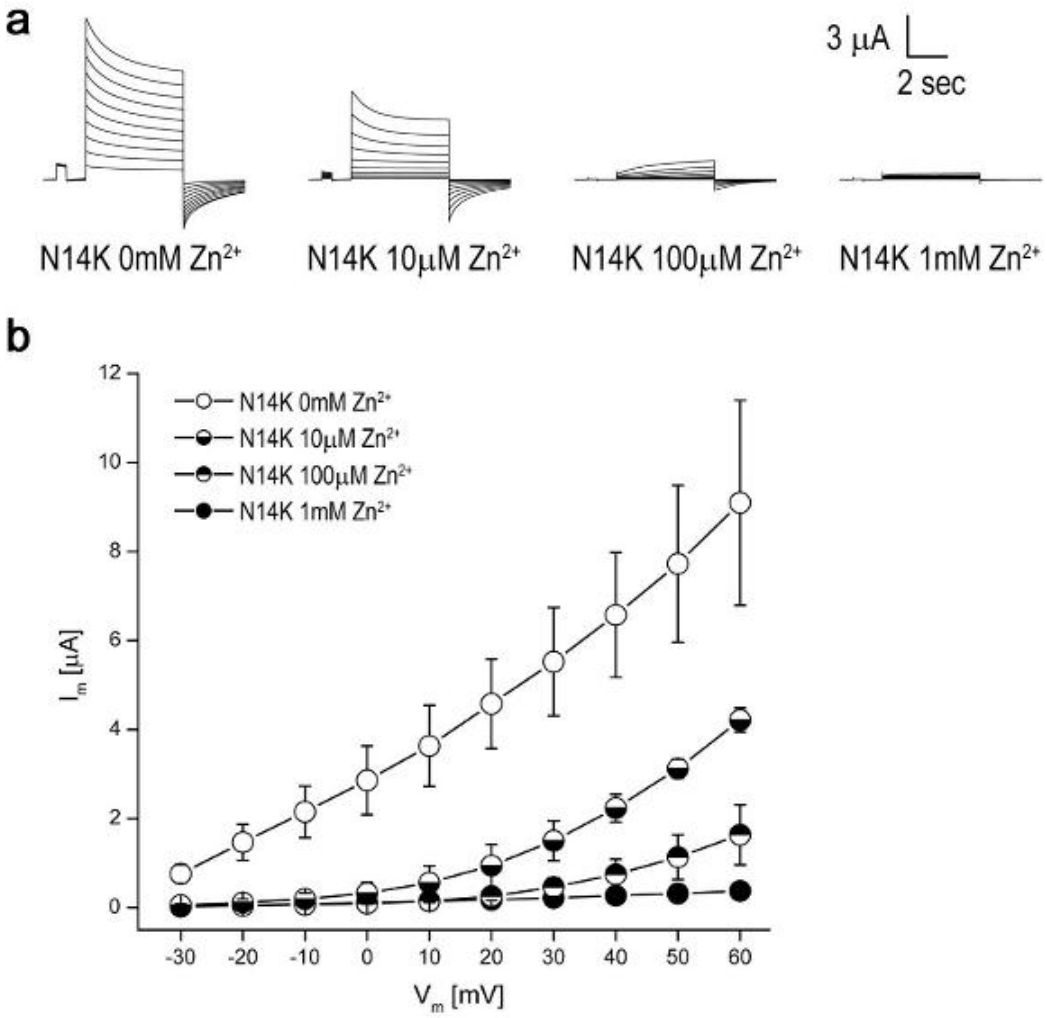
a
3 μA
2 sec
N14K 0mM Zn2+
N14K 10μM Zn2+
N14K 100μM Zn2+
N14K 1mM Zn2+
b
N14K 0mM Zn2+
N14K 10μM Zn2+
N14K 100μM Zn2+
N14K 1mM Zn2+
Im [μA]
Vm [mV]
12
10
8
6
4
2
0
-30
-20
-10
0
10
20
30
40
50
60

Figure IV-5. Whole-cell current recordings from *Xenopus* oocytes expressing Cx26 mutation N14K proteins at 0 and 100 μM FFA concentrations.

a) Whole-cell current expressed while treated with FFA and after washout. b) Different current traces from 0μM before drug application, 100μM during FFA application, and 0μM after washout. c) Displaying the channel block at 100μM FFA.

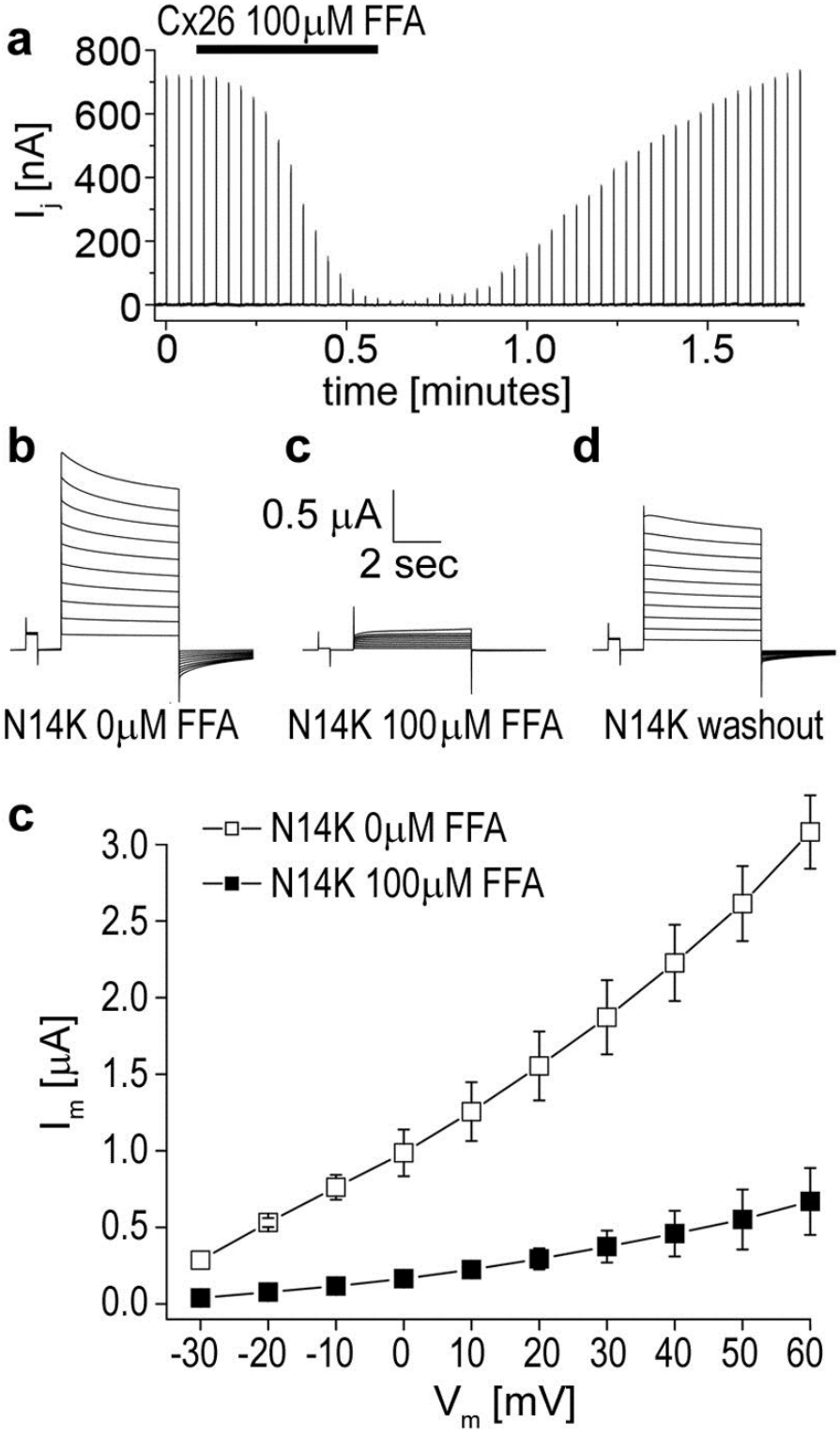
a
Cx26 100μM FFA
800
600
400
200
0
I_j [nA]
0
0.5
1.0
1.5
time [minutes]
b
c
d
0.5 μA
2 sec
N14K 0μM FFA
N14K 100μM FFA
N14K washout
c
N14K 0μM FFA
N14K 100μM FFA
3.0
2.5
2.0
1.5
1.0
0.5
0.0
I_m [μA]
-30
-20
-10
0
10
20
30
40
50
60
V_m [mV]

Chapter V

Concluding Remarks and Observations

Gap junctions are expressed throughout the body and take part in many processes that are necessary for normal physiological function. Gap junction channels are formed by connexin protein subunits, six of which combine to produce a hemichannel [3]. Two hemichannels from the plasma membranes of adjacent cells align in the extracellular space to form a complete gap junctional channel [4], which allows ions and other small molecules to pass between the connected cells. In addition, connexin hemichannels can be functional in non-junctional membranes, allowing the exchange of solutes with the extracellular space [5,6]. There are more than 20 connexin genes that are expressed throughout the body in overlapping and unique patterns [2]. Gap junction channels may be assembled from the same connexin, or a combination of different connexins, depending on the cell type. Each connexin protein has four transmembrane domains (TM1–TM4), connected by two extracellular loops (EC1 and EC2) and a cytoplasmic loop (CL). The N- and C-termini of the protein extend into the cytoplasm of the cell. Two organs where connexins and gap junctions are necessary for normal function are the skin and the inner ear. Mutations in connexin genes have been linked to human hereditary diseases affecting both the epidermis and cochlea.

There are numerous mutations in Cx26 that are linked to both non-syndromic and syndromic deafness. The difference between these two groups is that non-syndromic deafness is caused by a loss of typical wild-type Cx26 function within the cochlea. Mutations that cause deafness in addition to other clinical complications such as skin disease in KID syndrome can be linked to a gain of function within the skin. When severely truncated proteins [28] are caused by mutations in Cx26 (stop codon at the 13th amino acid) the result is not syndromic deafness. Cx26 function in the epidermis is either completely unnecessary or at least compensated for by some redundant expression of other connexins/proteins. It follows that the skin complications in KID syndrome can be traced to a function of Cx26 that is not present in wild-type proteins, or a gain of function.

In this dissertation, six KID syndrome related mutations, G12R, N14K, N14Y, S17F, D50N, and D50Y were examined to determine what gain of function these mutations have that causes the manifestation of the skin complications. While it was previously suggested that in a few mutations (A40V and G45E) that KID syndrome may be due to aberrant hemichannel activity [98,99,106] it was unclear if this function was complete. Another mutation (N14Y) was found to reduce dye transfer between cells and have lowered channel functionality [153]. To better understand what actual channel functionality and what trafficking patterns the proteins may have we recorded single-cell currents and

paired dual-cell conductances from ooctyes injected with the six mutations we probed. We also used immunocytochemistry in transfected HeLa cells with antibodies for markers in different cellular organelles to determine where the protein may localize within cells. Our tests indicated that while a majority of KID syndrome related mutations (G12R, N14K, A40V, G45E, and D50N) cause hemichannels that are several fold larger in current than wild-type proteins, there are a few mutations (N14Y, S17F, and D50Y) which create proteins with no channel functionality in oocytes. Interestingly, none of the mutations we tested had typical gap junction formation when we stained cells for them. While the mutations which cause larger hemichannels appear to occur in diffuse patterns around the cell, those without channel functionality look like they remain in the perinuclear area near markers for the early endosome and endoplasmic reticulum. This suggests that while most KID-related mutations cause a gain of channel function by increasing native hemichannel currents across many different voltages, that there is a secondary pathway by which some KID mutations do not traffic to the plasma membrane. While they both end up causing the same clinical phenotype in patients, it's clear that there accomplish this end by different pathways.

In the future an investigation into these two pathways might analyze the signal cascade that leads to the same phenotype. This could be useful for the development of therapeutic treatments by determine what new cellular pathways

are activated leading ultimately to a disruption of the skin. These treatments can take advantage of the relative ease of skin treatment by application of topical agents. There should be further studies to establish whether there are mechanisms and agents which would reduce the hemichannel currents of KID mutations that produce increased hemichannel activity. A hemichannel blocker that could operate in physiological ranges (μM) and be applied to the skin in a manageable treatment would be extremely useful to patients which suffer dramatically from KID syndrome.

In conclusion, this dissertation determined that syndromic deafness mutations differ dramatically from wild-type Cx26 in channel function and trafficking patterns in the cell. While several mutations lead to larger single connexon functionality and presumably lead to a severe disruption of cellular homeostasis, there are also a few mutations that lead to complete lack of plasma membrane channel functionality. Those few mutations do not traffic to the plasma membrane like typical Cx26 proteins. Their disruption comes from interactions within the cell. Ultimately either pathway may cause a complete destruction of epidermis homeostasis through non-typical connexin functionality.

References

1 Bennett, M. V. & Goodenough, D. A. Gap junctions, electrotonic coupling, and intercellular communication. *Neurosciences Research Program bulletin* **16**, 1-486 (1978).

2 Sohl, G. & Willecke, K. An update on connexin genes and their nomenclature in mouse and man. *Cell communication & adhesion* **10**, 173-180 (2003).

3 Goodenough, D. A. & Paul, D. L. Beyond the gap: functions of unpaired connexon channels. *Nature reviews. Molecular cell biology* **4**, 285-294, doi:10.1038/nrm1072 (2003).

4 Harris, A. L. Emerging issues of connexin channels: biophysics fills the gap. *Quarterly reviews of biophysics* **34**, 325-472 (2001).

5 Jiang, J. X. & Gu, S. Gap junction- and hemichannel-independent actions of connexins. *Biochimica et biophysica acta* **1711**, 208-214, doi:10.1016/j.bbamem.2004.10.001 (2005).

6 Saez, J. C., Retamal, M. A., Basilio, D., Bukauskas, F. F. & Bennett, M. V. Connexin-based gap junction hemichannels: gating mechanisms. *Biochimica et biophysica acta* **1711**, 215-224, doi:10.1016/j.bbamem.2005.01.014 (2005).

7 Bruzzone, R., White, T. W. & Paul, D. L. Connections with connexins: the molecular basis of direct intercellular signaling. *European journal of biochemistry / FEBS* **238**, 1-27 (1996).

8 Oh, S., Rubin, J. B., Bennett, M. V., Verselis, V. K. & Bargiello, T. A. Molecular determinants of electrical rectification of single channel conductance in gap junctions formed by connexins 26 and 32. *The Journal of general physiology* **114**, 339-364 (1999).

9 Barrio, L. C. *et al.* Gap junctions formed by connexins 26 and 32 alone and in combination are differently affected by applied voltage. *Proceedings of the National Academy of Sciences of the United States of America* **88**, 8410-8414 (1991).

10 Musil, L. S. & Goodenough, D. A. Multisubunit assembly of an integral plasma membrane channel protein, gap junction connexin43, occurs after exit from the ER. *Cell* **74**, 1065-1077 (1993).

11 Evans, W. H. *et al.* Trafficking pathways leading to the formation of gap junctions. *Novartis Foundation symposium* **219**, 44-54; discussion 54-49 (1999).

12 Martin, P. E., Blundell, G., Ahmad, S., Errington, R. J. & Evans, W. H. Multiple pathways in the trafficking and assembly of connexin 26, 32 and 43 into gap junction intercellular communication channels. *Journal of cell science* **114**, 3845-3855 (2001).

13 Musil, L. S. & Goodenough, D. A. Gap junctional intercellular communication and the regulation of connexin expression and function. *Current opinion in cell biology* **2**, 875-880 (1990).

14 Gaietta, G. *et al.* Multicolor and electron microscopic imaging of connexin trafficking. *Science* **296**, 503-507, doi:10.1126/science.1068793 (2002).

15 Thomas, T. *et al.* Mechanisms of Cx43 and Cx26 transport to the plasma membrane and gap junction regeneration. *Journal of cell science* **118**, 4451-4462, doi:10.1242/jcs.02569 (2005).

16 Fallon, R. F. & Goodenough, D. A. Five-hour half-life of mouse liver gap-junction protein. *The Journal of cell biology* **90**, 521-526 (1981).

17 Beardslee, M. A., Laing, J. G., Beyer, E. C. & Saffitz, J. E. Rapid turnover of connexin43 in the adult rat heart. *Circulation research* **83**, 629-635 (1998).

18 Jordan, K., Chodock, R., Hand, A. R. & Laird, D. W. The origin of annular junctions: a mechanism of gap junction internalization. *Journal of cell science* **114**, 763-773 (2001).

19 White, T. W. & Paul, D. L. Genetic diseases and gene knockouts reveal diverse connexin functions. *Annual review of physiology* **61**, 283-310, doi:10.1146/annurev.physiol.61.1.283 (1999).

20 Wei, C. J., Xu, X. & Lo, C. W. Connexins and cell signaling in development and disease. *Annual review of cell and developmental biology* **20**, 811-838, doi:10.1146/annurev.cellbio.19.111301.144309 (2004).

21 Anand, R. J. & Hackam, D. J. The role of gap junctions in health and disease. *Critical care medicine* **33**, S535-538 (2005).

22 Mese, G., Richard, G. & White, T. W. Gap junctions: basic structure and function. *The Journal of investigative dermatology* **127**, 2516-2524, doi:10.1038/sj.jid.5700770 (2007).

23 Gerido, D. A. & White, T. W. Connexin disorders of the ear, skin, and lens. *Biochimica et biophysica acta* **1662**, 159-170, doi:10.1016/j.bbamem.2003.10.017 (2004).

24 Richard, G. Connexin disorders of the skin. *Clinics in dermatology* **23**, 23-32, doi:10.1016/j.clindermatol.2004.09.010 (2005).

25 van Steensel, M. A. Gap junction diseases of the skin. *American journal of medical genetics. Part C, Seminars in medical genetics* **131C**, 12-19, doi:10.1002/ajmg.c.30030 (2004).

26 Lai-Cheong, J. E., Arita, K. & McGrath, J. A. Genetic diseases of junctions. *The Journal of investigative dermatology* **127**, 2713-2725, doi:10.1038/sj.jid.5700727 (2007).
27 Petit, C. From deafness genes to hearing mechanisms: harmony and counterpoint. *Trends in molecular medicine* **12**, 57-64, doi:10.1016/j.molmed.2005.12.006 (2006).
28 Petit, C. Usher syndrome: from genetics to pathogenesis. *Annual review of genomics and human genetics* **2**, 271-297, doi:10.1146/annurev.genom.2.1.271 (2001).
29 Smith, R. J. Clinical application of genetic testing for deafness. *American journal of medical genetics. Part A* **130A**, 8-12, doi:10.1002/ajmg.a.30053 (2004).
30 Apps, S. A., Rankin, W. A. & Kurmis, A. P. Connexin 26 mutations in autosomal recessive deafness disorders: a review. *International journal of audiology* **46**, 75-81, doi:10.1080/14992020600582190 (2007).
31 Tranebaerg, L. Genetics of congenital hearing impairment: a clinical approach. *International journal of audiology* **47**, 535-545, doi:10.1080/14992020802249259 (2008).
32 Zhao, H. B., Kikuchi, T., Ngezahayo, A. & White, T. W. Gap junctions and cochlear homeostasis. *The Journal of membrane biology* **209**, 177-186, doi:10.1007/s00232-005-0832-x (2006).
33 White, T. W. Functional analysis of human Cx26 mutations associated with deafness. *Brain research. Brain research reviews* **32**, 181-183 (2000).
34 Bruzzone, R. *et al.* Loss-of-function and residual channel activity of connexin26 mutations associated with non-syndromic deafness. *FEBS letters* **533**, 79-88 (2003).
35 Kelsell, D. P. *et al.* Connexin 26 mutations in hereditary non-syndromic sensorineural deafness. *Nature* **387**, 80-83, doi:10.1038/387080a0 (1997).
36 Jonard, L. *et al.* A familial case of Keratitis-Ichthyosis-Deafness (KID) syndrome with the GJB2 mutation G45E. *European journal of medical genetics* **51**, 35-43, doi:10.1016/j.ejmg.2007.09.005 (2008).
37 Santos-Sacchi, J. & Dallos, P. Intercellular communication in the supporting cells of the organ of Corti. *Hearing research* **9**, 317-326 (1983).
38 Jagger, D. J. & Forge, A. Compartmentalized and signal-selective gap junctional coupling in the hearing cochlea. *The Journal of neuroscience : the official journal of the Society for Neuroscience* **26**, 1260-1268, doi:10.1523/JNEUROSCI.4278-05.2006 (2006).

39 Kikuchi, T., Adams, J. C., Paul, D. L. & Kimura, R. S. Gap junction systems in the rat vestibular labyrinth: immunohistochemical and ultrastructural analysis. *Acta oto-laryngologica* **114**, 520-528 (1994).

40 Kikuchi, T., Kimura, R. S., Paul, D. L. & Adams, J. C. Gap junctions in the rat cochlea: immunohistochemical and ultrastructural analysis. *Anatomy and embryology* **191**, 101-118 (1995).

41 Johnstone, B. M., Patuzzi, R., Syka, J. & Sykova, E. Stimulus-related potassium changes in the organ of Corti of guinea-pig. *The Journal of physiology* **408**, 77-92 (1989).

42 Oesterle, E. C. & Dallos, P. Intracellular recordings from supporting cells in the guinea pig cochlea: DC potentials. *Journal of neurophysiology* **64**, 617-636 (1990).

43 Kikuchi, T., Adams, J. C., Miyabe, Y., So, E. & Kobayashi, T. Potassium ion recycling pathway via gap junction systems in the mammalian cochlea and its interruption in hereditary nonsyndromic deafness. *Medical electron microscopy : official journal of the Clinical Electron Microscopy Society of Japan* **33**, 51-56, doi:10.1007/s007950000009 (2000).

44 Wangemann, P. K(+) cycling and its regulation in the cochlea and the vestibular labyrinth. *Audiology & neuro-otology* **7**, 199-205 (2002).

45 Hibino, H. & Kurachi, Y. Molecular and physiological bases of the K+ circulation in the mammalian inner ear. *Physiology (Bethesda)* **21**, 336-345, doi:10.1152/physiol.00023.2006 (2006).

46 Schulte, B. A. & Adams, J. C. Distribution of immunoreactive Na+,K+-ATPase in gerbil cochlea. *The journal of histochemistry and cytochemistry : official journal of the Histochemistry Society* **37**, 127-134 (1989).

47 Crouch, J. J., Sakaguchi, N., Lytle, C. & Schulte, B. A. Immunohistochemical localization of the Na-K-Cl co-transporter (NKCC1) in the gerbil inner ear. *The journal of histochemistry and cytochemistry : official journal of the Histochemistry Society* **45**, 773-778 (1997).

48 Bruzzone, R. & Cohen-Salmon, M. Hearing the messenger: Ins(1,4,5)P3 and deafness. *Nature cell biology* **7**, 14-16, doi:10.1038/ncb0105-14 (2005).

49 Beltramello, M., Piazza, V., Bukauskas, F. F., Pozzan, T. & Mammano, F. Impaired permeability to Ins(1,4,5)P3 in a mutant connexin underlies recessive hereditary deafness. *Nature cell biology* **7**, 63-69, doi:10.1038/ncb1205 (2005).

50 Madison, K. C. Barrier function of the skin: "la raison d'etre" of the epidermis. *The Journal of investigative dermatology* **121**, 231-241, doi:10.1046/j.1523-1747.2003.12359.x (2003).

51 Stucker, M. *et al.* The cutaneous uptake of atmospheric oxygen contributes significantly to the oxygen supply of human dermis and epidermis. *The Journal of physiology* **538**, 985-994 (2002).
52 Hennings, H. *et al.* Calcium regulation of growth and differentiation of mouse epidermal cells in culture. *Cell* **19**, 245-254 (1980).
53 Menon, G. K. New insights into skin structure: scratching the surface. *Advanced drug delivery reviews* **54 Suppl 1**, S3-17 (2002).
54 Cornelissen, L. H., Oomens, C. W., Huyghe, J. M. & Baaijens, F. P. Mechanisms that play a role in the maintenance of the calcium gradient in the epidermis. *Skin Res Technol* **13**, 369-376, doi:10.1111/j.1600-0846.2007.00239.x (2007).
55 Forslind, B., Lindberg, M., Roomans, G. M., Pallon, J. & Werner-Linde, Y. Aspects on the physiology of human skin: studies using particle probe analysis. *Microscopy research and technique* **38**, 373-386, doi:10.1002/(SICI)1097-0029(19970815)38:4<373::AID-JEMT5>3.0.CO;2-K (1997).
56 Caputo, R. & Peluchetti, D. The junctions of normal human epidermis. A freeze-fracture study. *Journal of ultrastructure research* **61**, 44-61 (1977).
57 Risek, B., Klier, F. G. & Gilula, N. B. Multiple gap junction genes are utilized during rat skin and hair development. *Development* **116**, 639-651 (1992).
58 Kam, E., Melville, L. & Pitts, J. D. Patterns of junctional communication in skin. *The Journal of investigative dermatology* **87**, 748-753 (1986).
59 Salomon, D., Saurat, J. H. & Meda, P. Cell-to-cell communication within intact human skin. *The Journal of clinical investigation* **82**, 248-254, doi:10.1172/JCI113578 (1988).
60 Kelsell, D. P. *et al.* Connexin mutations associated with palmoplantar keratoderma and profound deafness in a single family. *European journal of human genetics : EJHG* **8**, 141-144, doi:10.1038/sj.ejhg.5200407 (2000).
61 Di, W. L., Rugg, E. L., Leigh, I. M. & Kelsell, D. P. Multiple epidermal connexins are expressed in different keratinocyte subpopulations including connexin 31. *The Journal of investigative dermatology* **117**, 958-964, doi:10.1046/j.0022-202x.2001.01468.x (2001).
62 Rouan, F. *et al.* trans-dominant inhibition of connexin-43 by mutant connexin-26: implications for dominant connexin disorders affecting epidermal differentiation. *Journal of cell science* **114**, 2105-2113 (2001).
63 Masgrau-Peya, E., Salomon, D., Saurat, J. H. & Meda, P. In vivo modulation of connexins 43 and 26 of human epidermis by topical retinoic acid treatment. *The journal of histochemistry and cytochemistry : official journal of the Histochemistry Society* **45**, 1207-1215 (1997).

64 Lucke, T. *et al.* Upregulation of connexin 26 is a feature of keratinocyte differentiation in hyperproliferative epidermis, vaginal epithelium, and buccal epithelium. *The Journal of investigative dermatology* **112**, 354-361, doi:10.1046/j.1523-1747.1999.00512.x (1999).

65 Djalilian, A. R. *et al.* Connexin 26 regulates epidermal barrier and wound remodeling and promotes psoriasiform response. *The Journal of clinical investigation* **116**, 1243-1253, doi:10.1172/JCI27186 (2006).

66 Majumder, P. *et al.* ATP-mediated cell-cell signaling in the organ of Corti: the role of connexin channels. *Purinergic signalling* **6**, 167-187, doi:10.1007/s11302-010-9192-9 (2010).

67 Petersen, M. B. & Willems, P. J. Non-syndromic, autosomal-recessive deafness. *Clinical genetics* **69**, 371-392, doi:10.1111/j.1399-0004.2006.00613.x (2006).

68 Chang, E. H., Van Camp, G. & Smith, R. J. The role of connexins in human disease. *Ear and hearing* **24**, 314-323, doi:10.1097/01.AUD.0000079801.55588.13 (2003).

69 Guilford, P. *et al.* A non-syndrome form of neurosensory, recessive deafness maps to the pericentromeric region of chromosome 13q. *Nature genetics* **6**, 24-28, doi:10.1038/ng0194-24 (1994).

70 del Castillo, I. *et al.* A deletion involving the connexin 30 gene in nonsyndromic hearing impairment. *The New England journal of medicine* **346**, 243-249, doi:10.1056/NEJMoa012052 (2002).

71 Dai, P. *et al.* Distinct and novel SLC26A4/Pendrin mutations in Chinese and U.S. patients with nonsyndromic hearing loss. *Physiological genomics* **38**, 281-290, doi:10.1152/physiolgenomics.00047.2009 (2009).

72 Rabionet, R., Gasparini, P. & Estivill, X. Molecular genetics of hearing impairment due to mutations in gap junction genes encoding beta connexins. *Human mutation* **16**, 190-202, doi:10.1002/1098-1004(200009)16:3<190::AID-HUMU2>3.0.CO;2-I (2000).

73 Antoniadi, T. *et al.* Mutation analysis of the GJB2 (connexin 26) gene by DGGE in Greek patients with sensorineural deafness. *Human mutation* **16**, 7-12, doi:10.1002/1098-1004(200007)16:1<7::AID-HUMU2>3.0.CO;2-A (2000).

74 Alvarez, A. *et al.* High prevalence of the W24X mutation in the gene encoding connexin-26 (GJB2) in Spanish Romani (gypsies) with autosomal recessive non-syndromic hearing loss. *American journal of medical genetics. Part A* **137A**, 255-258, doi:10.1002/ajmg.a.30884 (2005).

75 Joseph, A. Y. & Rasool, T. J. High frequency of connexin26 (GJB2) mutations associated with nonsyndromic hearing loss in the population of

Kerala, India. *International journal of pediatric otorhinolaryngology* **73**, 437-443, doi:10.1016/j.ijporl.2008.11.010 (2009).

76 Khandelwal, G., Bhalla, S., Khullar, M. & Panda, N. K. High frequency of heterozygosity in GJB2 mutations among patients with non-syndromic hearing loss. *The Journal of laryngology and otology* **123**, 273-277, doi:10.1017/S0022215108002892 (2009).

77 Bouwer, S. *et al.* Carrier rates of the ancestral Indian W24X mutation in GJB2 in the general Gypsy population and individual subisolates. *Genetic testing* **11**, 455-458, doi:10.1089/gte.2007.0048 (2007).

78 Bors, A. *et al.* Frequencies of two common mutations (c.35delG and c.167delT) of the connexin 26 gene in different populations of Hungary. *International journal of molecular medicine* **14**, 1105-1108 (2004).

79 Dong, J., Katz, D. R., Eng, C. M., Kornreich, R. & Desnick, R. J. Nonradioactive detection of the common Connexin 26 167delT and 35delG mutations and frequencies among Ashkenazi Jews. *Molecular genetics and metabolism* **73**, 160-163, doi:10.1006/mgme.2001.3182 (2001).

80 Dai, P. *et al.* The prevalence of the 235delC GJB2 mutation in a Chinese deaf population. *Genetics in medicine : official journal of the American College of Medical Genetics* **9**, 283-289, doi:10.1097/GIM.0b013e31804d2371 (2007).

81 Abe, S., Usami, S., Shinkawa, H., Kelley, P. M. & Kimberling, W. J. Prevalent connexin 26 gene (GJB2) mutations in Japanese. *Journal of medical genetics* **37**, 41-43 (2000).

82 Lautermann, J. *et al.* Expression of the gap-junction connexins 26 and 30 in the rat cochlea. *Cell and tissue research* **294**, 415-420 (1998).

83 Forge, A. *et al.* Gap junctions and connexin expression in the inner ear. *Novartis Foundation symposium* **219**, 134-150; discussion 151-136 (1999).

84 Xia, A. P. *et al.* Expression of connexin 31 in the developing mouse cochlea. *Neuroreport* **11**, 2449-2453 (2000).

85 Ahmad, S., Chen, S., Sun, J. & Lin, X. Connexins 26 and 30 are co-assembled to form gap junctions in the cochlea of mice. *Biochemical and biophysical research communications* **307**, 362-368 (2003).

86 Kudo, T. *et al.* Transgenic expression of a dominant-negative connexin26 causes degeneration of the organ of Corti and non-syndromic deafness. *Human molecular genetics* **12**, 995-1004 (2003).

87 Cohen-Salmon, M. *et al.* Expression of the connexin43- and connexin45-encoding genes in the developing and mature mouse inner ear. *Cell and tissue research* **316**, 15-22, doi:10.1007/s00441-004-0861-2 (2004).

88 Zhao, H. B. Connexin26 is responsible for anionic molecule permeability in the cochlea for intercellular signalling and metabolic communications. *The European journal of neuroscience* **21**, 1859-1868, doi:10.1111/j.1460-9568.2005.04031.x (2005).

89 Grob, J. J., Breton, A., Bonafe, J. L., Sauvan-Ferdani, M. & Bonerandi, J. J. Keratitis, ichthyosis, and deafness (KID) syndrome. Vertical transmission and death from multiple squamous cell carcinomas. *Archives of dermatology* **123**, 777-782 (1987).

90 Nazzaro, V., Blanchet-Bardon, C., Lorette, G. & Civatte, J. Familial occurrence of KID (keratitis, ichthyosis, deafness) syndrome. Case reports of a mother and daughter. *Journal of the American Academy of Dermatology* **23**, 385-388 (1990).

91 Szymko-Bennett, Y. M., Russell, L. J., Bale, S. J. & Griffith, A. J. Auditory manifestations of Keratitis-Ichthyosis-Deafness (KID) syndrome. *The Laryngoscope* **112**, 272-280, doi:10.1097/00005537-200202000-00014 (2002).

92 Janecke, A. R. *et al.* GJB2 mutations in keratitis-ichthyosis-deafness syndrome including its fatal form. *American journal of medical genetics. Part A* **133A**, 128-131, doi:10.1002/ajmg.a.30515 (2005).

93 Richard, G. *et al.* Missense mutations in GJB2 encoding connexin-26 cause the ectodermal dysplasia keratitis-ichthyosis-deafness syndrome. *American journal of human genetics* **70**, 1341-1348, doi:10.1086/339986 (2002).

94 van Steensel, M. A., van Geel, M., Nahuys, M., Smitt, J. H. & Steijlen, P. M. A novel connexin 26 mutation in a patient diagnosed with keratitis-ichthyosis-deafness syndrome. *The Journal of investigative dermatology* **118**, 724-727, doi:10.1046/j.1523-1747.2002.01735.x (2002).

95 van Geel, M. *et al.* HID and KID syndromes are associated with the same connexin 26 mutation. *The British journal of dermatology* **146**, 938-942 (2002).

96 van Steensel, M. A. *et al.* A phenotype resembling the Clouston syndrome with deafness is associated with a novel missense GJB2 mutation. *The Journal of investigative dermatology* **123**, 291-293, doi:10.1111/j.0022-202X.2004.23204.x (2004).

97 Mazereeuw-Hautier, J. *et al.* Keratitis-ichthyosis-deafness syndrome: disease expression and spectrum of connexin 26 (GJB2) mutations in 14 patients. *The British journal of dermatology* **156**, 1015-1019, doi:10.1111/j.1365-2133.2007.07806.x (2007).

98 Montgomery, J. R., White, T. W., Martin, B. L., Turner, M. L. & Holland, S. M. A novel connexin 26 gene mutation associated with features of the keratitis-ichthyosis-deafness syndrome and the follicular occlusion triad.

Journal of the American Academy of Dermatology **51**, 377-382, doi:10.1016/j.jaad.2003.12.042 (2004).

99 Stong, B. C., Chang, Q., Ahmad, S. & Lin, X. A novel mechanism for connexin 26 mutation linked deafness: cell death caused by leaky gap junction hemichannels. *The Laryngoscope* **116**, 2205-2210, doi:10.1097/01.mlg.0000241944.77192.d2 (2006).

100 Arita, K. *et al.* A novel N14Y mutation in Connexin26 in keratitis-ichthyosis-deafness syndrome: analyses of altered gap junctional communication and molecular structure of N terminus of mutated Connexin26. *The American journal of pathology* **169**, 416-423, doi:10.2353/ajpath.2006.051242 (2006).

101 Yotsumoto, S. *et al.* Novel mutations in GJB2 encoding connexin-26 in Japanese patients with keratitis-ichthyosis-deafness syndrome. *The British journal of dermatology* **148**, 649-653 (2003).

102 Terrinoni, A. *et al.* Connexin 26 (GJB2) mutations, causing KID Syndrome, are associated with cell death due to calcium gating deregulation. *Biochemical and biophysical research communications* **394**, 909-914, doi:10.1016/j.bbrc.2010.03.073 (2010).

103 Arndt, S. *et al.* A novel dominant and a de novo mutation in the GJB2 gene (connexin-26) cause keratitis-ichthyosis-deafness syndrome: implication for cochlear implantation. *Otology & neurotology : official publication of the American Otological Society, American Neurotology Society [and] European Academy of Otology and Neurotology* **31**, 210-215, doi:10.1097/MAO.0b013e3181cc09cd (2010).

104 Cushing, S. L. *et al.* Successful cochlear implantation in a child with Keratosis, Icthiosis and Deafness (KID) Syndrome and Dandy-Walker malformation. *International journal of pediatric otorhinolaryngology* **72**, 693-698, doi:10.1016/j.ijporl.2008.01.017 (2008).

105 Koppelhus, U. *et al.* A novel mutation in the connexin 26 gene (GJB2) in a child with clinical and histological features of keratitis-ichthyosis-deafness (KID) syndrome. *Clinical and experimental dermatology* **36**, 142-148, doi:10.1111/j.1365-2230.2010.03936.x (2011).

106 Gerido, D. A., DeRosa, A. M., Richard, G. & White, T. W. Aberrant hemichannel properties of Cx26 mutations causing skin disease and deafness. *American journal of physiology. Cell physiology* **293**, C337-345, doi:10.1152/ajpcell.00626.2006 (2007).

107 Lee, J. R., Derosa, A. M. & White, T. W. Connexin mutations causing skin disease and deafness increase hemichannel activity and cell death when expressed in Xenopus oocytes. *The Journal of investigative dermatology* **129**, 870-878, doi:10.1038/jid.2008.335 (2009).

108 Hara-Chikuma, M. & Verkman, A. S. Aquaporin-3 functions as a glycerol transporter in mammalian skin. *Biology of the cell / under the auspices of the European Cell Biology Organization* **97**, 479-486, doi:10.1042/BC20040104 (2005).
109 Maeda, S. *et al.* Structure of the connexin 26 gap junction channel at 3.5 A resolution. *Nature* **458**, 597-602, doi:10.1038/nature07869 (2009).
110 Bondeson, M. L., Nystrom, A. M., Gunnarsson, U. & Vahlquist, A. Connexin 26 (GJB2) mutations in two Swedish patients with atypical Vohwinkel (mutilating keratoderma plus deafness) and KID syndrome both extensively treated with acitretin. *Acta dermato-venereologica* **86**, 503-508, doi:10.2340/00015555-0164 (2006).
111 Snoeckx, R. L., Hassan, D. M., Kamal, N. M., Van Den Bogaert, K. & Van Camp, G. Mutation analysis of the GJB2 (connexin 26) gene in Egypt. *Human mutation* **26**, 60-61, doi:10.1002/humu.9350 (2005).
112 Korge, B. P. *et al.* Loricrin mutation in Vohwinkel's keratoderma is unique to the variant with ichthyosis. *The Journal of investigative dermatology* **109**, 604-610 (1997).
113 Maestrini, E. *et al.* A missense mutation in connexin26, D66H, causes mutilating keratoderma with sensorineural deafness (Vohwinkel's syndrome) in three unrelated families. *Human molecular genetics* **8**, 1237-1243 (1999).
114 Maestrini, E. *et al.* A molecular defect in loricrin, the major component of the cornified cell envelope, underlies Vohwinkel's syndrome. *Nature genetics* **13**, 70-77, doi:10.1038/ng0596-70 (1996).
115 Peris, K., Salvati, E. F., Torlone, G. & Chimenti, S. Keratoderma hereditarium mutilans (Vohwinkel's syndrome) associated with congenital deaf-mutism. *The British journal of dermatology* **132**, 617-620 (1995).
116 Drummond, A. A Case of Unusual Skin Lesions. *Irish Journal of Medical Sciences* **2**, 85-90 (1939).
117 Vohwinkel, K. H. Keratoma hereditarium mutilans. *Archives of Dermatology and Syphilology* **158**, 354-364 (1929).
118 Richard, G., Brown, N., Ishida-Yamamoto, A. & Krol, A. Expanding the phenotypic spectrum of Cx26 disorders: Bart-Pumphrey syndrome is caused by a novel missense mutation in GJB2. *The Journal of investigative dermatology* **123**, 856-863, doi:10.1111/j.0022-202X.2004.23470.x (2004).
119 Bart, R. S. & Pumphrey, R. E. Knuckle pads, leukonychia and deafness. A dominantly inherited syndrome. *The New England journal of medicine* **276**, 202-207, doi:10.1056/NEJM196701262760403 (1967).
120 Ramer, J. C., Vasily, D. B. & Ladda, R. L. Familial leuconychia, knuckle pads, hearing loss, and palmoplantar hyperkeratosis: an additional family

with Bart-Pumphrey syndrome. *Journal of medical genetics* **31**, 68-71 (1994).

121 Alexandrino, F., Sartorato, E. L., Marques-de-Faria, A. P. & Steiner, C. E. G59S mutation in the GJB2 (connexin 26) gene in a patient with Bart-Pumphrey syndrome. *American journal of medical genetics. Part A* **136**, 282-284, doi:10.1002/ajmg.a.30822 (2005).

122 Sharland, M., Bleach, N. R., Goberdhan, P. D. & Patton, M. A. Autosomal dominant palmoplantar hyperkeratosis and sensorineural deafness in three generations. *Journal of medical genetics* **29**, 50-52 (1992).

123 Verbov, J. Palmoplantar keratoderma, deafness and atopy. *The British journal of dermatology* **116**, 881-882 (1987).

124 Heathcote, K., Syrris, P., Carter, N. D. & Patton, M. A. A connexin 26 mutation causes a syndrome of sensorineural hearing loss and palmoplantar hyperkeratosis (MIM 148350). *Journal of medical genetics* **37**, 50-51 (2000).

125 Leonard, N. J., Krol, A. L., Bleoo, S. & Somerville, M. J. Sensorineural hearing loss, striate palmoplantar hyperkeratosis, and knuckle pads in a patient with a novel connexin 26 (GJB2) mutation. *Journal of medical genetics* **42**, e2, doi:10.1136/jmg.2003.017376 (2005).

126 Uyguner, O. *et al.* The novel R75Q mutation in the GJB2 gene causes autosomal dominant hearing loss and palmoplantar keratoderma in a Turkish family. *Clinical genetics* **62**, 306-309 (2002).

127 Iossa, S. *et al.* New evidence for the correlation of the p.G130V mutation in the GJB2 gene and syndromic hearing loss with palmoplantar keratoderma. *American journal of medical genetics. Part A* **149A**, 685-688, doi:10.1002/ajmg.a.32462 (2009).

128 Richard, G. *et al.* Functional defects of Cx26 resulting from a heterozygous missense mutation in a family with dominant deaf-mutism and palmoplantar keratoderma. *Human genetics* **103**, 393-399 (1998).

129 de Zwart-Storm, E. A. *et al.* A novel missense mutation in the second extracellular domain of GJB2, p.Ser183Phe, causes a syndrome of focal palmoplantar keratoderma with deafness. *The American journal of pathology* **173**, 1113-1119, doi:10.2353/ajpath.2008.080049 (2008).

130 Akiyama, M. *et al.* A novel GJB2 mutation p.Asn54His in a patient with palmoplantar keratoderma, sensorineural hearing loss and knuckle pads. *The Journal of investigative dermatology* **127**, 1540-1543, doi:10.1038/sj.jid.5700711 (2007).

131 Messmer, E. M., Kenyon, K. R., Rittinger, O., Janecke, A. R. & Kampik, A. Ocular manifestations of keratitis-ichthyosis-deafness (KID) syndrome. *Ophthalmology* **112**, e1-6, doi:10.1016/j.ophtha.2004.07.034 (2005).

132 Schnyder, U. W. & Gloor, M. [Congenital bullous ichthyosiform erythroderma (case 20)]. *Zeitschrift fur Hautkrankheiten* **52**, 809-811 (1977).
133 Gulzow, J. & Anton-Lamprecht, I. [Ichthyosis hystrix gravior typus Rheydt: an otologic-dermatologic syndrome (author's transl)]. *Laryngologie, Rhinologie, Otologie* **56**, 949-955 (1977).
134 Traupe, H., Macher, E., Hamm, H. & Happle, R. Mutation rate estimates are not compatible with autosomal dominant inheritance of the dysplastic nevus "syndrome". *American journal of medical genetics* **32**, 155-157, doi:10.1002/ajmg.1320320203 (1989).
135 Brown, C. W. *et al.* A novel GJB2 (connexin 26) mutation, F142L, in a patient with unusual mucocutaneous findings and deafness. *The Journal of investigative dermatology* **121**, 1221-1223, doi:10.1046/j.1523-1747.2003.12550_4.x (2003).
136 Thomas, T., Aasen, T., Hodgins, M. & Laird, D. W. Transport and function of cx26 mutants involved in skin and deafness disorders. *Cell communication & adhesion* **10**, 353-358 (2003).
137 Marziano, N. K., Casalotti, S. O., Portelli, A. E., Becker, D. L. & Forge, A. Mutations in the gene for connexin 26 (GJB2) that cause hearing loss have a dominant negative effect on connexin 30. *Human molecular genetics* **12**, 805-812 (2003).
138 Forge, A., Marziano, N. K., Casalotti, S. O., Becker, D. L. & Jagger, D. The inner ear contains heteromeric channels composed of cx26 and cx30 and deafness-related mutations in cx26 have a dominant negative effect on cx30. *Cell communication & adhesion* **10**, 341-346 (2003).
139 Piazza, V. *et al.* Functional analysis of R75Q mutation in the gene coding for Connexin 26 identified in a family with nonsyndromic hearing loss. *Clinical genetics* **68**, 161-166, doi:10.1111/j.1399-0004.2005.00468.x (2005).
140 Mani, R. S. *et al.* Functional consequences of novel connexin 26 mutations associated with hereditary hearing loss. *European journal of human genetics : EJHG* **17**, 502-509, doi:10.1038/ejhg.2008.179 (2009).
141 Chen, Y., Deng, Y., Bao, X., Reuss, L. & Altenberg, G. A. Mechanism of the defect in gap-junctional communication by expression of a connexin 26 mutant associated with dominant deafness. *The FASEB journal : official publication of the Federation of American Societies for Experimental Biology* **19**, 1516-1518, doi:10.1096/fj.04-3491fje (2005).
142 Bennett, M. V., Contreras, J. E., Bukauskas, F. F. & Saez, J. C. New roles for astrocytes: gap junction hemichannels have something to communicate. *Trends in neurosciences* **26**, 610-617 (2003).

143 Mese, G., Londin, E., Mui, R., Brink, P. R. & White, T. W. Altered gating properties of functional Cx26 mutants associated with recessive non-syndromic hearing loss. *Human genetics* **115**, 191-199, doi:10.1007/s00439-004-1142-6 (2004).
144 Horton, R. M., Cai, Z. L., Ho, S. N. & Pease, L. R. Gene splicing by overlap extension: tailor-made genes using the polymerase chain reaction. *BioTechniques* **8**, 528-535 (1990).
145 Turner, D. L. & Weintraub, H. Expression of achaete-scute homolog 3 in Xenopus embryos converts ectodermal cells to a neural fate. *Genes & development* **8**, 1434-1447 (1994).
146 Bruzzone, R., Haefliger, J. A., Gimlich, R. L. & Paul, D. L. Connexin40, a component of gap junctions in vascular endothelium, is restricted in its ability to interact with other connexins. *Molecular biology of the cell* **4**, 7-20 (1993).
147 Spray, D. C., Harris, A. L. & Bennett, M. V. Equilibrium properties of a voltage-dependent junctional conductance. *The Journal of general physiology* **77**, 77-93 (1981).
148 Ripps, H., Qian, H. & Zakevicius, J. Properties of connexin26 hemichannels expressed in Xenopus oocytes. *Cellular and molecular neurobiology* **24**, 647-665 (2004).
149 Gonzalez, D., Gomez-Hernandez, J. M. & Barrio, L. C. Species specificity of mammalian connexin-26 to form open voltage-gated hemichannels. *The FASEB journal : official publication of the Federation of American Societies for Experimental Biology* **20**, 2329-2338, doi:10.1096/fj.06-5828com (2006).
150 Ebihara, L. & Steiner, E. Properties of a nonjunctional current expressed from a rat connexin46 cDNA in Xenopus oocytes. *The Journal of general physiology* **102**, 59-74 (1993).
151 Kelsell, D. P., Di, W. L. & Houseman, M. J. Connexin mutations in skin disease and hearing loss. *American journal of human genetics* **68**, 559-568, doi:10.1086/318803 (2001).
152 Essenfelder, G. M. *et al.* Connexin30 mutations responsible for hidrotic ectodermal dysplasia cause abnormal hemichannel activity. *Human molecular genetics* **13**, 1703-1714, doi:10.1093/hmg/ddh191 (2004).
153 de Zwart-Storm, E. A. *et al.* Molecular analysis of connexin26 asparagine14 mutations associated with syndromic skin phenotypes. *Experimental dermatology* **20**, 408-412, doi:10.1111/j.1600-0625.2010.01222.x (2011).
154 Matos, T. D. *et al.* A novel M163L mutation in connexin 26 causing cell death and associated with autosomal dominant hearing loss. *Hearing research* **240**, 87-92, doi:10.1016/j.heares.2008.03.004 (2008).

155 Tattersall, D., Scott, C. A., Gray, C., Zicha, D. & Kelsell, D. P. EKV mutant connexin 31 associated cell death is mediated by ER stress. *Human molecular genetics* **18**, 4734-4745, doi:10.1093/hmg/ddp436 (2009).